

THE SULFUR CONTENT AND SULFUR ISOTOPIC COMPOSITION OF
ARCHEAN BASALTIC ROCKS AT MATAGAMI, QUEBEC
AND THEIR RELATIONSHIP TO
MASSIVE SULFIDES

by

ANNA PASITSCHNIAK

A thesis submitted to the Faculty of Graduate Studies
and Research of McGill University, in partial fulfilment
of the requirements for the degree of Master of Science.

Department of Geological Sciences
McGill University, Montreal, Quebec, Canada

Copyright © Anna Pasitschniak, 1982

Sulfur Content and Isotopic Composition of Basalts.

A. Pasitschniak - The Sulfur Content and Sulfur Isotopic Composition of Archean Basaltic Rocks at Matagami, Québec and their Relationship to Massive Sulfides - Department of Geological Sciences - Master of Science

ABSTRACT

The concentration of sulfur in Archean basaltic rocks belonging to the Watson Lake Group is highly variable. Least altered basalts contain an average of 980 ppm sulfur whereas the altered basalts contain approximately 1300 ppm. This indicates an addition of sulfur to the altered rocks due to convective circulation of hydrothermal fluids.

The sulfur isotopic composition, $\delta^{34}\text{S}$, of these basalts ranges from -0.3 to +1.8 per mil in the least altered rocks and from -1.8 to +3.9 per mil in the altered rocks. The sulfur present in the least altered rocks is derived from a magmatic source whereas that present in the altered rocks is derived from a mixed magmatic and seawater source.

Ore metals which were leached in the core of the geothermal system were probably transported exclusively as chloride complexes. Sulfur, on the other hand, was transported as H_2S and SO_4^{2-} .

Ore deposition at the Garon Lake mine probably resulted from mixing of a metal-rich chloride brine with a sulfur-bearing solution.

A. Pasitschniak - La Concentration en Soufre et sa
Composition Isotopique dans les Roches Basaltiques Archéennes
à Matagami, Québec et Leur Relation avec le Minéral de Sul-
fures Massifs - Département des Sciences Géologiques -
Maîtrise en Sciences

SOMMAIRE

La concentration de soufre dans les roches basaltiques Archéennes du groupe du Lac Watson (Matagami, Québec) est très variable. Les basaltes les plus frais en contiennent en moyenne 980 ppm, tandis que les basaltes altérés en contiennent 1300 ppm. Cette augmentation serait due à la circulation de fluides hydrothermaux en convection.

La composition isotopique du soufre, $\delta^{34}\text{S}$, dans ces roches varie de -0.3 à +1.8 par mille dans les roches les plus fraîches et de -1.8 à +3.9 par mille dans les roches altérées. Dans les roches les plus fraîches, le soufre a une origine magmatique, mais dans les roches altérées, on trouve une origine mixte, en partie magmatique, en partie provenant d'eau de mer.

Les métaux du minéral lessivés dans le centre du système géothermique ont probablement migré exclusivement sous forme de complexes chlorurés. Le soufre, par contre, a été transporté sous forme de H_2S et de SO_4^{2-} .

A la mine Garon Lake, la déposition du minéral aurait résulté du mélange d'une saumure chlorurée métallifère et d'une solution sulfurée.

Table of Contents

	Page
CHAPTER 1 - <u>INTRODUCTION</u>	
Previous work	3
Outline of the Study	5
Acknowledgements	5
CHAPTER 2 - <u>REGIONAL GEOLOGY</u>	
2.1 <u>Introduction</u>	7
2.2 <u>Volcanic Stratigraphy</u>	7
2.3 <u>Intrusive Rocks</u>	10
2.4 <u>Extrusive Rocks</u>	12
2.5 <u>Alteration in the Extrusive Rocks</u>	12
2.6 <u>Interpretation of the Alteration in the Extrusive Rocks</u>	16
2.7 <u>Structural History</u>	17
2.8 <u>Metamorphism of the Volcanic Rocks</u>	19
CHAPTER 3 - <u>SULFUR GEOCHEMISTRY OF THE BASALTIC ROCKS</u>	
3.1 <u>Introduction</u>	21
3.2 <u>Analytical Techniques</u>	22
3.2.1 Sulfur Determination by X-ray Fluorescence Spectrometry	23
3.2.2 Sulfur Determination by LECO Analysis	27
3.2.3 Comparison of Results Obtained by Using Both Methods of Analysis	28
3.3 <u>Bulk Sample Analysis by X-ray Fluorescence</u>	30
3.4 <u>Sulfur Distribution in Basaltic Rocks</u>	32
3.5 <u>Correlation Between Sulfur and Iron</u>	34
3.6 <u>Juvenile Sulfur Content of Basalts</u>	41
3.7 <u>Factors Controlling the Solubility of Sulfur</u>	47

3.8	<u>Solubility and Saturation of Sulfur in Basaltic Rocks</u>	49
3.9	<u>Discussion</u>	51
3.10	<u>Conclusion</u>	57
CHAPTER 4 - <u>SULFUR ISOTOPE DETERMINATION</u>		
4.1	<u>Introduction</u>	58
4.2	<u>Analyses of the Volcanic Rocks</u>	62
4.3	<u>Isotopic Composition of the Rocks</u>	62
4.4	<u>Interpretation of the Isotopic Composition</u>	64
4.5	<u>Conclusion</u>	68
CHAPTER 5 - <u>HYDROTHERMAL FLUIDS AND MASSIVE SULFIDE GENESIS</u>		
5.1	<u>Introduction</u>	69
5.2	<u>Major Element, Trace Element and Trans- ition Element Redistribution</u>	70
5.3	<u>Sulfur Redistribution</u>	70
5.4	<u>Solubility and Transport of Ore Metals and Sulfur</u>	71
5.5	<u>Stability of Metal Bisulfide and Metal Chloride Complexes</u>	76
5.6	<u>Mechanism of Ore Metal Transport and its Relationship to the Genesis of Massive Sulfides</u>	77
5.7	<u>Conclusion</u>	83
CONCLUSION		84
CONTRIBUTION TO KNOWLEDGE		86
BIBLIOGRAPHY		87

APPENDICIES

I	<u>Sample Preparation and Analytical Procedure</u>	109
II	<u>Geochemical Composition of Basaltic and Rhyolitic Units</u>	123

NR Norita Rhyolite
B1 Basalt
B2 Basalt
B3 Basalt
B4 Basalt
GLR Garon Lake Rhyolite
B5 Basalt
B6 Basalt
B7 Basalt

MAPS

1. Sample Location Map: Bell Channel Property
2. Sample Location Map: Garon Lake Property

LIST OF FIGURES

	Page
1.1 Regional geology and location of mines in the Matagami district.	2
2.1 Geological Map of the study area.	8
2.2 Restored stratigraphic section through the volcanic rocks in the western part of the study area, bordering the Bell River.	9
2.3 Restored stratigraphic section through the extrusive volcanic rocks.	13
3.1 Calibration line used to determine the sulfur content of unknown samples.	25
3.2 Plot of XRF versus LECO results.	29
3.3 Frequency diagrams illustrating the distribution of sulfur analyses.	35
3.4a Plot of sulfur versus iron content of least altered basalts.	37
3.4b Plot of the geometric mean of sulfur against the arithmetic mean of iron for least altered basalts.	39
3.5a Plot of sulfur versus iron content of altered basalts.	42
3.5b Plot of the geometric mean of sulfur against the arithmetic mean of iron for altered basalts.	43
3.6 Plot of sulfur concentration versus iron content for Archean basaltic rocks.	52
4.1 Isotopic enrichment factors for important sulfur species.	60
4.2 Plot of $\delta^{34}\text{S}$ values against SiO_2 content.	65
4.3 Comparison of the positions of $\delta^{34}\text{S}$ contours with the stability fields of Fe-S-O minerals and barite at $T = 350^\circ\text{C}$.	67
5.1 Rate of dissolution of sulfur for B2 basalts.	74

5.2	Rate of dissolution of sulfur for B3 basalts.	74
5.3	Rate of dissolution of sulfur for B4 basalts.	75
5.4	Longitudinal vertical projection of the three sulfide lenses at the Garon Lake mine.	79
5.5	Stability fields of Fe-Zn-Cu-S minerals at T = 350°C.	82

LIST OF TABLES

	Page
3.1 Comparison of Results Obtained by XRF and LECO Analysis.	26
3.2 Variation of Sulfur Concentration Within a Bulk Sample.	31
3.3 Distribution of the Mean Sulfur Content and Corresponding Standard Error of the Mean in each Unit.	33
3.4 Average Fe and S Compositions of the Volcanic Rocks.	40
3.5 Losses and Gains of FeO and S during Alteration as Indicated by the Differences in these Components Between Altered and Least Altered Basalts.	44
3.6 Sulfur Content of Least Altered Submarine Basalts.	45
4.1 Sulfur Isotopic Compositions of the Basalts.	63
5.1 Approximate Ore Reserve at the Garon Lake mine.	80

CHAPTER 1 - INTRODUCTION

There appears to be an increasing awareness that the formation of a number of massive sulfide ore deposits and surrounding rocks is syngenetic. Consequently, more attention is currently being drawn to the sulfur content of the wallrocks.

In this study, attention is focused on the sulfur content of Archean basaltic rocks in Matagami, Québec, with special reference to those basalts which were part of a hydrothermal system responsible for the generation of a geothermal massive sulfide ore deposit. A wide range of sulfur values now exists within these basalts. Moreover, the least hydrothermally altered rocks appear to contain less sulfur than the altered ones. This suggests an addition of sulfur to the latter, perhaps due to interaction with hydrothermal fluids.

The study area has been described in detail by MacGeehan (1979) and is located just northeast of Matagami, which lies 352 kilometers north of Amos, Québec, as shown in Figure 1.1. The town and surrounding mining district are part of the Abitibi greenstone belt of the Superior Province (Goodwin and Ridler, 1970). A sequence of very old volcanics was intruded by a large mafic intrusion known as the Bell River Igneous Complex. As increasing amounts of magma were supplied to this magma chamber, a thick succession of interlayered basaltic and rhyolitic rocks was extruded. Since the entire sequence of basalts was both porous and submarine, all of these rocks became saturated with water. Moreover, some of these rocks

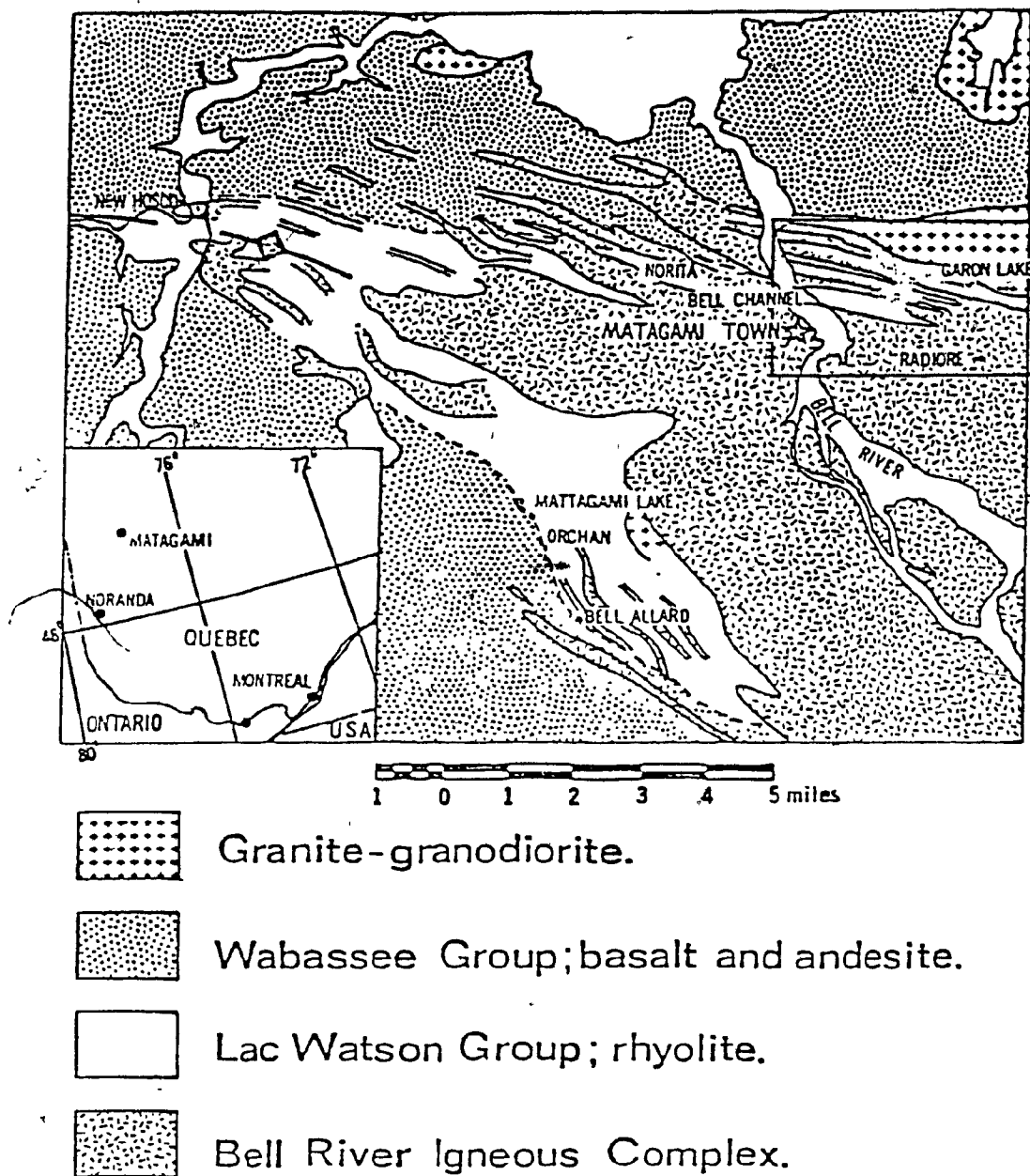


Figure 1.1 - Regional geology and location of mines in the Matagami district. The location of Matagami in Quebec is shown as in inset (lower left), and the area covered by this study is shown as an inset (right). The geology is simplified by MacGeehan (1979) from Sharpe (1968).

() were also hydrothermally altered as a consequence of the convective circulation of heated seawater. Following hydration, and in some cases hydrothermal alteration, these rocks were folded into a westward-plunging anticline whereby the Bell River Complex occupies the core of the anticline and the overlying basaltic and rhyolitic rocks flank the north and south limbs. Massive sulfide deposits occur on both the north and south limbs and are interpreted to be of volcanogenic exhalative origin.

Previous Work

Bell (1895, 1900), Bancroft (1912) and Freeman (1936) were among the first to attempt to unravel the complex geological history of this area. Later, I.W. Jones of the Québec Bureau of Mines ~~undertook~~ the task of mapping the area on a scale of 1 inch = 1 mile. This was then published by Longley (1943), Freeman and Black (1944) and Beland (1953). In the years that followed, additional work was carried out by Joklik (1960), Jenney (1961), Sharpe (1964, 1968) and most recently by MacGeehan (1979) whose work provides the most comprehensive geochemical and petrographic study of the volcanic rocks and associated massive sulfide ore deposit.

Earlier work regarding the amount of sulfur present in fresh basalts was initiated by Moore and Fabbi (1971), Schilling (1973), Mathez (1976), MacLean (1977) and Czamanske and Moore (1977). The results of these studies indicate

that the amount of sulfur present in these basalts is variable, ranging from 800 to 1800 ppm.

Apart from some preliminary sulfur analyses by MacGeehan (1979), few studies have been done to determine the amount of sulfur present in hydrothermally altered and metamorphosed basalts. However, a couple of recent investigations (ie. Naldrett & Goodwin, 1977; Naldrett et al., 1978) are relevant. The study area in both cases has been restricted to the Abitibi greenstone belt in northeastern Ontario and the various types of rocks comprising this belt. As a result of their study, Naldrett & Goodwin (1977) have shown that the sulfur content of the Blake River Group rocks is very erratic. They also found that there is a systematic increase in sulfur with the total iron content in the volcanic rocks belonging to the Blake River and the Rankin-Ennadai Groups. In addition, Naldrett et al. (1978) noted that these rocks were probably saturated with sulfur at the time of their extrusion.

Finally, previous work on sulfur isotopes has established that sulfur occurring in fresh igneous rocks probably originated from an igneous source. Consequently, the $\delta^{34}\text{S}$ value of primary igneous sulfide minerals is expected to be close to zero (Sasaki, 1970; Schneider, 1970; Kanetaira et al., 1973; Ohmoto et al., 1979). On the other hand, sulfur found in altered igneous rocks was probably derived from a multiple source. Therefore, the $\delta^{34}\text{S}$ values of the resulting sulfide minerals are expected to be more variable (Ohmoto,

1972; Ripley et al., 1977; Ohmoto et al., 1979).

Outline of the Study

No detailed study of sulfur concentration in the volcanic rocks in the Matagami area has yet been made. Apart from the $\delta^{34}\text{S}$ analyses of ore rocks at the Norita mine, which is part of an M.Sc. study by P. Bernard (in preparation) at McGill University, no other sulfur isotopic study has been done on these volcanics and/or the associated ore rocks.

The objectives of this study are the following:

- (1) to examine the distribution of sulfur in both least altered and altered basalts exhibiting an iron-enrichment trend and occurring within a limited stratigraphic range.
- (2) to account for the present distribution of sulfur within these rocks.
- (3) to determine whether there is a correlation between degree of alteration, sulfur content and sulfur isotopic composition.
- (4) to propose a mechanism for the transport of sulfur and ore metals.

Acknowledgements

The author wishes to thank Dr. G. R. Webber, the thesis supervisor, for suggesting this topic of research. Many thanks to F. Bonavia and Dr. W. H. MacLean for their assistance in the field during the summer of 1980. Sincere thanks to

() Drs. R. Doig, W. H. MacLean, E. W. Mountjoy, G. R. Webber and A. E. Williams-Jones and to my colleagues F. Bonavia, B. J. McKay, B. Noguez, M. Prahbu, E. Schandal and K. St. Seymour for their valuable discussions, helpful suggestions, support and encouragement toward the completion of this work. Thanks to Drs. C. E. Rees of McMaster University and C. Riddle of the Geological Survey of Canada for providing sulfur isotope analyses and LECO sulfur analyses, respectively. Thanks also to A. M. Collins, the departmental geochemist, for determining the iron contents of some of the samples. A special thank you to Dr. R. F. Martin who kindly supplied a French translation of the abstract.

Financial support for this research was provided by a Carl Reinhardt Scholarship as well as N.R.C. Grant A7719 to Dr. W. H. MacLean. Analytical expenses were supported by F.C.A.C. Grant 649 to Drs. W. H. MacLean and G. R. Webber.

CHAPTER 2 - REGIONAL GEOLOGY

2.1 Introduction

The general geology of the study area located just northeast of Matagami, Québec, is illustrated in Figure 2.1. It is characterized by intrusive and extrusive volcanic rocks which generally face to the north. The direction of strike in these rocks is E-SE and the angle of dip is close to 90° (MacGeehan, 1979). The earlier intrusive rocks comprise several dykes and sills as well as the Bell River Igneous Complex. The compositional range of the dykes and sills is gabbroic to quartz dioritic whereas the Bell River Igneous Complex consists of rocks which are dominantly of gabbroic composition. The Granodiorite Pluton is a later intrusion which outcrops to the north of the Garon Lake mine. This pluton, unlike the other intrusions, was intruded after the regional metamorphism.

The mineralization in the area is associated with three stratigraphic horizons: the Norita rhyolite, the Bell Channel rhyolite and the Garon Lake rhyolite.

2.2 Volcanic Stratigraphy

The stratigraphy of the area has been established by MacGeehan (1979) and is illustrated in Figure 2.2. The lowest stratigraphic unit to be exposed is a pillowed basalt designated as unit B1. Underlying this unit is the Norita rhyolite. Although this rhyolite does not outcrop, it has

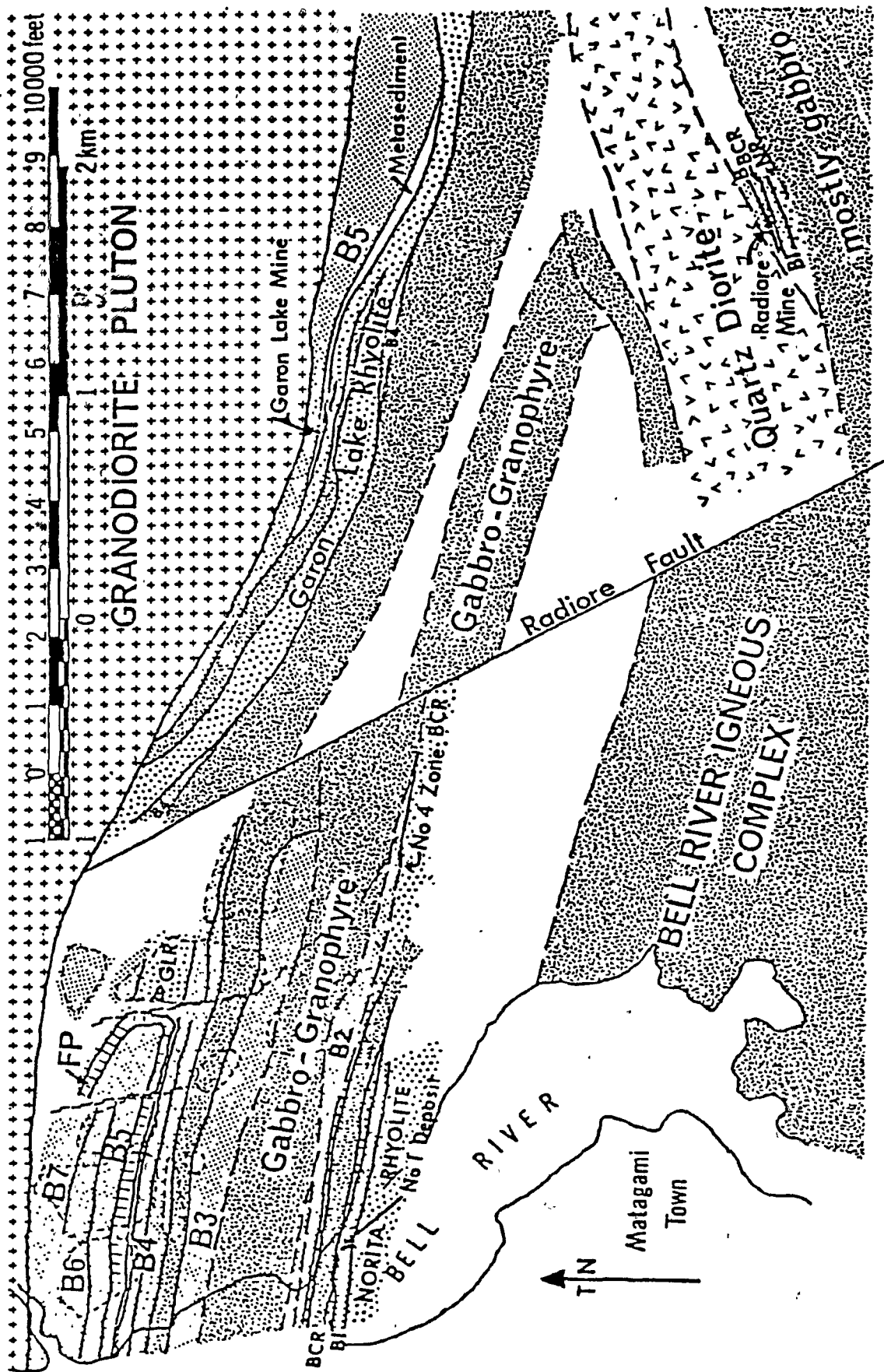


Figure 2.1 - Geological Map of the study area. The acronyms identifying each rock unit are explained in Figure 2.2 (after MacGeehan, 1979).

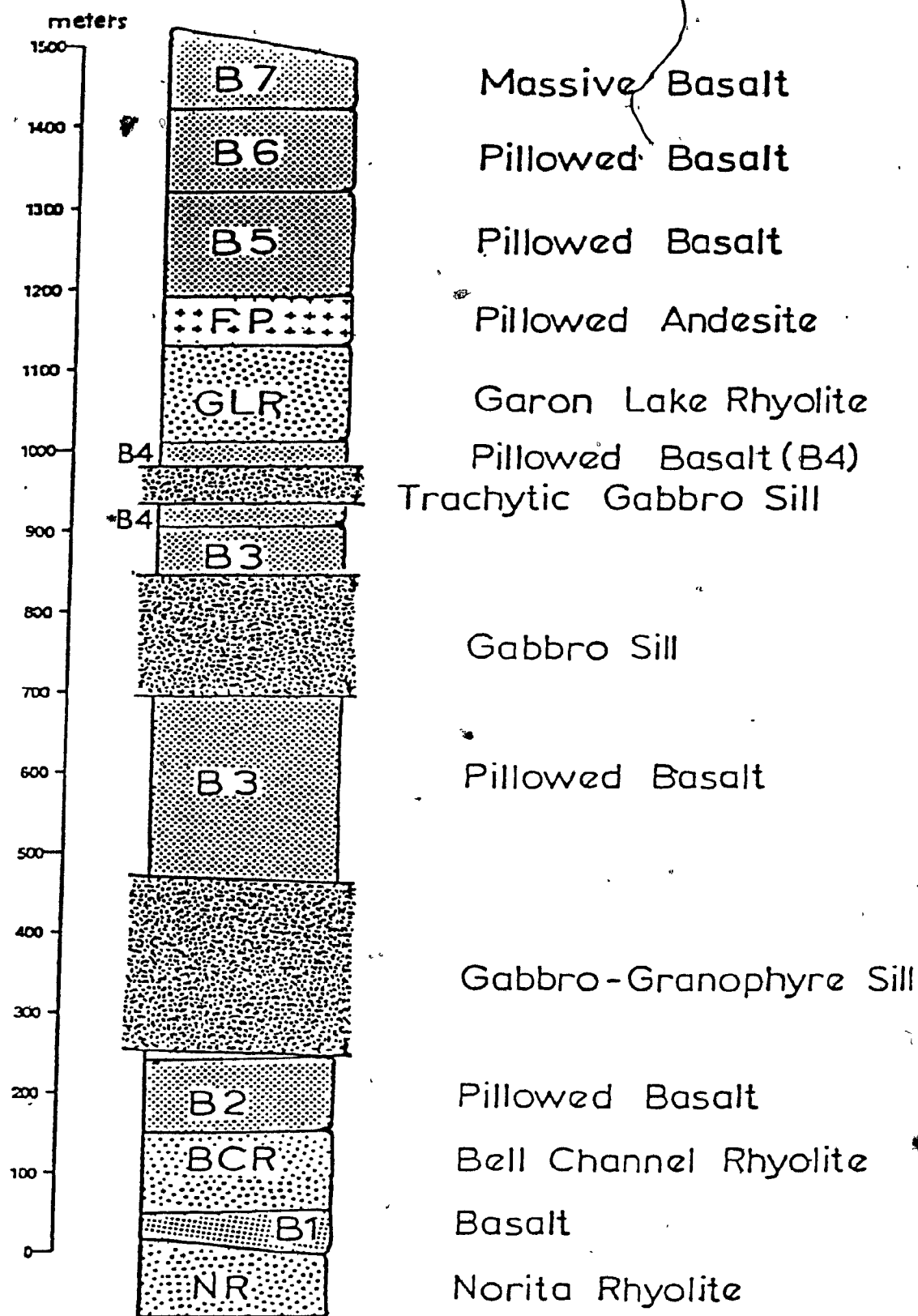


Figure 2.2 - Restored stratigraphic section through the volcanic rocks in the western part of the study area, bordering the Bell River. The section includes the lowest volcanic rocks in the stratigraphic succession which have been intersected in diamond drilling. The intrusive gabbro sills which are well known due to good outcrop and drill intersection have been included in the section, but other intrusive gabbroic rocks are present which have not been included in this illustration (after MacGeehan, 1979).

been exposed underground at the Norita mine. The Norita rhyolite hosted the Bell Channel No. 1 and Radiore deposits. A study of the petrology and geochemistry of the Radiore deposit is the subject of an M.Sc. thesis by F. Bonavia (1982) at McGill University. Overlying unit B1 is yet another rhyolitic unit known as the Bell Channel rhyolite. This unit hosted the Bell Channel No.4 deposit. Located directly above the Bell Channel rhyolite is a 450m thick sequence of pillowed basalts. This sequence of basaltic flows has been subdivided into three units (ie. B2, B3 and B4) by the contemporaneous intrusion of three gabbroic sills. Basalt unit B4 is overlain by another rhyolitic unit called the Garon Lake rhyolite. This unit has a general thickness of 120m but thickens eastward from the Radiore fault. It reaches its maximum thickness in the vicinity of the Garon Lake mine which is located on the east side of this domal accumulation. Lying stratigraphically above the Garon Lake rhyolite is a 65m thick pillowed feldspar porphyry. This unit is overlain by a 375m thick sequence of more pillowed basalts designated as B5, B6 and B7.

2.3 Intrusive Rocks

The volcanic rocks in this area are transected by four types of intrusions: (1) gabbro sills (2) diorite sills (3) the Bell River Igneous Complex and (4) the granodiorite pluton (MacGeehan, 1979).

The gabbro sills range in thickness from 20 to 240m.

The thicker ones are commonly zoned in that the base of the sill is gabbroic in composition whereas the top is almost dioritic. Most of these sills lie parallel to stratigraphy. Sharpe (1964, 1968) stated that they were partly co-magmatic with the basalts. MacGeehan (1979) feels that the association of the gabbro sills with the basalts as well as the similarity in their petrography and geochemistry support the idea that they were probably contemporaneous.

Another intrusion which is associated with the volcanic rocks is a 600m thick dioritic to quartz dioritic sill located just east of the Radiore fault. However, unlike the above mentioned sills, this one cuts across stratigraphy at a low angle and is probably a later phase intrusion of the gabbroic intrusive event.

The Bell River Igneous Complex is one of the larger intrusions in this area. The rocks comprising this Complex grade northward from banded gabbro-anorthosites through to oxide-rich gabbros and finally to finely layered gabbroic units.

The last intrusion in this area was the emplacement of the granodiorite pluton. Along its southern boundary, it truncates both the extrusive volcanics and the intrusive gabbro sills. In addition, it also cuts across the Bell River Igneous Complex, indicating that it postdated the intrusion of the Complex. As a consequence of this latest intrusion, a number of large-scale faults were formed. One example is

the Radiore fault which is characterized by a strong dip-slip component, indicating considerable vertical displacement. The granodiorite pluton is thought to have been intruded after the folding and the regional metamorphism.

2.4 Extrusive Rocks

An illustration of the stratigraphic column showing only the extrusive volcanics is presented in Figure 2.3. In a recent study of the three different extrusive volcanic units, MacGeehan (1979) noted that all are sub-alkaline and tholeiitic. He showed that the basalts are all very iron rich having an $Fe/Fe + Mg$ ratio of more than 0.45. Moreover, these rocks exhibit an iron enrichment trend characteristic of tholeiitic rocks. Additional geochemical evidence supported the conclusions that (1) the basalts are all genetically inter-related (2) the rhyolites are all genetically inter-related (3) the rhyolites are probably genetically related to the basalts and (4) the feldspar porphyry unit is a hybrid rock type of the surrounding basaltic and rhyolitic rocks.

2.5 Alteration in the Extrusive Volcanic Rocks

Virtually all the volcanics in this area are altered; the basalts are spilitized and silicified whereas the rhyolites are chloritized. Geochemical evidence further suggests that these alteration processes were contemporaneous and pre-dated regional metamorphism. The spilitization exper-

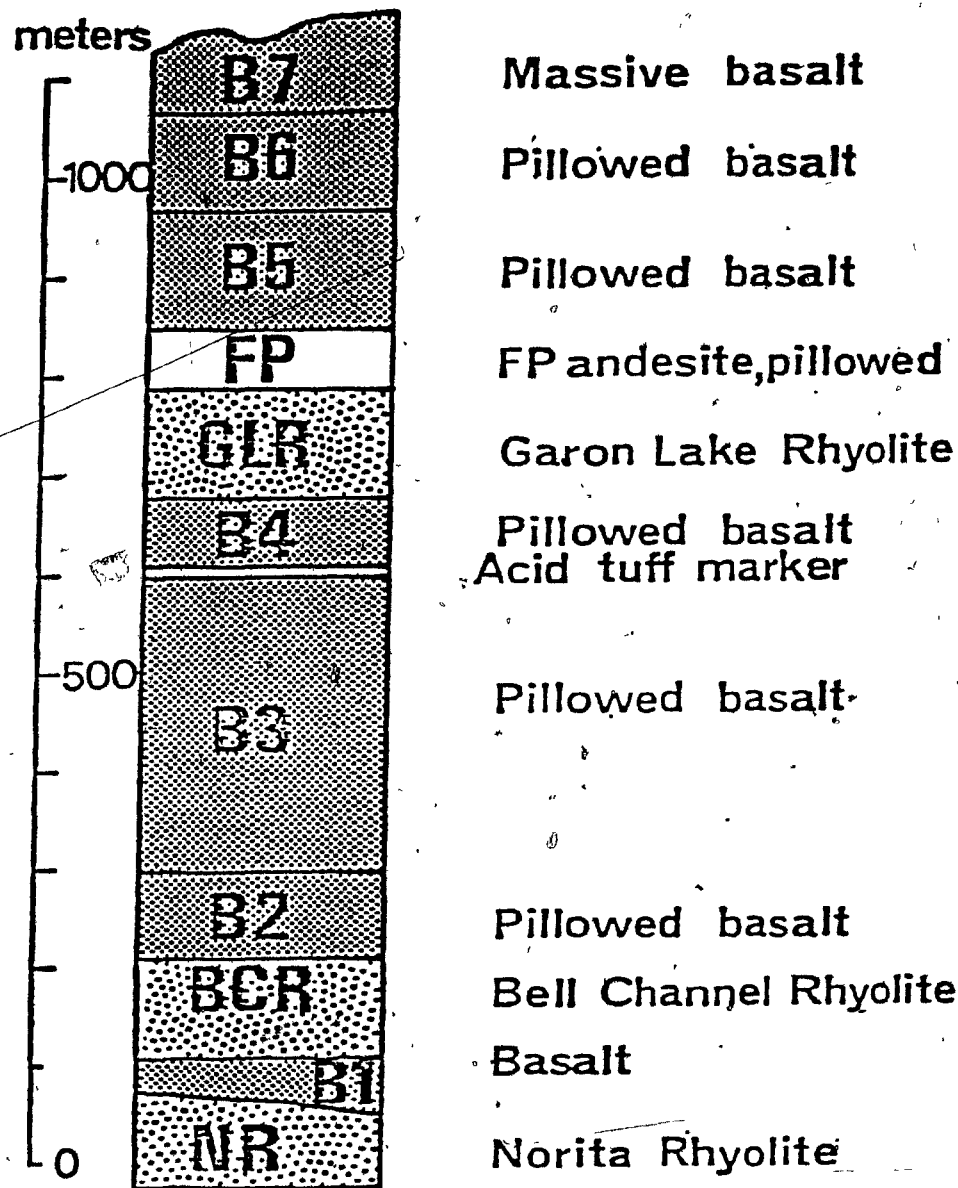


Figure 2.3 - Restored stratigraphic section through the extrusive volcanic rocks (after MacGeehan, 1979).

() ienced by the rocks is characterized by (1) the alteration of calcium feldspars to sodium feldspars, and (2) the alteration of pyroxenes to actinolite. Silicification, on the other hand, comprises fine-scale silicic veinlets (0.1-5.0mm) which cut through spilitized and non-spilitized basalt.

Intense alteration is found in basalts bordering both the upper and lower contact zones of gabbro sills. These basalts are typically bleached to a pale grey color and are strongly silicified.

MacGeehan (1979) showed that progressive alteration of the B3 basalts has resulted in a depletion of FeO and Fe_2O_3 and an enrichment in SiO_2 .

Basalts belonging to unit B4 exhibit the same general geochemical trends as the B3 basalts except that unit B4, as a whole, is more strongly silicified.

Basalts belonging to unit B2 are largely similar geochemically to those belonging to units B3 and B4.

Units B5, B6 and B7 also exhibit the same general trends as outlined for units B2, B3 and B4. The similarity in the trends between the two groups indicates that basalts B5, B6 and B7 have also been subjected to hydrothermal alteration, although it was essentially unrelated to hydrothermal activity in the Garon Lake geothermal system.

() On the other hand, the results of geochemical analyses of samples belonging to unit B1 do not comply with the trends established for the overlying units. The following two points

suggest possible explanations for the observed irregularities in the chemistry of this unit.

- (1) According to the stratigraphic column (Figure 2.2), unit B1 is overlain and underlain by the Bell Channel rhyolite and the Norita rhyolite, respectively. As a result, it is not clear whether the degree of differentiation experienced by this unit was analogous to that experienced by units B2 to B4.
- (2) Since it is located very close to the base of the stratigraphic column, it has undoubtedly been subjected to many phases of alteration. Judging by the mean silica content of this unit ($\%SiO_2 = 59.9$), it is certain that it has undergone intensive hydrothermal alteration between the time of deposition and the present. Similarly, it is equally certain that it has been subjected to intense potassic alteration as well ($\%K_2O = 0.67$).

In view of this, it is difficult to compare unit B1 with the rest of the overlying basalts. Consequently, this study will be restricted to units B2 through B7 since they have all experienced a similar degree of alteration. A further study of unit B1 is currently being carried out by MacLean (in preparation) at McGill University.

The Garon Lake rhyolite experienced a loss of SiO_2 and an addition of FeO and Fe_2O_3 . However, the geochemistry of the Norita and the Bell Channel rhyolites cannot be compared

to that of the Garon Lake rhyolite because of similar arguments to the ones presented above, concerning unit B1.

2.6 Interpretation of the Alteration in the Extrusive Rocks

Alteration of basaltic rocks involved the leaching of nearly all of the major elements and their replacement by $\text{SiO}_2 + \text{Na}_2\text{O}$ (MacGeehan, 1979). Leaching and enrichment of certain elements appears to be related to stratigraphic height. For instance, silicification increased with increasing stratigraphic height. In addition, the exchange of elements between the rocks and the fluid increased with increasing temperature of the fluid.

Chloritization of the Garon Lake rhyolite was accompanied by desilicification as well as enrichment in FeO and Fe_2O_3 .

This alteration developed because of the high permeability of the basalts. After the gabbro sills were emplaced and began to cool, heat flow was directed toward the basalts. Since these basalts were saturated with water, the heat exchange caused the fluid to heat up and circulate convectively from the margins of the sills outward through the basalts via the quartz-epidote structures which have been preserved in the rocks.

MacGeehan (1979) also established that silicification and chloritization were contemporaneous and that they shared the same fluid. Furthermore, he concluded that the geothermal system developed shortly after the volcanic rocks were laid down and dissipated before the overlying basalts were extruded.

Finally, given that the geothermal system terminated prior to the extrusion of unit B5 and other overlying units, MacGeehan (1979) was able to estimate that the hydrostatic pressure under which the geothermal system was operative was less than 600 bars and on the basis of the alteration mineral assemblage now present in these rocks, he estimated that the rock-fluid interaction occurred at $T < 400^{\circ}\text{C}$.

2.7 Structural History

The outcrops in this area form low-lying hills which strike roughly E-W and are bound by faults on both the east and west sides. The traces of the fault planes have been obliterated by glaciation and can only be recognized by the linear alignment of valleys.

Detailed structure of the area has been established by MacGeehan (1979) on the basis of mapping and determination of facing directions. The latter was evaluated on the basis of (1) pillow basalts (2) grading in the tuffaceous units (3) the arrangement of massive sulfide lenses in mineralized rhyolite and (4) the relationship of feeder dykes to overlying flow units.

Since all of the large and some of the small gabbro sills are fractionated, and because it has been established that the gabbro sills and the basalts were penecontemporaneous, the fractionation pattern of the sills was also used as a means of determination or confirmation of facing direction.

The strike of the rocks in this area is E-SE. They dip

vertically and commonly face northward. The latter is evident in outcrops along the Bell River as well as east of the Radiore fault.

There is evidence of folding in the area. The presence of a synclinal fold which plunges to the west and has an interlimb angle of 0° - 30° has been noted. It is bounded by a small N-S fault to the west, located between 8N,30E and 34N,27E, and the Radiore fault to the east. The folding is indicated by the sequence of B3-acid tuff-B4-Garon Lake Rhyolite-Feldspar porphyry units on the south limb and by the reverse pattern on the north limb. A thick, well fractionated sill intrudes the B3 unit on the south limb and has been traced to the north limb. On the basis of the position of the upper fractionated portion of the sill with respect to the B3 unit, and the reverse order of the sequence mentioned above, MacGeehan (1979) was able to establish a south-facing direction in this particular area.

An examination of the faults in the area has shown that there was considerable dip-slip movement along N-S faults. For instance, the dip-slip displacement across the fault extending from 8N,30E to 34N,27E on the south limb of the syncline was found to be greater than 750m with the east side moving up with respect to the west side. The large dip-slip movement is attributed to the vertical displacement of volcanics which were vertically inclined to begin with.

(In contrast to the above mentioned displacement along

N-S faults, the displacement of volcanics along the Radiore fault trending NW-SE had a significant strike-slip component. This is evidenced by an offset of approximately 400m of the Bell Channel rhyolite across the Radiore fault.

Finally, the development of N-S and NW-SE faults in the area is a consequence of the emplacement of the granodiorite pluton.

2.8 Metamorphism of the Volcanic Rocks

MacGeehan (1979) established that there were three stages of metamorphism in this area:

- (1) "burial" metamorphism comprising widespread hydrothermal alteration .
- (2) folding and regional metamorphism
- (3) contact metamorphism of rocks adjacent to the granodiorite pluton

The hydrothermal alteration was a low to medium grade metamorphic event which occurred fairly early in the history of the area. The alteration was characterized by spilitization and silicification of basalts and concomitant chloritization of rhyolites. The mineral assemblage produced as a result of this alteration was albite-actinolite-chlorite-epidote, which is characteristic of the greenschist facies.

This early stage of alteration was then followed by folding and regional metamorphism. Although most of the rocks in this area experienced greenschist facies metamorphism, certain rocks did experience some amphibolite facies metamor-

phism as evidenced by the presence of hornblende and spessartine garnet in their mineral assemblages.

Lastly, some of the volcanic rocks in this area, particularly those bordering the granodiorite pluton, were subjected to contact metamorphism as evidenced by the progressive mineral zonation from pyroxene hornfels in the inner zone, to hornblende hornfels in the middle zone, through to a partially degraded assemblage of albite-actinolite-chlorite-epidote in the outer zone.

In summary, virtually all of the rocks in this area have been affected by one or more phases of alteration. However, each phase is characterized by a specific mineral assemblage and it is therefore possible to determine the degree of alteration experienced by any given rock unit.

CHAPTER 3 - SULFUR GEOCHEMISTRY OF THE BASALTIC ROCKS

3.1 Introduction

The bulk of the sulfur within these basalts is believed to be contained in sulfide minerals, predominantly as pyrite. In view of this, it is worthwhile to discuss the crystal structure of this sulfide as well as the geochemistry of sulfur, in general.

According to Wedepohl (1978), sulfur in sulfides typically forms purely ionic bonds with ions of low charge of the most electropositive elements. However, the structure of pyrite is not truly ionic. The arrangement of atoms in pyrite is similar to that found in the sodium chloride structure except that the anion has been replaced by a covalently bonded pair of sulfur atoms whose interatomic distance is 2.14 Å. There are four S-S pairs per cell, each oriented along a different body diagonal. Each sulfur is co-ordinated by 1S and 3Fe resulting in an octahedron being formed about the S-S pair.

The behavior of sulfur in a magma is related to its physical and chemical properties. For instance, because of its bonding energy, sulfur ($r = 1.84 \text{ Å}$) will preferentially compete with oxygen ($r = 1.40 \text{ Å}$) to form compounds with Fe^{2+} in a magma. However, due to the limited solubility of sulfide liquids in silicate melts, unmixing will commonly occur (MacLean, 1969; Anderson, 1974). The separation process generally takes place during magma generation and is sometimes

evident in the occurrence of exsolved iron, nickel and copper sulfides within basalts. Furthermore, this unmixing can lead to the formation of economic ore deposits (Ewers et al., 1972; Hudson, 1972; Naldrett, 1973; Woodall et al., 1969).

3.2 Analytical Techniques

The preferred method for the determination of sulfur content in unknowns is the LECO method. Very few sulfur analyses have been done by X-ray fluorescence due to difficulties in achieving both accurate and even reproducible results. However, this study succeeds in establishing an analytical method for sulfur determination by XRF. Moreover, the study also demonstrates that X-ray fluorescence can produce reliable results. The analytical method, as it pertains to the XRF, consists of three stages. The first stage involves the identification of the sulfide phase in the rocks which are of interest. The second stage is the preparation of standards. Special care should be taken to ensure that the sulfide phase is ground uniformly prior to its addition to a given matrix. The grain size of both the sulfide phase and the matrix as well as the homogeneity of the resulting standard are critical to the achievement of accurate and reproducible sulfur values. The third stage of this analytical method is to set up a calibration curve which can be used to determine the amount of sulfur contained in an unknown sample. The following discussion is an introduction to the analytical techniques employed in this study.

All of the samples were analysed for sulfur with a Philips PW 1220 X-ray fluorescence spectrometer. A description of the sample preparation procedure is contained in Appendix I. A careful study of both the handspecimens and available polished sections showed that the only sulfur-bearing mineral present in the basalts was pyrite. Consequently, a set of standards was prepared by addition of finely ground pyrite to pulverized basalt. Details of the standard preparation procedure are also contained in Appendix I.

In addition to the analyses obtained from the XRF, several others have been done using the LECO analytical method. Some of the samples were analysed by Dr. C. Riddle of the Ontario Geological Survey using the Canmet certified standard SL-1. Other samples were also analysed by Dr. C. E. Rees of McMaster University.

The results of the X-ray fluorescence and LECO analyses are tabulated in Appendix II, or presented in the text.

Accuracy and precision calculations of both analytical methods are reported in Appendix I. The accuracy and precision of the XRF analytical method at a level of confidence of 95%, is 9.8% and 4.4%, respectively. The precision of the LECO analytical method is within 4.2% of the sulfur concentration.

3.2.1 Sulfur Determination by X-ray Fluorescence Spectrometry

To determine the sulfur content of unknowns, six standards, with sulfur concentrations covering the range of sulfur expected

()
()
in these rocks, were prepared. The same six standards were analysed several times. Each time that a set of six was analysed, the results were seen to represent a line on a graph. This line became more refined with each successive run, and eventually a line of best fit, or a calibration line as it is otherwise known, emerged. This calibration line is shown in Figure 3.1 and the following equation is derived from it.

$$\text{ppm } S_{\text{unk}} = X(5300 + 100) \text{ ppm}$$

where ppm S_{unk} is the amount of sulfur present in the unknown and X is the ratio of net counts per second of the unknown to the net counts per second of the standard. The value 5300 is the x-coordinate of the standard against which all of the unknowns were run and the value 100 is the x intercept representing the amount of sulfur initially in the basalt. Once this calibration line was established, the analysis of all the samples was begun. The results of these analyses are tabulated, in part, in column two of Table 3.1.

(
(
The analytical method outlined above works exclusively for samples of rocks which contain pyrite as the main or only sulfide-bearing mineral phase. Consequently, if the principal sulfide mineral was not pyrite, this calibration line would not give an accurate determination of sulfur content because of different mass absorption corrections. This has been tested by creating standards using other sulfide minerals such as

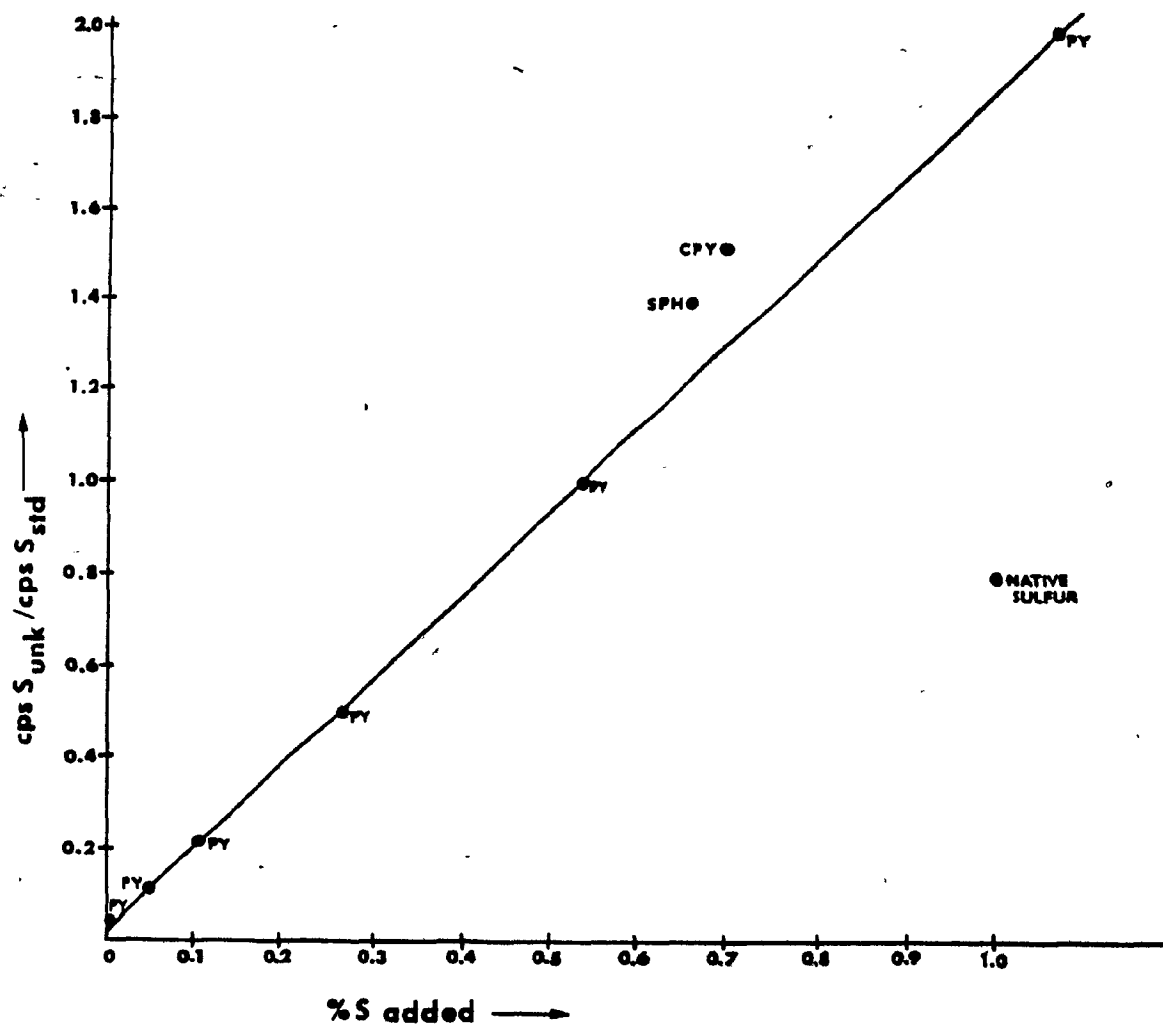


Figure 3.1 - Calibration line used to determine the sulfur content of unknown samples.

TABLE 3.1: Comparison of Results Obtained by XRF and LECO Analysis

Sample No.	%S(XRF)	%S(L.A.)*	%S(L.A.)*	%S(L.A.)**
AP-1	0.032	0.028	0.027	
AP-5	0.119	0.112	0.112	
AP-7	0.021	0.018	0.018	
AP-9	0.053	0.052	0.052	
AP-13	0.192	0.162	0.162	
AP-18	0.008	0.007	0.007	
AP-26	0.017	0.017	0.019	
AP-29	0.234	0.194	0.192	
AP-30	1.612	1.71	1.72	1.56
AP-31	0.466	0.454	0.450	
AP-38	0.169	0.143	0.140	
AP-39	0.013	0.014	0.013	
AP-41	0.007	0.009	0.009	
AP-42	0.086			0.063
AP-43	0.058			0.049
AP-44	0.040	0.039	0.040	0.035
AP-49	0.016			0.015
AP-50	0.008	0.009	0.009	
AP-55	0.016	0.013	0.014	
AP-64	0.005	0.007	0.007	
M-330	0.332			0.29
M-316	0.007			0.0075
M-317	0.077			0.077
M-655	0.017			0.012
M-38	0.019			0.015

*Ontario Geological Survey (Geoservices Laboratory)

**McMaster University

chalcopyrite and sphalerite. For instance, two per cent of each of these minerals was added to two separate aliquots of the same rock powder which was used in making the pyrite standards. After the powdered pellets were made, they were analysed on the XRF. The results of the analyses are presented in Figure 3.1 which shows that although these and the 2% pyrite standard contain the same amount of sulfur added, none of them are superimposed. The same appears to be true if one compares the 1% native sulfur to the 1% pyrite standard.

Therefore, in the simplest monomineralic cases, sulfur content can best be determined by creating standards containing only the one mineral which represents the dominant sulfur-bearing phase in a rock. However, in cases where there are many sulfur-bearing phases present, this particular analytical method would not be recommended.

3.2.2 Sulfur Determination by LECO Analysis

The LECO analytical method is currently thought to be the best technique for the determination of sulfur content. Hence, in an attempt to see whether the sulfur values obtained by X-ray fluorescence are indeed close to the true values, several of the samples previously analysed by XRF were selected for LECO analysis at McMaster University.

The analytical procedure of this method involves initial combustion of samples in a stream of oxygen in a LECO induction furnace. The sulfur dioxide which was produced was swept by the oxygen into a flask containing bromine water, where it

was oxidized to sulfate. The sulfate was then precipitated as barium sulfate and the sulfur content was determined gravimetrically at this stage. The results of these analyses are presented in column five of Table 3.1.

Additional analyses were carried out by the Ontario Geological Survey using the LECO analyser as well. The results of these analyses appear in columns three and four of Table 3.1.

In examining the results contained in columns three and four, one can see that there is good evidence for reproducibility of results. The precision, at a level of confidence of 95%, is 4.2% (Appendix 1). Moreover, there are two samples (ie. AP-30 and AP-44) which columns three, four and five have in common and the results of these two samples indicate that the interlab bias, expressed as an average difference, is 0.083 (Appendix 1).

3.2.3 Comparison of Results Obtained by Using Both Methods of Analysis

Comparing all four sets of results presented in Table 3.1, one can see that, with few exceptions, there is no significant difference between values. In fact, most values seem to lie remarkably close to one another.

Figure 3.2 is a graphic illustration of the relationship between values obtained as a result of both methods of analysis. The sulfur content determined by LECO analysis is plotted as the abscissa and the sulfur content determined by XRF is plotted as the ordinate. One high sulfur value repre-

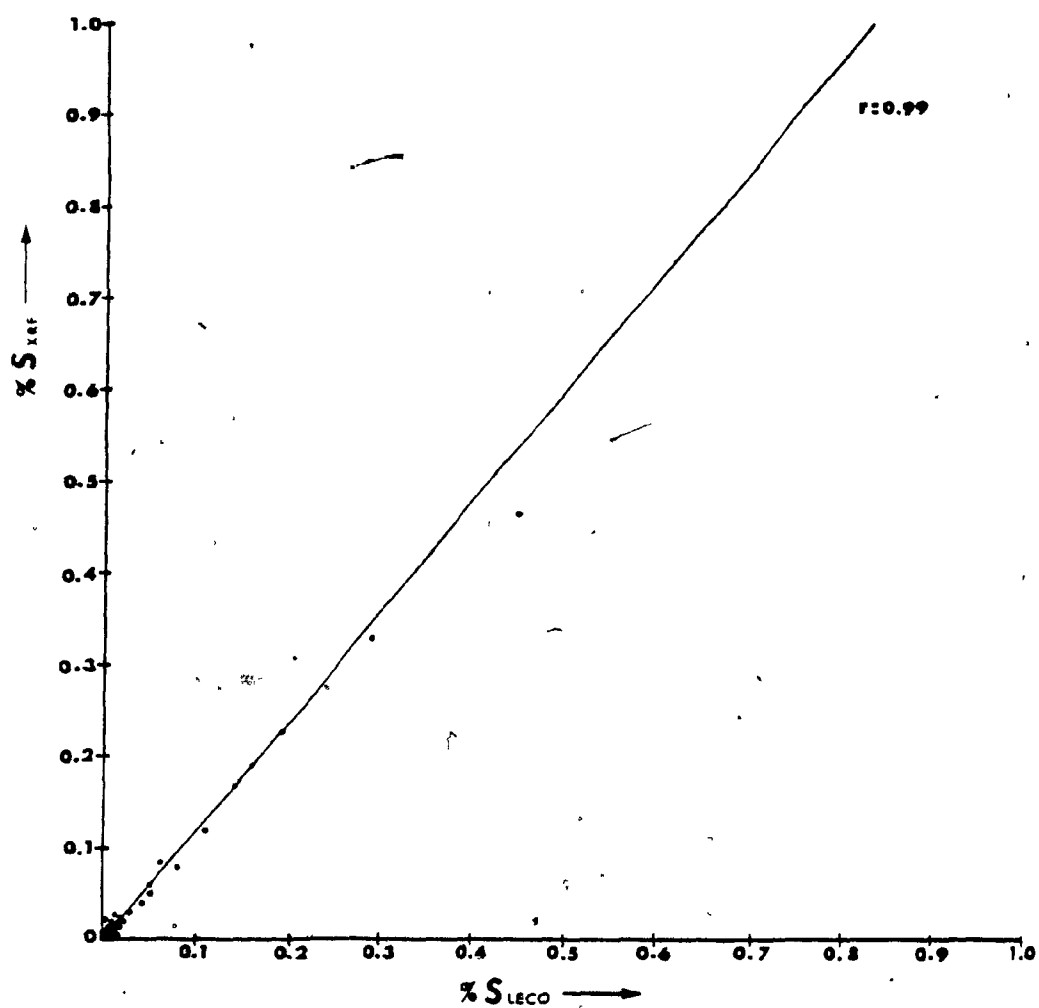


Figure 3.2 - Plot of XRF versus LECO results.

sentative of sample AP-30 is not shown. The solid line is a computed regression line for the case in which y is considered the dependent variable and x the independent variable. The calculated correlation coefficient is 0.998. Therefore, it is concluded that there is good correlation between the two sets of values.

3.3 Bulk Sample Analysis by X-ray Fluorescence

Approximately 50 kilograms of sample were collected from one sample location and subsequently sub-divided into 46 smaller samples, each weighing about one to two kilograms. The reason for collecting such an unusually large amount of sample was to test the magnitude of variation of sulfur concentration throughout this bulk sample. In so doing, one would then be able to determine whether the samples which had been collected during the course of this study could be considered to be representative samples of each of the field areas sampled. The results of the bulk sample analysis are presented in Table 3.2. On the basis of these results, the range of the sulfur concentration is 122 ppm and the mean and corresponding standard deviation are 79.4 and 30.3 ppm, respectively. The relative deviation in sulfur concentration at this level is 38%. Unfortunately, the concentration of sulfur in this bulk sample is low relative to all of the other samples. Consequently, it is difficult to estimate the magnitude of variation in sulfur concentration at higher levels.

TABLE 3.2: Variation of Sulfur Concentration Within a BulkSample

Sample No.	ppm S
AP-45	138
AP-46	90
AP-47	69
AP-48	58
AP-49	164
AP-50	80
AP-51	58
AP-52	159
AP-53	80
AP-54	64
AP-55	164
AP-56	64
AP-57	95
AP-58	64
AP-59	85
AP-60	85
AP-61	85
AP-62	75
AP-63	58
AP-64	45
AP-65	106
AP-66	138
AP-67	101
AP-68	74
AP-69	58
AP-70	80
AP-71	58
AP-72	74
AP-73	74
AP-74	80
AP-75	53
AP-76	53
AP-77	69
AP-78	90
AP-79	48
AP-80	106
AP-81	53
AP-82	69
AP-83	74
AP-84	58
AP-85	54
AP-86	54
AP-87	42
AP-88	74
AP-89	58
AP-90	75

3.4 Sulfur Distribution in Basaltic Rocks

The distribution of sulfur in basalt samples within each of the units is shown in Table 3.3. Individual analyses appear in Appendix II, although the overall distribution of values between the different units and between least altered and altered basalts within those units is presented in Table 3.3. In examining the data presented in the first two columns of Table 3.3, one can see that there is a noticeable difference in the mean sulfur content between units and, that the mean sulfur content increases from unit B3 through B4 and up to B5 and then decreases through B6 down to B7. Moreover, there is the added difference between the mean sulfur content of least altered and altered basalts. Generally, the mean sulfur contents of the altered basalts are consistently higher than those of the least altered basalts. The sole unit which takes exception to this pattern is unit B7 in which the sulfur content of the least altered basalt is greater than the mean sulfur content of the altered basalts. However, this may be due to the fact that the one sample which constitutes least altered basalt is fairly high in sulfur and consequently, may not be representative of the sulfur content of this group. Since it is sometimes difficult to find local areas of least altered rock in a region which is dominantly altered, it is unfortunate that the one sample which was collected from unit B7 is not entirely reliable. Despite this, however, there is a strong indication that altered basalts

TABLE 3.3: Distribution of the Mean Sulfur Content and Corresponding Standard Error of the Mean in each Unit

Unit	Least altered & altered	Least altered	Altered
B2	914 \pm 258 (14)	780 \pm 285 (10)	1246 \pm 592 (4)
B3	695 \pm 185 (43)	598 \pm 202 (20)	780 \pm 301 (23)
B4	1428 \pm 310 (44)	1153 \pm 285 (24)	1759 \pm 591 (20)
B5	1915 \pm 389 (15)	1718 \pm 461 (9)	2210 \pm 722 (6)
B6	1200 \pm 637 (9)	583 (1)	1278 \pm 717 (8)
B7	330 \pm 77 (6)	398 (1)	317 \pm 93 (5)

The numbers in parentheses indicate the number of basalt samples.

generally contain more sulfur than least altered basalts within a given unit. In addition, both the least altered basalts and the altered basalts retain the above mentioned pattern in which the mean sulfur content increases from a certain value in unit B3 to a maximum in unit B5 and then decreases again through units B6 and B7.

3.5 Correlation Between Sulfur and Iron

The relationship between sulfur and iron is illustrated in Figures 3.4 and 3.5. In Figure 3.4a, the sulfur and iron contents of each individual sample are shown. A few very high values do not appear on the graph. However, the results of all the analyses performed on each of the samples are contained in Appendix II. The overall pattern of the data points in Figure 3.4a is suggestive of a trend of increasing sulfur with the total iron content of the rocks.

The sulfur in these basalts appears to have a log normal distribution as shown in Figure 3.3 (a similar plot to that used by Naldrett et al., 1977). The gap in the middle of Figure 3.3b is not considered to be critical because the height of the histogram in that region is four units on one side and two on the other. In the case of a Poisson distribution, this corresponds to a standard deviation of 2 and 1.4, respectively. Thus, a value of zero is not unlikely. However, even if the distribution is bimodal, it is still likely that each of the populations is reasonably log normally distributed to justify the calculation of the geometric mean of

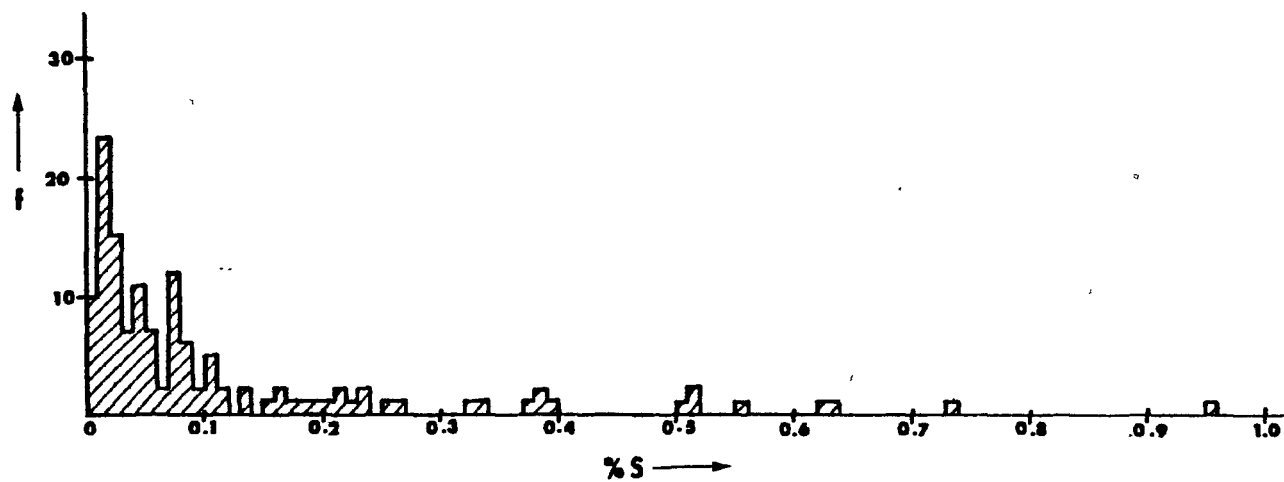


Figure 3.3a - Frequency diagram illustrating the distribution of sulfur analyses.

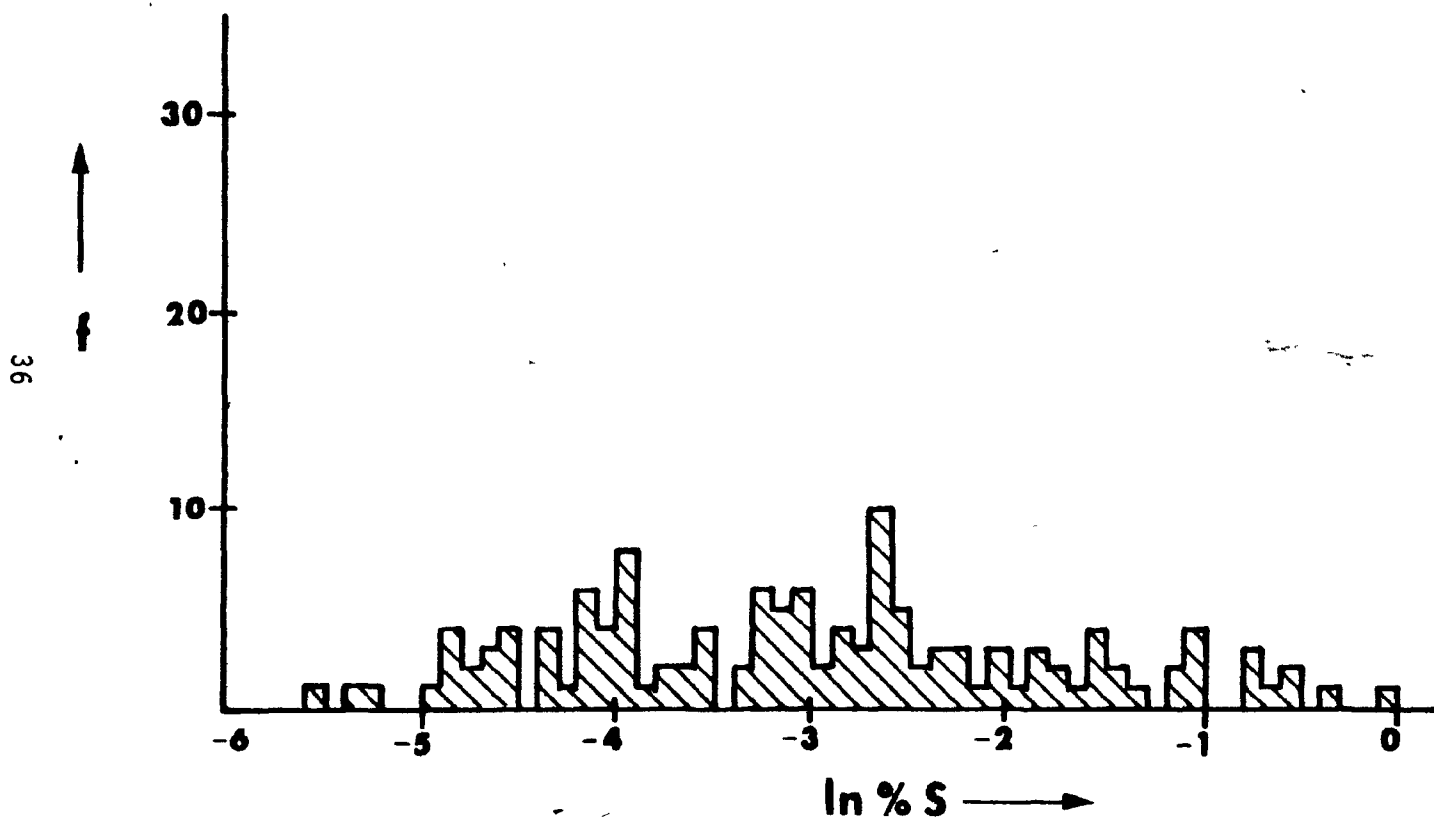


Figure 3.3b - Frequency diagram illustrating the distribution of sulfur analyses.

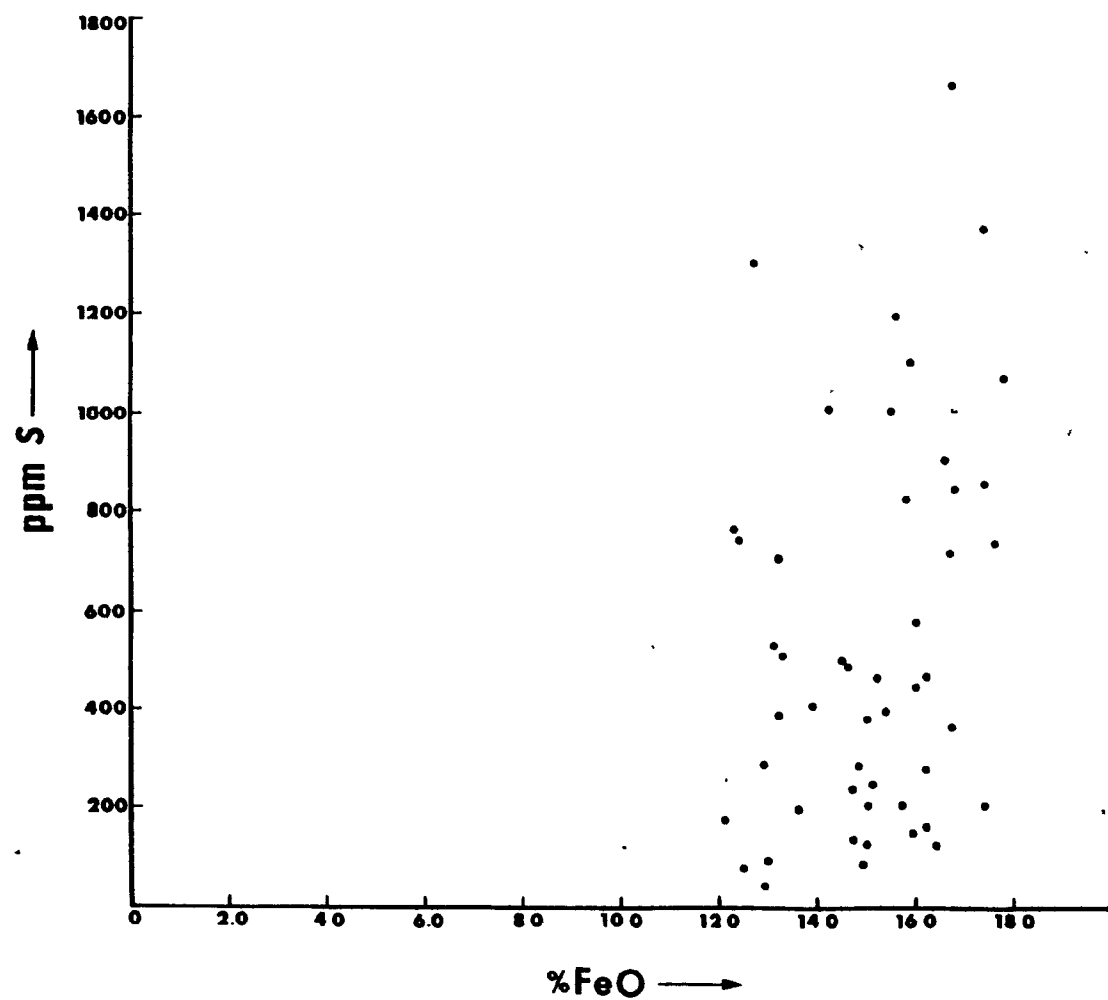


Figure 3.4a - Plot of sulfur versus iron content of least altered basalts.

sulfur. Moreover, a bimodal distribution, if it exists, is likely a reflection of the generally lower sulfur content of the least altered rocks as compared to that of the altered rocks as demonstrated in the previous section. In light of the above discussion, the trend observed in Figure 3.4a becomes more evident if, on the assumption that the distribution is log normal, the geometric means of sulfur are plotted against the average total iron content of each basalt group as shown in Figure 3.4b. The solid line in the above mentioned figure is drawn on the basis of the location of the mean data points of the different basalt units comprising the Watson Lake Group. These mean data points were calculated using all available iron and sulfur values. A list of the mean iron and sulfur contents of each unit is presented in Table 3.4. In examining the data presented for the least altered basalts in both Table 3.4 and Figure 3.4b, one can see that the pattern exhibited by the sulfur in units B3 to B7 corresponds exactly to that exhibited by iron. The iron contents of these units reflect an iron enrichment trend within these basalt flows as noted by MacGeehan (1979). The significance of the fact that the sulfur contents parallel increases and decreases in iron contents in the least altered rocks is that the relationship between iron and sulfur is a primary one and possibly related to sulfur saturation in the melt (to be discussed later).

Figure 3.5a illustrates the relationship between sulfur

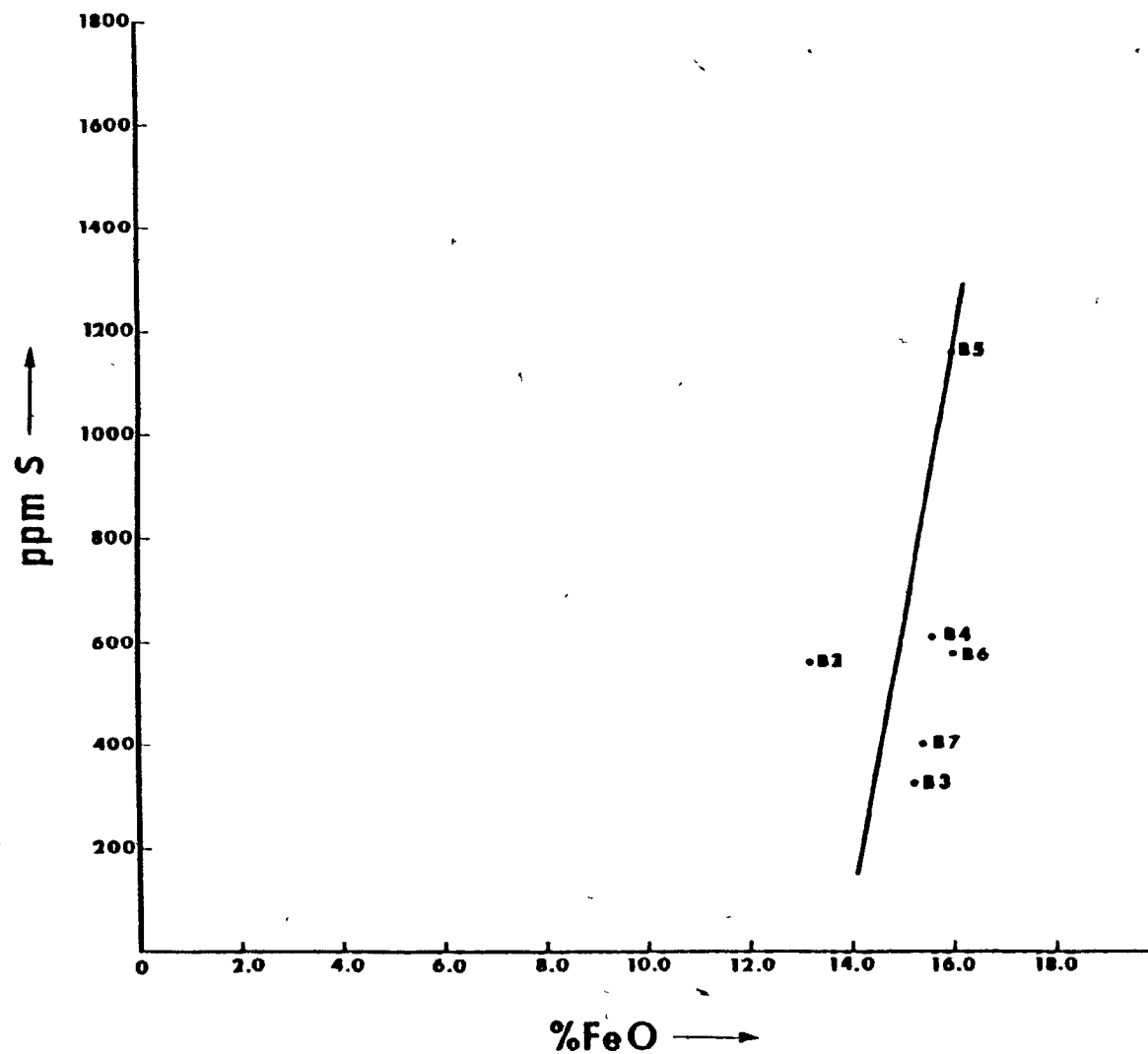


Figure 3.4b - Plot of the geometric mean of sulfur against the arithmetic mean of iron for least altered basalts.

TABLE 3.4: Average Fe^{*} and S^{**} Compositions of the Volcanic Rocks

Least altered basalts			Altered basalts		
Unit	%FeO [*]	S(ppm) ^{**}	Unit	%FeO [*]	S(ppm) ^{**}
B2	13.21	562	B2	12.08	649
B3	15.20	318	B3	11.97	302
B4	15.55	607	B4	10.71	647
B5	16.07	1158	B5	15.31	1755
B6	15.99	584	B6	14.51	724
B7	15.14	398	B7	12.09	270

*Total iron expressed as FeO

**Geometric means of sulfur

and iron contents in altered basalts. The trend between these two elements becomes more evident if the geometric means of sulfur are plotted against the average total iron content of each basalt group, as shown in Figure 3.5b. Since all of the samples represented in Figure 3.5b are altered, it is difficult to determine whether the relationship between iron and sulfur is a primary one or a secondary one. Therefore, in an attempt to resolve this problem, the igneous component of iron as well as that of sulfur was stripped from the altered basalts as shown in Table 3.5. The data presented in this table reveal that the unit which lost the greatest amount of iron (ie. B4) contains the least amount of secondary sulfur. Similarly, the unit which lost the least amount of iron (ie. B5) contains the greatest amount of secondary sulfur. This indicates that secondary sulfur distribution is controlled by the iron content of the rocks and, that the trend illustrated in Figure 3.5b is the result of a secondary alteration effect superimposed upon a primary igneous relationship.

3.6 Juvenile Sulfur Content of Basalts.

In order to estimate the amount of sulfur present in non-hydrothermally altered basalts in the study area, only least altered, submarine samples were used. Table 3.6 lists these basalts together with their respective sulfur contents. On the basis of the data presented in Table 3.6, the average

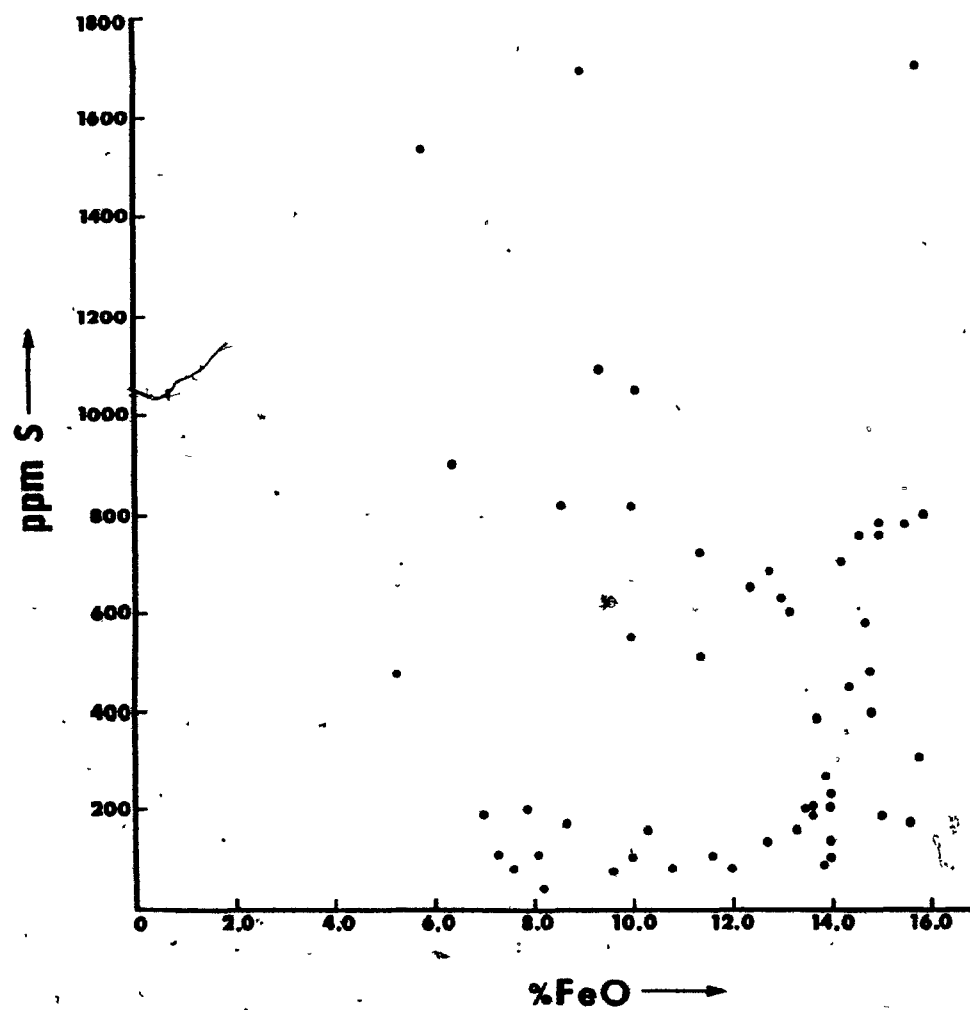


Figure 3.5a - Plot of sulfur versus iron content of altered basalts.

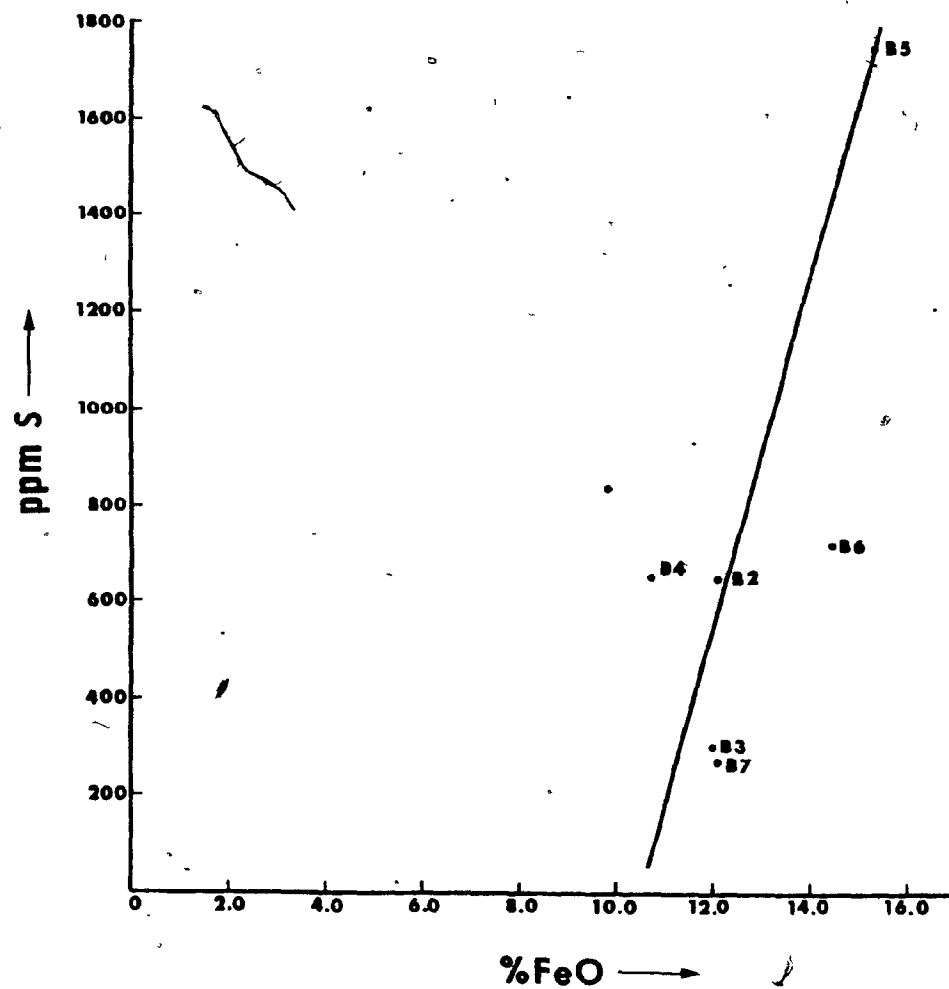


Figure 3.5b - Plot of the geometric mean of sulfur against the arithmetic mean of iron for altered basalts.

TABLE 3.5: Losses and Gains of FeO^{*} and S^{**} during Alteration
as Indicated by the Differences in these Components
Between Altered and Least Altered Basalts

Unit	%FeO [*]	S(ppm) ^{**}
B2	-1.13	87
B3	-3.23	—
B4	-4.84	40
B5	-0.76	597
B6	-1.48	140
B7	-3.05	—

* Total iron expressed as FeO.

** Geometric means of sulfur.

TABLE 3.6: Sulfur Content of Least Altered Submarine Basalts

Unit	Sample No.	S(ppm)
B2	M319	201
	M584	3291
	M322	392
	M585	747
	M317	770
	M569	509
	M321	710
	AP33	413
	AP34	477
	AP35	297
B3	M310	278
	M305	133
	M19	465
	M307	716
	M343	906
	M309	160
	M9	2152
	M308	3858
	M313	368
	M306-2	93
	M329	385
	M312	848
	M18	293
	M306-1	48
	M3	238
	AP3	175
	AP7	207
	AP36	408
	AP37	101
	AP39	133
B4	M92	2205
	M372	1670
	M89	210
	M256	1198
	M253	472
	M1	450
	M252	5109
	M350	253
	AP9	530
	AP12	292
	AP13	1919
	AP14	1309
	AP17	80

B4	AP20	832
	AP21	498
	AP23	1113
	AP24	2327
	M252-2	5109
	M395	213
	M398	490
	AP25	138
	AP26	170
	AP27	1018
	AP40	58
B5	M48	1076
	M85	742
	M47	1383
	M383	3811
	M384	1012
	M386	2528
	M388	101
	M389	3949
	AP42	864
B6	AP43	583
B7	AP44	398

sulfur content of 65 samples is 982 ± 150 ppm.

According to Moore and Fabbi (1971) the outer glassy part of submarine erupted basalt contains 800 ± 150 ppm S. This has been confirmed by Moore and Schilling (1973) who found that the average sulfur content of the outer 2cm of pillows is 843 ppm. Mathez (1976) also reports concentrations of sulfur dissolved in glasses and his values range from 1000 to 1800 ppm S. Other data from investigations carried out by MacLean (1977) show that sulfur analyses in basalt glasses ranged from 930 to 1160 ppm S. Finally, the sulfur content of basaltic glasses obtained by Czamanske and Moore (1977) ranges from 850 to 1400 ppm S.

3.7 Factors Controlling the Solubility of Sulfur

The solubility of sulfur in basaltic magmas depends, to a large extent, upon four parameters: (1) composition, in particular iron and silica contents (2) temperature (3) sulfur fugacity and (4) oxygen fugacity (Fincham and Richardson, 1954; Haughton et al., 1974; Shima and Naldrett, 1975).

Abraham et al. (1960) determined experimentally that an iron silicate melt is capable of dissolving more sulfur than any other melts. Later, MacLean (1969) demonstrated experimentally that the activity of FeO exerts a strong influence on the solubility of sulfur. In view of these experimental results, it is concluded that the iron content has a strong positive influence on the sulfur content of a magma. In

addition, Haughton et al. (1974) showed that the sulfide capacity of a melt decreases as the silica content increases. This indicates that the effect of increasing silica on the sulfide capacity of a melt is opposite to that of increasing iron.

The second factor affecting the solubility of sulfur is temperature. Experimental evidence indicates that a decrease in temperature causes a decrease in the solubility of sulfur. According to Haughton et al. (1974), the solubility of sulfur decreases by a factor of ten as the temperature drops from 1200°C to 1040°C, assuming the ratio of f_{O_2} and f_{S_2} is kept constant. However, as the magma cools, the values of f_{O_2} and f_{S_2} change. Hence, it is often difficult to estimate the effect of temperature on the solubility of sulfur without taking into consideration the oxygen and sulfur fugacities as well.

Regarding sulfur fugacity, an increase in sulfur solubility results as f_{S_2} increases. This has been confirmed by Haughton et al. (1974). Nagamori and Kameda (1965) suggested that the probable value of $\log f_{S_2}$ for most mafic magmas at 1200°C lies in the range of -1 ± 1.5 atm.

The fourth factor which influences the solubility of sulfur is oxygen fugacity. It has been found that the solubility of sulfur decreases with increasing f_{O_2} (MacLean, 1969; Haughton et al., 1974). According to Fudali (1965).

experimentally determined values of f_{O_2} for basalts range from $10^{-8.5}$ to $10^{-6.4}$ atm at 1200°C . Furthermore, Katsura and Nagashima (1974) have shown that at 1200°C , most of the sulfur in a basaltic melt occurs as dissolved sulfide at oxygen partial pressures below 10^{-8} atmospheres, and as dissolved sulfate at oxygen partial pressures above 10^{-8} atmospheres.

Pressure affects the solubility of sulfur indirectly since a magma emplaced at a confining pressure which is less than the vapor pressure of the volatile components will lose a substantial amount of sulfur, largely in the form of SO_2 .

In summary, the principal factors affecting the solubility of sulfur are iron and silica contents, temperature, sulfur fugacity and oxygen fugacity. Furthermore, experimental evidence indicates that increasing the activity of FeO , temperature and f_{S_2} while decreasing f_{O_2} and silica content causes an increase in the solubility of sulfur in a melt.

3.8 Solubility and Saturation of Sulfur in Basaltic Rocks

There is general agreement that modern mid-ocean ridge basalts form by partial melting of the mantle at a depth of 30 to 100 km and a temperature range of 1250°C to 1300°C . According to MacLean (1969), all available sulfides would be melted well before silicate melting began. As more and more silicate melt is formed, the sulfide melt will continually

dissolve into it. The dissolution of sulfides in silicate liquids is accomplished by displacing oxygen bonded to ferrous iron. Nockolds (1966) calculated bond energies for various elements present in the crust and found that the metal-oxide to metal-sulfide ratio for Fe^{2+} is 1.82. This value is lower than that obtained for any other major cations and indicates the preference of sulfur for displacing oxygen bonded only to ferrous iron in a magma. However, because the ionic radius of sulfur (1.84\AA) is greater than that of oxygen (1.40\AA), sulfur cannot substitute easily for oxygen in silicate systems. Hence, the solubility of sulfur in magmas is limited.

The presence of sulfide globules in present day mid-ocean ridge basalts is evidence of the existence of an immiscible sulfide liquid. Therefore, the occurrence of these globules in fresh submarine basalts is indicative of sulfur saturation in the melt. The hypothesis that most, if not all, submarine basalts are saturated with sulfur prior to eruption is not a novel one. Moore and Calk (1971), Vakhrushev and Prokoptsev (1972) and Anderson (1972) were among the first to note the presence of sulfide globules in Cenozoic basalts. Later, careful studies carried out by others (Kanehira et al., 1973; Moore and Schilling, 1973; Anderson, 1974; Mathez, 1976; Mathez and Yeats, 1976; MacLean, 1977; Czamanske and Moore, 1977) revealed that modern submarine basalts generally contain exsolved sulfides in their

vesicles, indicating that the basaltic melts were saturated with respect to sulfur at the point of eruption and quenching on the sea floor.

3.9 Discussion

Figure 3.6 illustrates the relationship between sulfur and total iron content. Line A corresponds to the data obtained from the Juan de Fuca Ridge by Mathez (1976). Line B corresponds to the data obtained from the Mid-Atlantic Ridge by Czamanske et al. (1977). Both these lines represent fresh submarine basalts which were quenched at moderate pressures (~ 500 atm). Curve C corresponds to Naldrett & Goodwin's (1977) data obtained from the Blake River Group rocks which comprise part of the Abitibi greenstone belt in northeastern Ontario. This curve represents various Archean volcanic rocks including altered basalts, some andesites, dacites and rhyolites. These rocks are submarine and were probably quenched at similar pressures to those investigated by Mathez (1976) and Czamanske et al. (1977). Curve D is an experimental curve obtained at 1200°C and 1 atm by Haughton, Roeder and Skinner (1974). Line E corresponds to the data collected by the author. This line represents only the least altered ($\text{wt.}\% \text{SiO}_2 < 52.0$) Archean, submarine ($P \sim 500$ atm) basalts from the Watson Lake Group which is part of the Abitibi greenstone belt in Québec. Lines A and B and curve D illustrate two important points: (1) the sulfur

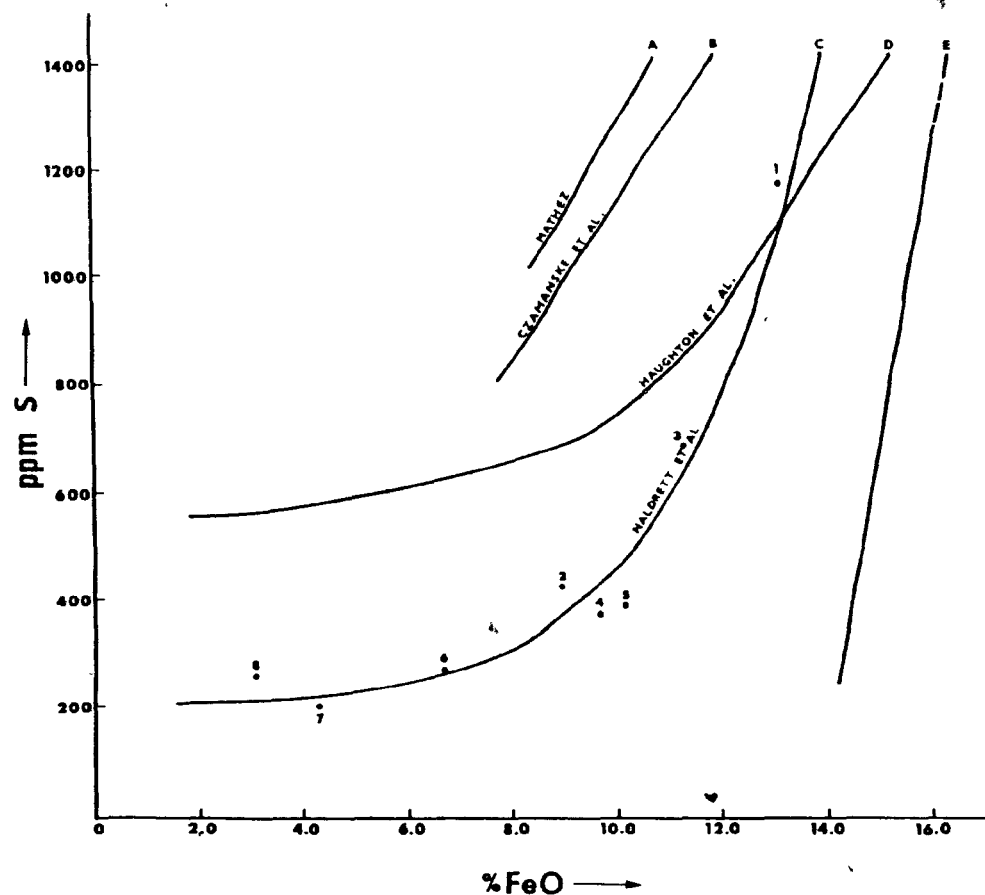


Figure 3.6 - Plot of sulfur concentration versus iron content for Archean basaltic rocks (curve E). Shown for comparison are curve A determined for natural submarine basalt from the Juan de Fuca Ridge by Mathez (1976); curve B determined for natural submarine basalt from the mid-Atlantic Ridge by Czamanske & Moore (1977); curve C determined for natural submarine volcanic rocks by Naldrett & Goodwin (1977); and curve D which is an experimental curve obtained at 1200°C and 1 atm by Haughton, Roeder & Skinner (1974).

content of basalts increases with increasing total iron content (2) the sulfur content is higher in basalts quenched at moderate pressures (~ 500 atm) as compared to that in basalts quenched at low pressures (1 atm). In addition, lines A and B represent a close approximation of the sulfide saturation trend for modern submarine basalts whereas curve D represents a basaltic sulfide saturation trend obtained experimentally at 1200°C and 1 atm.

Experimental evidence presented by Haughton et al. (1974) indicates that the sulfur content of basalts increases with increasing total iron content. The data of Mathez (1976) and Czamanske et al. (1977) confirm the positive correlation between sulfur and iron, although the levels of sulfur in their submarine basalts are higher than those in Haughton's (1974) experimental basalts. A likely reason for the high sulfur levels is pressure (Moore & Schilling, 1973). The sulfur levels obtained by Mathez (1976) and Czamanske (1977) appear to be representative of Cenozoic submarine basalts. In examining the data presented for Archean submarine basalts (line E) and that presented for modern submarine basalts (lines A and B), one can see that the Archean rocks have lower sulfur levels than the younger rocks. Moreover, there is less dependence of sulfur on iron in Archean basalts as compared to that in the younger rocks. A comparison of Archean and Cenozoic basalts, if it were valid, would indicate that the older rocks are clearly undersaturated.

Naldrett & Goodwin (1977) analysed various types of Archean volcanic rocks including altered and least altered basalts, some andesites, dacites and rhyolites and plotted the results of all these analyses on an FeO-S diagram as shown in Figure 3.6 (curve C). Points one through four each represent a group of analyses obtained from basalts. Points five and six each represent a group of andesites, point seven represents a group of dacites whereas point eight corresponds to a group of rhyolites. If points five through eight are indeed andesites, dacites and rhyolites, then one cannot plot them all on one curve, nor can one plot them on the same curve with basalts. The reason for this is that the sulfide capacity of a melt decreases with increasing silica content as discussed earlier in Section 3.7. In addition, recent analyses of rhyolites from the Matagami area confirm the fact that these rocks generally contain far less sulfur than the basalts (see Appendix II). Hence, the bottom portion of Naldrett & Goodwin's curve is unreliable on this basis. Points one through four, if they were representative of fresh or merely least altered basalts, could be plotted on an FeO-S diagram. However, closer inspection of Naldrett & Goodwin's analytical data suggests that their basalts include both least altered and altered rocks. Fresh metabasalts typically contain 48-52% SiO₂ whereas hydrothermally altered samples show a progressive increase in silica content (MacGeehan, 1979; MacGeehan and MacLean, 1980b). In view of

this, the upper portion of Naldrett & Goodwin's curve is not entirely reliable either. Naldrett & Goodwin (1977) also presented a diagram to show that the relationship between iron and sulfur in their rocks is similar to that obtained experimentally by Haughton et al. (1974). They were able to do this by plotting the arithmetic means of sulfur for each group against the respective mean FeO contents. Having established in their paper that the wide ranges of sulfur contents in their rocks make the arithmetic mean a poor estimator of the mean sulfur content of each group, it is not clear why they proceeded to use the arithmetic means, especially since they had determined the geometric means of sulfur for each group of rocks for that very reason. Nevertheless, by plotting the arithmetic mean of sulfur against the mean iron content for each group, they coincidentally obtained a curve which was slightly offset from the experimental curve obtained by Haughton et al. (1974). Consequently, Naldrett & Goodwin (1977) concluded that their Blake River Group rocks were probably saturated with respect to sulfur. This conclusion is obviously invalid on the basis of the above discussion. Furthermore, in another paper, Naldrett, Goodwin, Fisher & Ridler (1978) present more analyses of various types of Archean rocks from the same general area and compare them to the trend shown by curve C. Using an identical approach to that taken in the 1977 paper, they draw conclusions concerning sulfur saturation of the rocks

based on a comparison of these latest results with the trend that they showed for the Blake River Group rocks (curve C). These conclusions are somewhat erroneous since curve C, which is the basis of their comparisons, is invalid. A final point concerning Naldrett et al.'s (1977, 1978) papers is that their andesites, dacites and rhyolites may well be saturated but only because they are andesites, dacites and rhyolites and not on the basis that they can be fitted smoothly onto the lower portion of a basalt curve. Sulfur saturation levels decrease progressively as the composition of a melt varies from basaltic to rhyolitic as demonstrated by Haughton et al. (1974). Consequently, one should be able to produce a smooth curve, such as the one that Naldrett et al. (1977) produced, if one plots all of these rock types on one curve.

The results of the present study (curve E) indicate that hydrothermal alteration added sulfur to the altered rocks and depleted them of iron. Since the basalts of the present study are, in many ways, similar to the ones studied by Naldrett et al. (1977, 1978), the author suspects that if the lower portion of curve C were eliminated, as it should be, and if the upper portion of this curve were re-evaluated by considering only the least altered rocks, then the resulting line would be offset to the right of its present position while the slope would become slightly steeper. This is based on the likely assumption that the process of alteration operative on the Archean basalts of the Watson

Lake Group is similar to that operative on the Archean basalts of the Blake River Group. If this assumption is valid, then the resulting line for Naldrett's Blake River Group basalts would be very similar to line E.

3.10 Conclusion

The sulfur content of basaltic rocks from the Matagami area is highly variable. However, the mean sulfur content of the units comprising the Watson Lake Group increases from unit B3 through B4 to a maximum in B5 and then decreases through B6 to B7.

There is an added difference between the mean sulfur content of least altered and altered basalts. In all but one unit, the mean sulfur values of the altered basalts are consistently higher than those of the least altered basalts.

Increases and decreases in sulfur content of least altered basalts parallel increases and decreases in total iron content. This indicates that the relationship between iron and sulfur is a primary one, possibly related to sulfur saturation in the melt.

Addition of sulfur to the altered basalts reflects the amount of iron lost as a result of hydrothermal alteration. The unit which lost the greatest amount of iron contains the least amount of secondary sulfur whereas the unit which lost the least amount of iron contains the greatest amount of secondary sulfur. This suggests that secondary sulfur distribution is controlled by the iron content of the rocks.

CHAPTER 4 - SULFUR ISOTOPE DETERMINATION

4.1 Introduction

Sulfur has four isotopes: ^{32}S , ^{33}S , ^{34}S and ^{36}S . Of all of these, ^{32}S and ^{34}S are the most abundant (ie. $^{32}\text{S}=95.02\%$, $^{34}\text{S} = 4.2\%$). Due to the differences in mass, these isotopes can be segregated in nature. The heavier ^{34}S isotopes have a tendency to form S^{6+} ions and are fractionated rather strongly into sulfates. The lighter, ^{32}S isotopes, on the other hand, tend to form S^{2-} ions and are fractionated more into sulfide minerals and aqueous and gaseous sulfide species.

The determination of isotopic composition is accomplished by comparing the ratio of sulfur isotopes in an unknown to the ratio of isotopes in a known standard. All meteorites are characterized by the same sulfur isotope ratio. Thus, by convention, the isotopic composition of troilite in the Canon Diablo meteorite is taken as a standard. Troilite (FeS) has a very constant $^{34}\text{S}/^{32}\text{S}$ ratio of 0.0450045 (Ault & Jensen, 1963). Knowing this, the $\delta^{34}\text{S}$ value of unknown samples can be determined using the following mathematical expression:

$$\delta^{34}\text{S}(\text{per mil}) = \frac{(^{34}\text{S}/^{32}\text{S})_{\text{sample}} - (^{34}\text{S}/^{32}\text{S})_{\text{std}}}{(^{34}\text{S}/^{32}\text{S})_{\text{std}}} \times 10^3$$

Positive $\delta^{34}\text{S}$ values denote more ^{34}S than in the meteorite.

Mantle material is considered to be of the same isotopic composition as the meteorites. Therefore, sulfur derived

from the mantle is expected to have $\delta^{34}\text{S}$ equal to zero. Magmatic sulfides should also have $\delta^{34}\text{S}$ values close to zero.

Present day seawater has a uniform isotopic composition of +20 per mil. Virtually all of the sulfur in seawater is in the form of aqueous sulfates. On the basis of the data presented in Figure 4.1, sulfides formed in equilibrium with this seawater are expected to be negative at $T < 400^\circ\text{C}$. However, because the $\delta^{34}\text{S}$ values of seawater varied between +10 and +30 per mil from the base of the Cambrian to the present (Ohmoto et al., 1979), it is expected that the total range of $\delta^{34}\text{S}$ values of the resulting sulfides would be greater for any given temperature.

Aside from the influence of the isotopic composition of seawater, $\delta^{34}\text{S}$ values of sulfide minerals occurring in hydrothermally altered rocks have been shown to result from the interaction between several important inorganic parameters. Sakai (1968) and Ohmoto (1972) demonstrated that the chemistry of the ore-forming solutions (ie. aqueous sulfur species, f_{O_2} , pH and T) have a strong effect on the $\delta^{34}\text{S}$ values of hydrothermal minerals.

According to Ohmoto (1972), H_2S is an important aqueous species at low pH and low f_{O_2} . However, as the pH of the fluid increases, H_2S becomes less stable and HS^- becomes the predominant sulfur species. As pH continues to increase, S^{2-} eventually becomes the most stable species in solution.

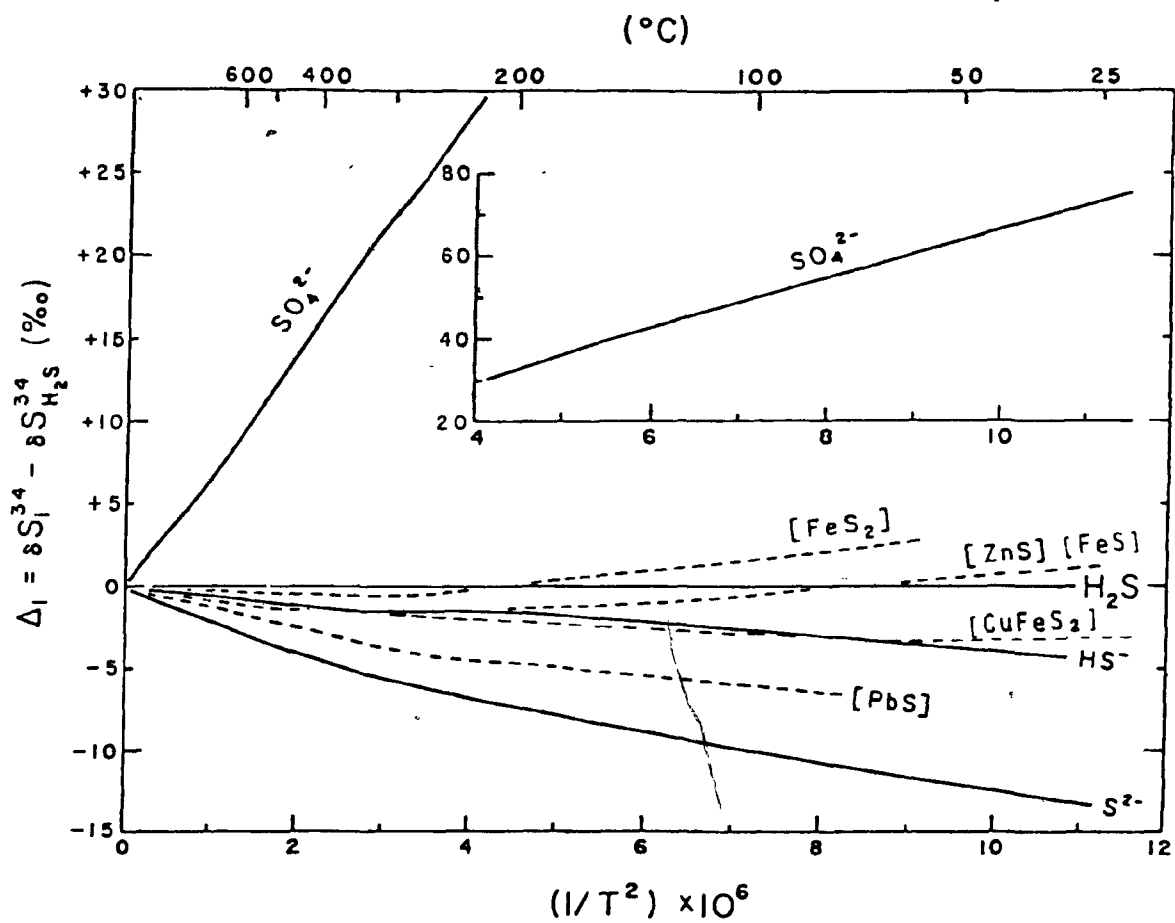


Figure 4.1 - Isotopic enrichment factors for important sulfur species (based on the data by Sakai, 1968; Rye & Czamanske, 1969; Kajiwarra & Krouse, 1971; Ohmoto, 1972).

Furthermore, at high f_{O_2} and low pH, HSO_4^- is an important aqueous species whereas at higher pH (and high f_{O_2}), SO_4^{2-} becomes the predominant sulfur species.

Having established the stability fields of the various aqueous sulfur species, it is now appropriate to examine the effect of pH and/or f_{O_2} on the isotopic composition of sulfide minerals. Ohmoto (1972) showed that the isotopic composition of sulfides forming in equilibrium with a fluid containing significant proportions of several aqueous species can change quite drastically with a slight change in pH and/or f_{O_2} . For instance, at 250°C, an increase in f_{O_2} by one unit and/or an increase of pH by one unit can account for a decrease in $\delta^{34}S$ by about 20 per mil.

Furthermore, a change in f_{O_2} and/or pH by one unit can produce a larger variation in $\delta^{34}S$ at lower temperatures than at higher temperatures since the fractionation factors are larger at lower temperatures (Figure 4.1).

On the basis of the above discussion, it is evident that the $\delta^{34}S$ values of hydrothermal minerals are a reflection of a complex geochemical history of the sulfur in hydrothermal fluids. Therefore, the interpretation of $\delta^{34}S$ values obtained from these minerals requires an understanding of both the geology and the geochemistry of the ore deposits in addition to the processes of isotopic fractionation occurring within these systems.

4.2 Analyses of the Volcanic Rocks

Sulfur isotope analyses were carried out by Dr. C. E. Rees of McMaster University. The analytical procedure involves initial combustion of samples in a stream of oxygen in a LECO induction furnace. The sulfur dioxide which is produced is swept by the oxygen into a flask containing bromine water and then oxidized to sulfate. The latter is precipitated as barium sulfate which is then converted to hydrogen sulfide, cadmium sulfide, silver sulfide and sulfur dioxide for mass spectrometric analysis.

Although these sulfur isotope analyses were essentially total sulfur analyses, it appears that there is little chance of there being anything but reduced sulfur in the samples. This is in accordance with petrological evidence because no sulfate-bearing minerals have been encountered in any of the samples.

4.3 Isotopic Composition of the Rocks

Sulfur isotope determinations have been performed on thirteen samples of basalt. The results of these analyses are tabulated in Table 4.1. The isotopic results show that the $\delta^{34}\text{S}$ values are generally low, ranging from -0.3 to +1.8 per mil in the least altered rocks and -1.8 to +3.9 per mil in the altered ones. It is assumed that the degree of alteration, measured by SiO_2 content, is proportional to water/rock ratios (MacGeehan, 1979; MacGeehan and MacLean, 1980).

TABLE 4.1: Sulfur Isotopic Compositions of the Basalts

Type of sample [*]	Unit	Sample No.	³⁴ S(per mil)
A	B3	M-330	-1.8
LA	B3	AP-49	1.8
LA	B5	AP-42	0.0
A	B5	M-34	0.9
A	B2	M-316	3.8
LA	B2	M-317	1.8
A	B4	M-655	1.2
A	B4	M-369	0.6
LA	B6	AP-43	-0.2
LA	B7	AP-44	1.4
A	B7	M-38	3.9
LA	B5	AP-30	1.1
LA	B6	AP-7	-0.3

* "A" refers to altered whereas "LA" refers to least altered samples.

4.4 Interpretation of the Isotopic Composition

Figure 4.2 illustrates the relationship between $\delta^{34}\text{S}$ and SiO_2 content of the rocks. Since at the present time, SiO_2 data is unavailable for the seven least altered samples, average SiO_2 values for least altered basalts in each B-unit were calculated and substituted for the missing data in four of the seven samples. Unfortunately, no such data is available for units B6 and B7. Hence, three of the seven samples do not appear in Figure 4.2, although it is assumed that the silica content of these three samples is less than 52.0 wt.%. It is evident from the data presented in both Table 4.1 and Figure 4.2 that the least altered samples plot within a narrow range of $\delta^{34}\text{S}$. However, as the silica content of the samples increases, the range of $\delta^{34}\text{S}$ values widens.

According to Schneider (1970), Sasaki (1970), Kanehira et al., (1973) and Ohmoto et al., (1979), the sulfur isotope composition of fresh tholeiitic basalts ranges from -1.0 to +2.0 per mil. Assuming that this is generally true, then all of the least altered samples plotted in Figure 4.2 would be accounted for. The fact that the $\delta^{34}\text{S}$ values of the least altered rocks fall within the range of values characteristic of fresh tholeiitic basalts indicates that the sulfur contained in the least altered rocks is primary, as expected.

The $\delta^{34}\text{S}$ values of the altered basalts range from -1.8 to +3.9 per mil. The greater range in the isotopic composition

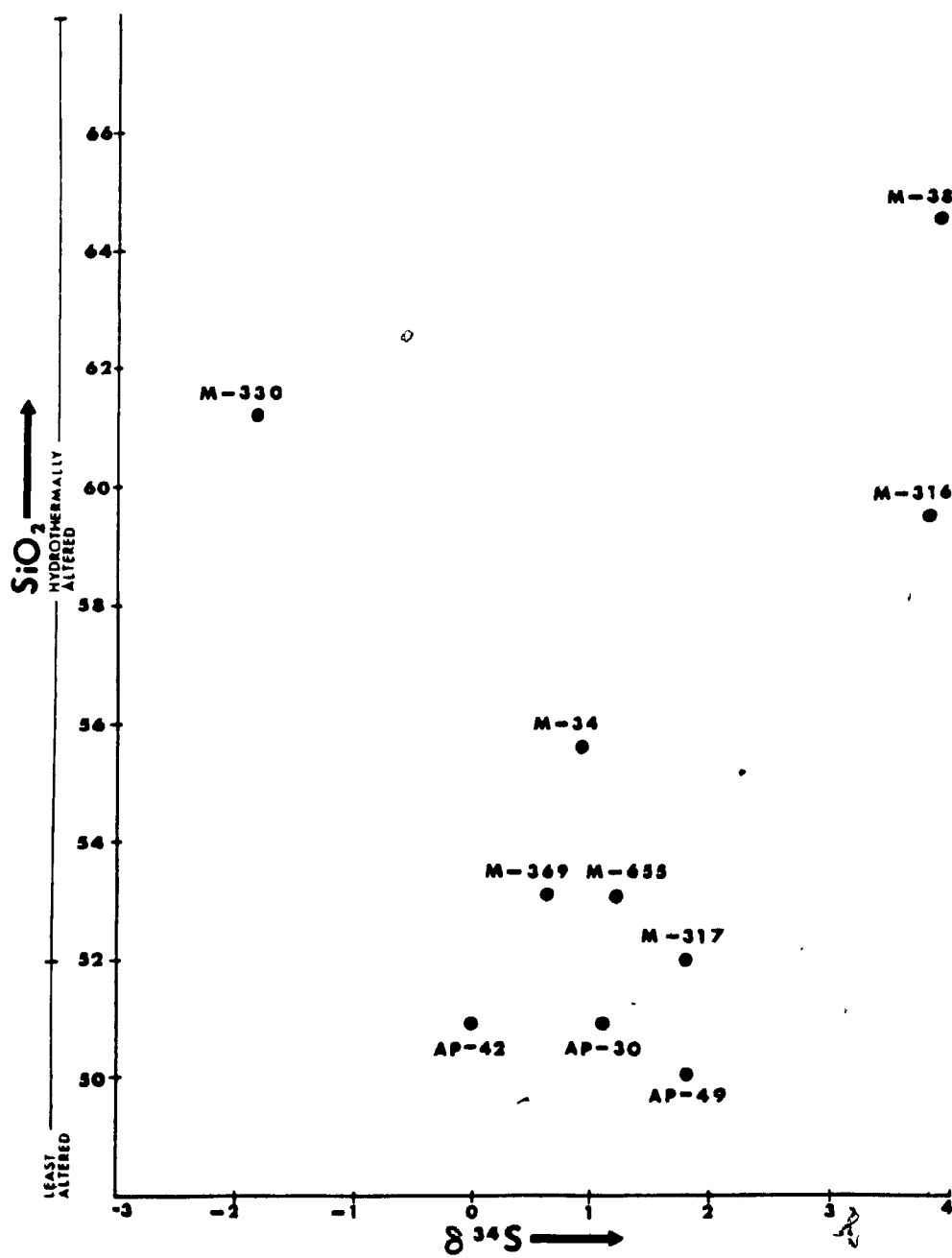


Figure 4.2 - Plot of $\delta^{34}\text{S}$ values against SiO_2 content.

of these basalts may be a reflection of the exchange of sulfur between the basalts and the altering fluid. As shown earlier in Chapter 3, this fluid generally added to the sulfur content of the altered basalts. Hence, a likely explanation for the strongly positive values is that they derive from an altering fluid of seawater origin. Although the isotopic composition of seawater in the Archean is not known, it will be assumed that it was similar to that of present day seawater. Thus, in terms of simple mixing, an addition of 7 %S (mean amount of sulfur added to units B2, B3 and B4) from seawater of $\delta^{34}\text{S} = +20$ per mil would increase the $\delta^{34}\text{S}_{\text{ES}}$ of the least altered rocks from an initial value of +1 per mil (mean isotopic composition of the least altered basalts) to +2.2 per mil in the altered rocks. This information enables one to superimpose $\delta^{34}\text{S}$ contours upon the stability fields of Fe-S-O minerals as shown in Figure 4.3. In examining the data presented in this figure, one can see that the range of $\delta^{34}\text{S}$ values exhibited by the altered basalts can be produced under conditions of (1) low f_{O_2} and near neutral pH (ie. by simply recirculating primary sulfur) or (2) high f_{O_2} and acidic pH (ie. by mixing primary sulfur with seawater sulfur). A choice between these two alternatives can only be made if the Eh/pH conditions of the hydrothermal fluid at the time of ore deposition are known. The restrictions on these two parameters will be evaluated in Chapter 5.

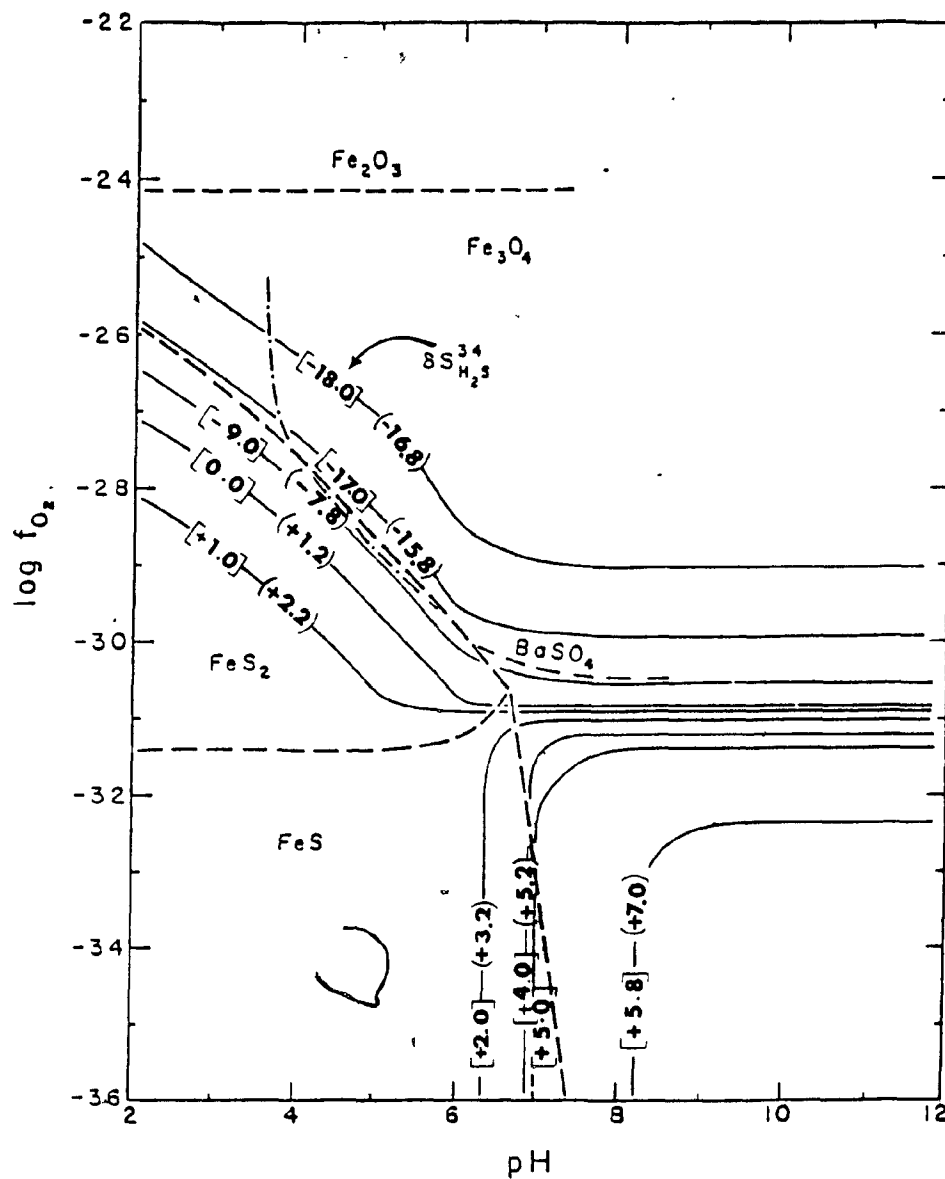


Figure 4.3 - Comparison of the positions of $\delta^{34}S$ contours with the stability fields of Fe-S-O minerals at $T = 350^\circ C$ and $I = 1.0$. FeS - FeS_2 - $BaSO_4$ - Fe_3O_4 - Fe_2O_3 boundaries are from Ohmoto (1972).

- : $\delta^{34}S$ contours. Values in [] and () are for H_2S at $\delta^{34}S_{\Sigma S} = +1.0$ and $+2.2$, respectively.
- - -: Fe-S-O mineral boundaries at $\Sigma S = 0.01$ moles/kg H_2O .
- · - · -: Barite soluble/insoluble boundary at $m_{Ba^{2+}} \cdot m_{SO_4^{2-}} = 10^{-3}$

This, in conjunction with $\delta^{34}\text{S}$ isopleths developed in this chapter, enables the author to trace and isolate the path of the ore-forming fluids.

4.5 Conclusion

The isotopic composition of sulfides occurring in the least altered basalts is indicative of a magmatic source of sulfur. *

In contrast, the isotopic composition of sulfide minerals in the altered basalts is indicative of either a recycled primary source or a mixed magmatic and seawater source.

CHAPTER 5 - HYDROTHERMAL FLUIDS AND MASSIVE SULFIDE GENESIS

5.1 Introduction

It has long been observed that seawater derived brines are both capable and efficient transport media. Indeed, hydrothermal leaching of transition metals and their subsequent transport as metal-rich brines can account for the genesis of a number of ore deposits (Degens & Ross, 1969; Parmentier & Spooner, 1978; Francheteau et al., 1979).

The origin of the brine involved in the Garon Lake geothermal system is thought to be seawater as well. According to MacGeehan (1979), these fluids were probably silica saturated and slightly basic originally, although as a result of their interaction with basalts, they later became more acidic. This is in agreement with Bischoff & Dickson (1975) who report that following the reaction of seawater with basalts at $T = 200^{\circ}\text{C}$ and $P = 500$ bars, the originally slightly basic $\text{Na-Mg-SO}_4\text{-Cl}$ solution loses its alkalinity and becomes a slightly acid Na-Ca-Cl solution.

The main effect of hydrothermal fluid interaction with the basalts was the development of alteration. As mentioned in Chapter 2, this alteration was dominantly a silicification and spilitization process. As a result, certain elements were leached from the rocks by the convecting hydrothermal fluid while others were added to the rocks. Details concerning the elements which were depleted from, and those which

were added to, the basalts are presented in the following section.

5.2 Major Element, Trace Element and Transition Element Redistribution

MacGeehan (1979) showed that the major elements, iron, magnesium, titanium and calcium, were leached from the basalts in the core of the geothermal system by the hydrothermal fluid. However, sodium and silica were added to the rocks as the alteration intensified.

Significant amounts of nickel, chromium and cobalt, and even greater amounts of manganese and vanadium were dissolved by the fluid, thereby depleting the basalts of these elements. On the other hand, elements such as zirconium, yttrium, niobium and the rare earths were added to the basalts (MacGeehan & MacLean, 1980).

Transition element redistribution involved the loss of copper, iron and zinc from the basalts. Zinc was dissolved progressively along with the other major elements, including iron. However, most of the copper appears to have been removed from basalts at the very beginning of the alteration.

5.3 Sulfur Redistribution

It was established earlier in Chapter 3 that altered basalts contain more sulfur than least altered basalts. This indicates an addition of sulfur to the altered basalts due to hydrothermal fluid interaction. A proposed model for sulfur

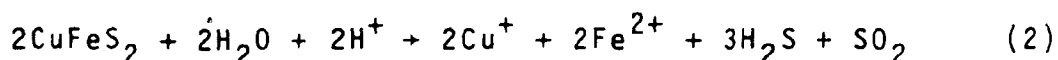
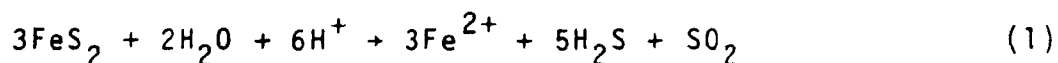
distribution within these basalts is presented below.

Shortly after the B2-B3-B4-GLR sequence of volcanics was laid down, seawater began to flow into the basalts due to the permeability of these units. However, the overlying rhyolitic unit was impermeable. This unit restricted fluid movement to the underlying basalts, thereby ensuring a closed system. As the seawater passed through the basalts, it was heated up by the rocks. This enabled the fluid to circulate convectively throughout the basalts. As it did so, it began to leach sulfur from the least altered rocks. In addition, the hydrothermal fluids also gained sulfur from seawater (Bischoff et al., 1981). Hence, the sulfur which was lost from the least altered basalts was incorporated into, and redistributed by, the hydrothermal fluids. These fluids continued to circulate through the rocks as long as there was sufficient energy in the system to do so. However, once most of the energy was dissipated, the geothermal system began to draw to a close. This was accompanied by re-precipitation of sulfur (as pyrite) within the altered basalts. The bulk of the sulfur, however, was precipitated in the form of metal sulfides at the sediment-seawater interface.

5.4 Solubility and Transport of Ore Metals and Sulfur

The principal ore metals of the Garon Lake mine are zinc, copper and iron. According to MacGeehan (1979), these

metals were leached from basalts in the core of the geothermal system at temperatures up to 400°C. At these elevated temperatures, pyrite and chalcopyrite, the most common sulfide minerals in igneous rocks, may decompose by reaction with acidic aqueous solutions to become the source of sulfur in ore-forming fluids (Ohmoto et al., 1979). These decomposition reactions may be represented by the following relations:



There is a possibility, however, that these metals may also have been leached at lower temperatures which would have prevailed closer to the intake zone of the system, provided that there was convective circulation of hydrothermal fluids in the area where these metals could have been leached. In the Red Sea geothermal system for instance, White (1968) found that zinc, copper and iron are being leached at temperatures less than 60°C. According to White (1968) as reported by Corliss (1971), "contact of a Na-Ca-Cl brine with solid phases that contain base metals which are crystallizing or recrystallizing at temperatures from 100 to 900°C; is the most favored circumstance for concentration of these metals in the liquid phase." Bischoff et al. (1975) conducted an experimental study in which seawater was reacted.

with basalt at 200°C and 500 bars and found that iron and copper were indeed leached from the basalts. Therefore, since the evidence in the literature indicates that base metals may be leached at low temperatures (ie. $T < 250^{\circ}\text{C}$), it is possible that the ore metals in the Garon Lake geothermal system may have been leached closer to the intake zone in addition to the core zone.

The dissolution rates of the base metals and sulfur appear to be variable. MacGeehan (1979) demonstrated that zinc was solubilized at a constant rate as alteration progressed. However, copper was dissolved rapidly at the outset of alteration. Iron was solubilized much like zinc in that it was leached at a constant rate as alteration progressed. The dissolution rate of sulfur, represented by the decreasing slope (m) of the least squares line in Figures 5.1, 5.2 and 5.3, indicates that sulfur was dissolved rapidly during the early stages of alteration and progressively slower during subsequent later stages.

Estimated temperatures within the intake zone as well as in the core suggest that sulfur was probably transported as aqueous H_2S , HS^- and SO_4^{2-} while the ore metals may have been transported as bisulfide and chloride complexes. In a study of hydrothermal ore formation at low temperatures and alkaline conditions, Barnes & Czamanske (1967) found that in the presence of HS^- species, zinc preferentially forms $\text{Zn}(\text{HS})_3^-$. Crerar & Barnes (1976) demonstrated that, in the

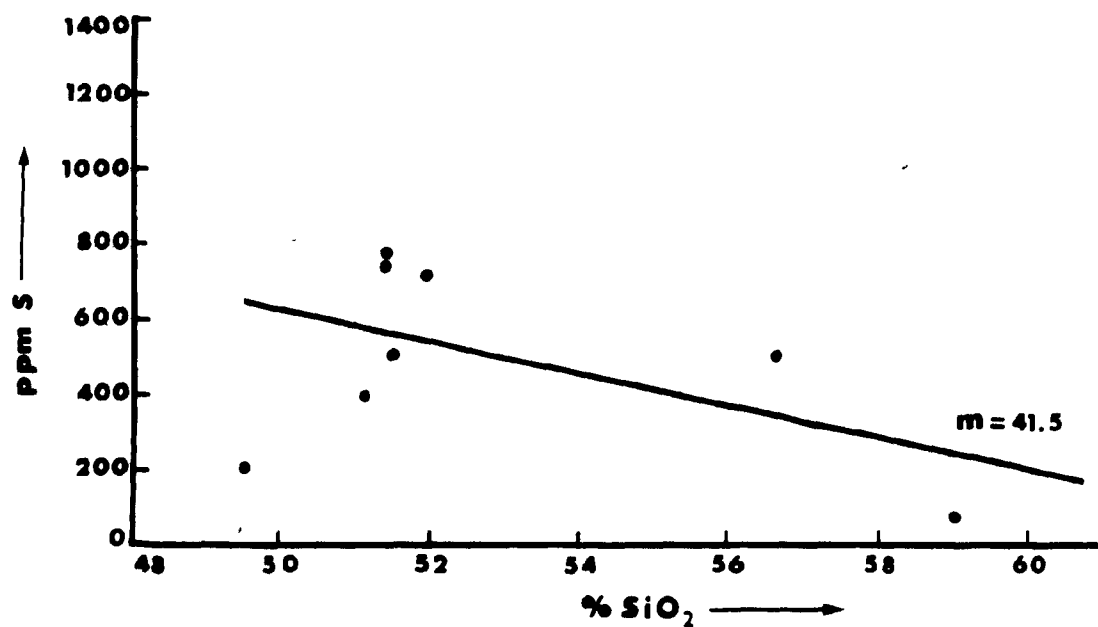


Figure 5.1 - Rate of dissolution of sulfur for B2 basalts.

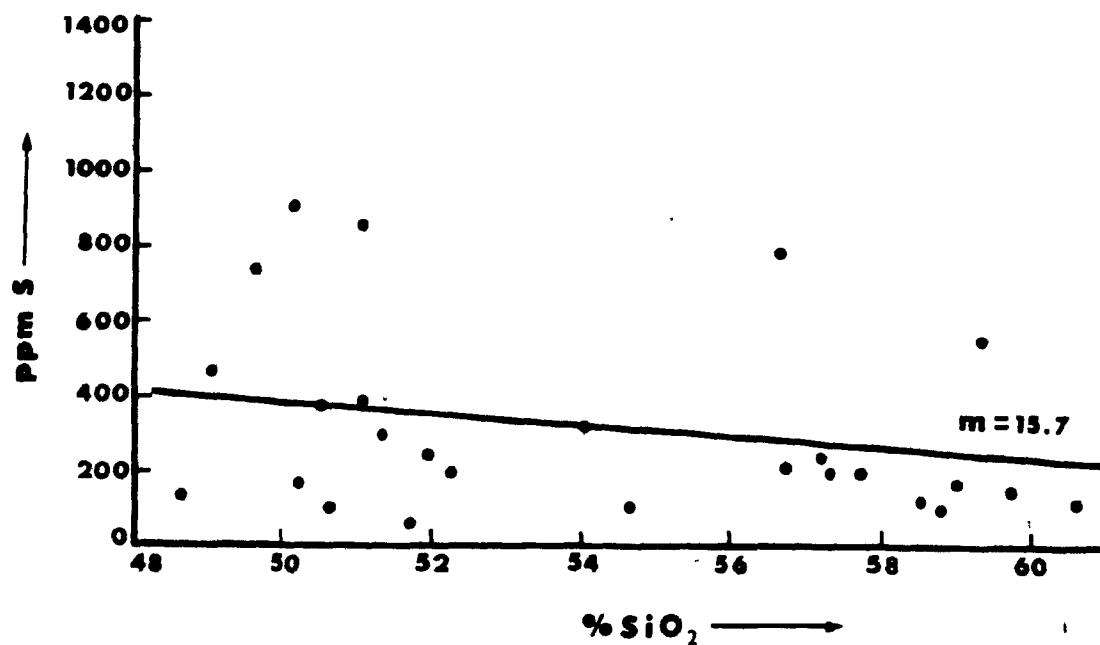


Figure 5.2 - Rate of dissolution of sulfur for B3 basalts.

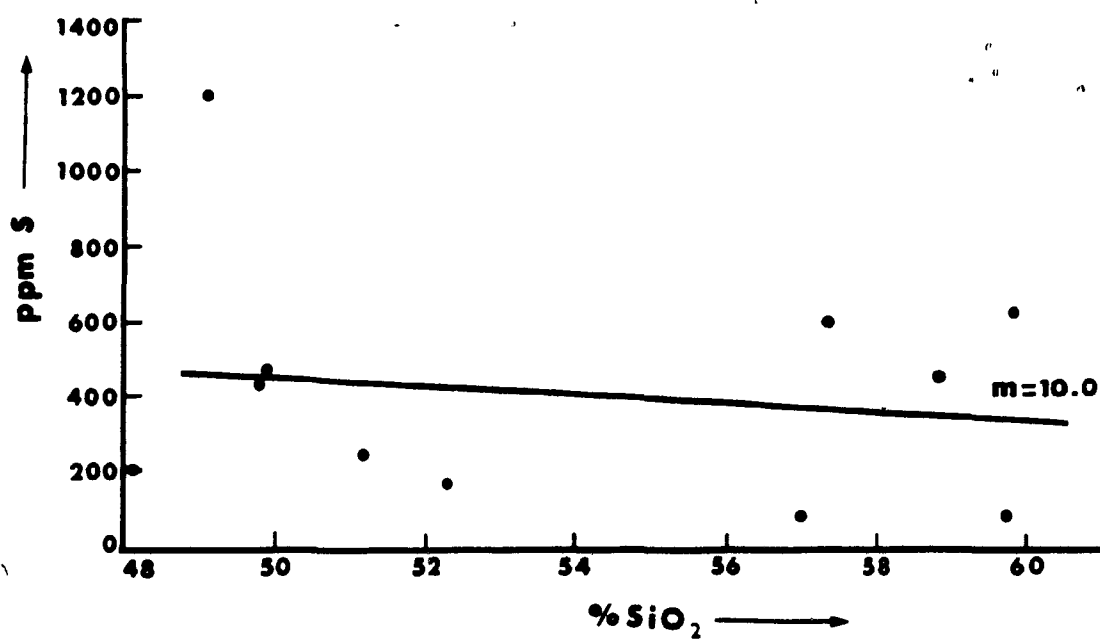


Figure 5.3 - Rate of dissolution of sulfur for B4 basalts.

presence of HS^- , the dominant Cu^+ species changes with increasing temperature from $\text{Cu}(\text{HS})_3^{2-}$ at $T \sim 200^\circ\text{C}$ to $\text{Cu}(\text{HS})_2^-$ at $T \sim 250^\circ\text{C}$. In a study of the thermodynamics of hydrothermal systems at elevated temperatures, Helgeson (1969, 1970) found that ZnCl_2 , CuCl , FeCl_2 , FeCl_3 , H_2S and H_2SO_4 are important components of natural hydrothermal systems.

Since it is believed that the prevailing pH conditions in the intake zone were alkaline as opposed to the dominantly acidic conditions within the core, it is highly probable that zinc and copper were transported as bisulfide complexes close to the intake zone (ie. $T < 350^\circ\text{C}$, $6.5 < \text{pH} < 9$) and as chloride complexes in the core zone (ie. $T \approx 350^\circ\text{C}$, $\text{pH} > 2.5$). Iron, on the other hand, was transported exclusively as a chloride complex since it cannot form bisulfide complexes (Crerar & Barnes, 1976; Barnes, 1979). Finally, sulfur was transported as aqueous H_2S and SO_4^{2-} (in the core) and as HS^- (in the intake zone).

5.5 Stability of Metal Bisulfide and Metal Chloride Complexes

The stability field of bisulfide complexes extends from $\text{pH} = 6.5$ to $\text{pH} = 9.0$ at $T < 350^\circ\text{C}$. At $T \geq 350^\circ\text{C}$, however, these complexes are stable at $\text{pH} > 9.0$ (Barnes, 1979). The break-up of metal bisulfide complexes may be caused by any of the following factors:

- (1) a decrease in pH. This can be in response to oxidation which may be caused mainly by reaction with wallrocks, other solutions and gases containing oxidized species (ie. CO_2 , SO_2 , O_2 etc.). Oxidation

releases H^+ ions, lowers pH and ultimately causes precipitation of sulfides.

- (2) an increase in temperature
- (3) dilution by other solutions
- (4) a change in ΣS . Crerar & Barnes (1976) report that nearly all of the copper in the form of cuprous bisulfide ($Cu(HS)_2^-$) will precipitate as a result of a change of $0.1 \times \Sigma S$.

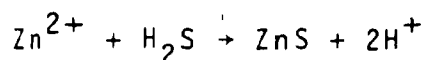
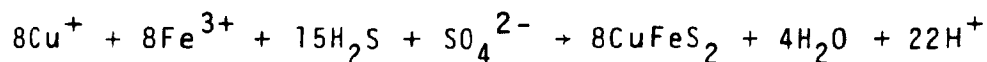
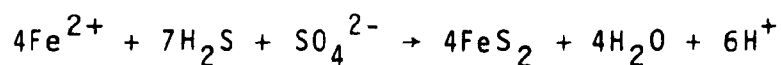
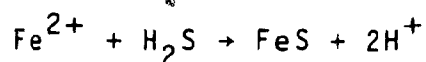
The stability field of metal chloride complexes is restricted to $pH < 2.5$ at $T < 350^\circ C$. At $T \geq 350^\circ C$, these complexes are stable at $pH > 2.5$ (Barnes, 1979). The break-up of these complexes can be attributed to the following factors:

- (1) a change in pH or a change in f_{O_2}
- (2) an increase in temperature
- (3) dilution by other solutions (ie. intermixing with a sulfur-bearing solution will cause precipitation of metal sulfides).
- (4) a change in ΣS

5.6 Mechanism of Ore Metal Transport and its Relationship to the Genesis of Massive Sulfides

Thermal conditions at the time of base metal leaching as well as the probable pH of the ore-forming fluids suggest that the ore metals which were leached in the core of the geothermal system were transported exclusively as chloride complexes. According to Ohmoto and Rye (1979), the formation of pyrrhotite, pyrite, chalcopyrite and sphalerite under

equilibrium hydrothermal conditions from Fe^{2+} , Fe^{3+} , Cu^{+} and Zn^{2+} chloride complexes requires H_2S and/or SO_4^{2-} as illustrated by the following reactions:



On the basis of this information, it appears that under equilibrium hydrothermal conditions, the interaction of metal complexes with sulfur-bearing species commonly results in the precipitation of metal sulfides.

Furthermore, earlier work by MacGeehan (1979) and Aftabi (1980) provides a basis for the upcoming discussion concerning the path of the ore-forming fluids. According to MacGeehan (1979), the development of a geothermal system beneath the Garon Lake rhyolite resulted in the leaching of ore metals and ultimately in their deposition in the form of massive sulfides. These massive sulfides comprise three orebodies as shown in Figure 5.4. Although the sulfide mineralogy of each orebody is the same, the concentration of ore metals varies from one orebody to the next as illustrated in Table 5.1. In addition, on the basis of mineralogical and textural evidence, Aftabi (1980) established that Po-Py-Cpy-Mt-Sph is a common equilibrium mineral assemblage in lens "A"

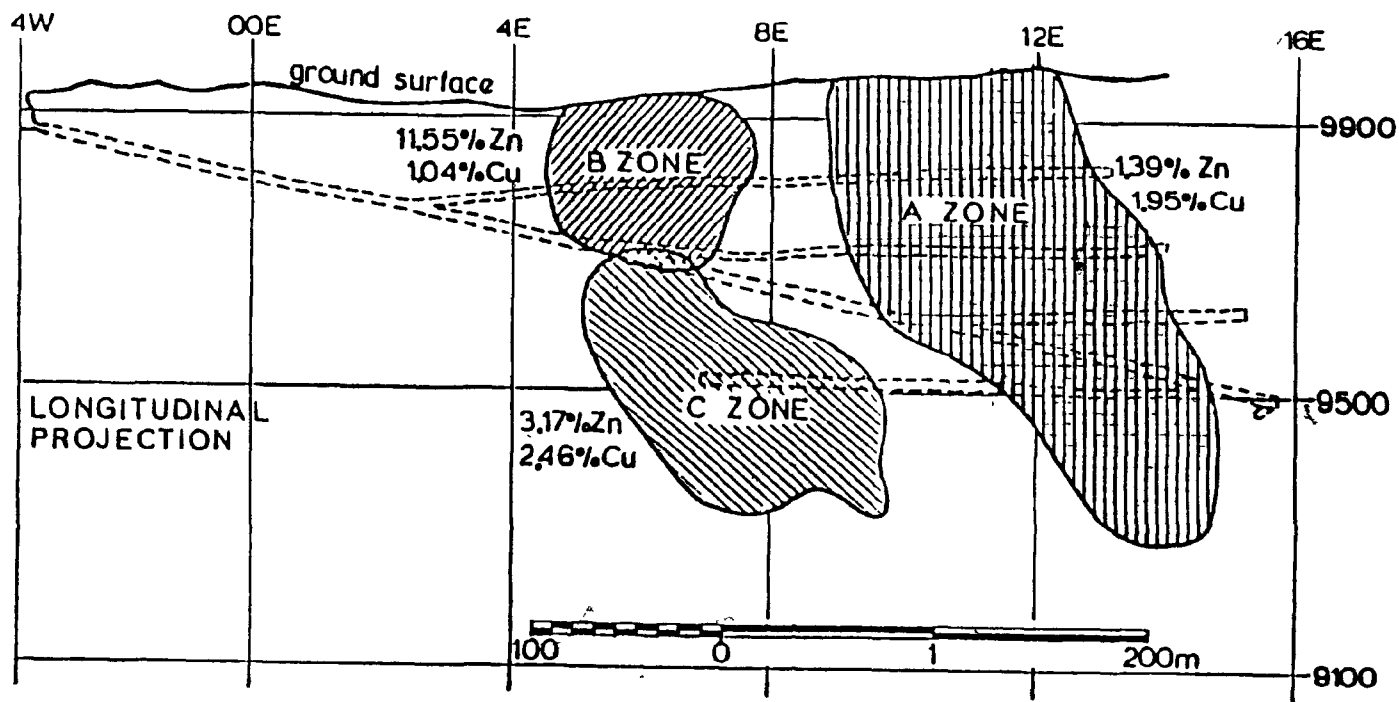


Figure 5.4- Longitudinal vertical projection of the three sulphide lenses, showing the economic or mineable perimeter of each orebody (after MacGeehan, 1979)

Table 5.1 : Approximate Ore Reserve at the Garon Lake Mine

<u>Orebody</u>	<u>Tonnage</u>	<u>% Zn</u>	<u>% Cu</u>	<u>Zn/Cu</u>
B-Zone	88,000	11.55	1.04	11.1
C-Zone	54,000	3.17	2.46	1.3
A-Zone	<u>309,000</u>	<u>1.39</u>	<u>1.95</u>	<u>0.7</u>
Total	451,000	3.59	1.83	1.96

(after MacGeehan, 1979)

whereas Py-Cpy-Sph is the equilibrium mineral assemblage in lens "C" as well as in lens "B".

(\ D

Therefore, all of the above mentioned evidence suggests that the ore-forming fluids evolved and progressed in the manner indicated in Figure 5.5. The initial fluid was probably centered at, or close to, the invariant point, as shown. This is consistent with the equilibrium mineral assemblage observed in lens "A". However, as the ore-forming fluid evolved, it progressed further into the pyrite stability field, as indicated. This is in accordance with the mean composition of the sphalerites in each lens as determined by Aftabi (1980). The lack of zonation within these sphalerites indicates compositional homogeneity within this mineral group and lends further support to the idea that the ore-forming fluid did not progress far beyond the $(\text{Zn}_{.9}\text{Fe}_{.1})\text{S}$ isopleth. Furthermore, it was suggested earlier in Chapter 4 that the isotopic composition of the altered basalts could be produced under conditions of (1) low f_{O_2} and near neutral pH or (2) high f_{O_2} and acidic pH. The first possibility can now be eliminated on the basis of the Eh/pH conditions established by the equilibrium mineral assemblages in the ore rocks. In addition, the mean isotopic composition of the sphalerites further restricts Eh/pH conditions of the hydrothermal fluid at the time of ore deposition. Consequently, the above mentioned mineralogical and petrographic evidence is consistent with the hypothesis that the sulfur

(

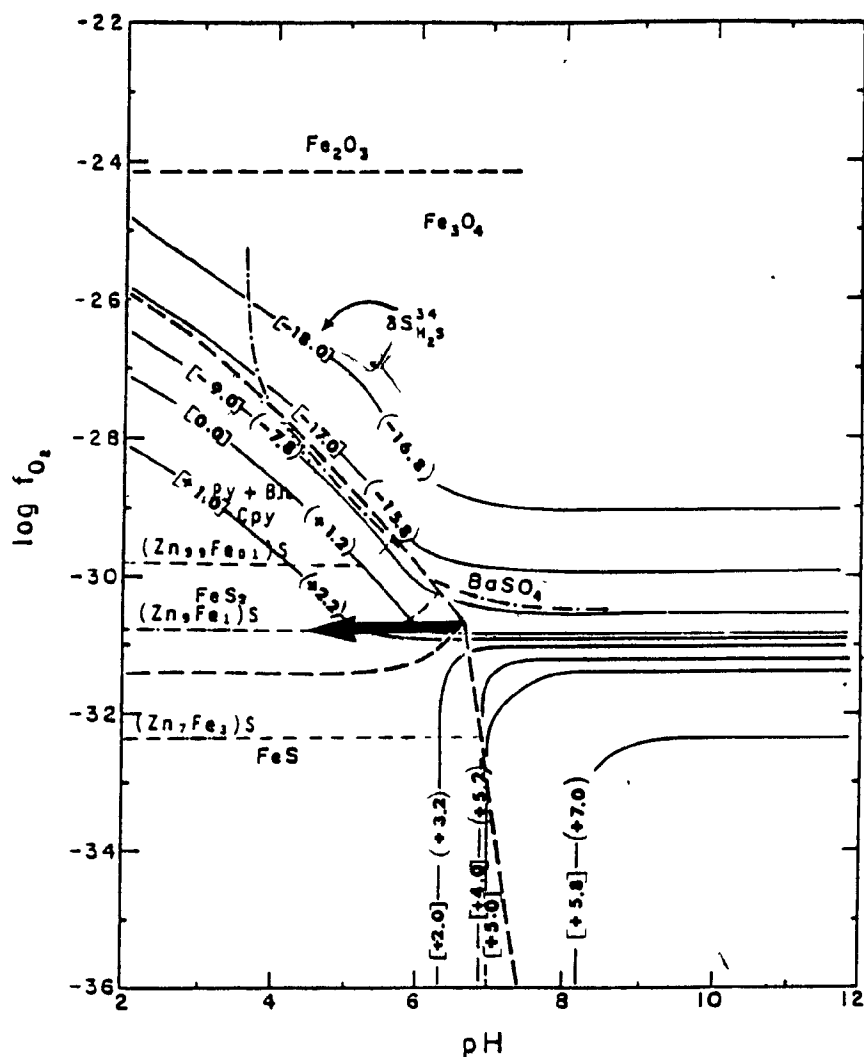


Figure 5.5 - Stability fields of Fe-Zn-Cu-S minerals at $T = 350^{\circ}\text{C}$. The Po-Mt, Po-Py and Py-Mt boundaries are from Ohmoto (1972). The Cpy-Py-Bh boundary is from Barton & Skinner (1979). Sphalerite isopleths within the Py and Po stability fields are from Scott & Barnes (1971).

- : $\delta^{34}\text{S}$ contours. Values in [] and () are for H_2S at $\delta^{34}\text{S}_{\Sigma\text{S}} = 1.0$ and 2.2 , respectively.
- - -: Fe-S-O mineral boundaries at $\Sigma\text{S} = 0.01$ moles/kg H_2O .
- · - · -: Barite soluble/insoluble boundary at $m_{\text{Ba}^{2+}} \cdot m_{\Sigma\text{S}} = 10^{-3}$

present in the altered basalts is derived from mixing of primary, igneous sulfur with lesser amounts of seawater sulfur.

5.7 Conclusion

The temperature of the ore-forming fluid in the core of the geothermal system was $\sim 350^{\circ}\text{C}$. The acidity of this fluid varied from $\text{pH} = 4.0$ to $\text{pH} = 6.8$ while the oxygen fugacity remained essentially constant at $\log f_{\text{O}_2} = -31.0$. Consequently, it appears likely that a possible cause of the break-up of metal chloride complexes within the Garon Lake geothermal system may have been the intermixing of a metal-chloride brine with a sulfur-bearing solution.

CONCLUSION

On the basis of the sulfur content and sulfur isotopic composition of Archean basaltic rocks at Matagami, it is concluded that:

- (1) The sulfur content of these Archean basaltic rocks is highly variable.
- (2) The sulfur content of the least altered basalts parallels the total iron content in each flow unit indicating that the relationship between the two elements is a primary one, possibly related to sulfur saturation in the melt.
- (3) The mean sulfur contents of the altered basalts are consistently higher than those of the least altered basalts. This is a reflection of initial leaching of sulfur from the least altered basalts and subsequent addition of sulfur to the altered basalts due to hydrothermal fluid interaction. Furthermore, the addition of sulfur to the altered basalts parallels the loss of iron, thereby suggesting that secondary sulfur distribution is controlled by the iron content of the rocks.
- (4) Sulfur isotopic results indicate that the sulfur present in the least altered basalts is of magmatic origin whereas that present in the altered basalts is of a mixed magmatic and seawater origin.

(5) On the basis of thermochemical evidence, ore deposition at the Garon Lake mine resulted from mixing of a metal-rich chloride brine with a sulfur-bearing solution.

CONTRIBUTION TO KNOWLEDGE

- (1) The analytical method outlined in the text presents an alternate means of analyzing for sulfur, provided that the rocks which are of interest contain one predominant sulfide-bearing mineral phase.
- (2) Hydrothermally altered basalts preserve the original, positive trend exhibited by iron and sulfur in the least altered basalts. However, the altered basalts are more sulfur-rich as compared to the least altered ones indicating that hydrothermal fluid interaction results in an addition of sulfur to altered basalts.
- (3) The amount of sulfur added to the altered basalts is inversely proportional to the amount of iron lost, thereby suggesting that secondary sulfur distribution is controlled by the iron content of the rocks.

BIBLIOGRAPHY

Abraham, K. P., Davies, M. W. and Richardson, R. D., 1960. Sulfide capacities of silicate melts. Part I: Jour. Iron Steel Inst., v. 196, p. 309-312.

_____ and Richardson, F. D., 1960. Sulfide capacities of silicate melts. Part II: Jour. Iron Steel Inst., v. 196, p. 313-317.

Aftabi, A., 1980. Polymetamorphism, textural relations and mineralogical changes in Archean massive sulfide deposits at the Garon Lake mine, Matagami, Québec. M.Sc. thesis, McGill University, Montreal, Québec.

Anderson, A. T., 1972. Sulfur and chlorine contents of glass inclusions in phenocrysts and basaltic host glasses. (Abstract) Fluid Inclusion Res. Proc. COFFI, v.2, p. 12-13.

_____, 1974. Chlorine, sulfur and water in magmas and oceans. Geol. Soc. Amer. Bull., v. 85, p. 1485-1492.

Andrews, A. J., 1979. On the effect of low temperature seawater-basalt interaction on the distribution of sulfur in the oceanic crust, Layer 2. Earth and Planetary Science Letters, v. 46, p. 68-80.

_____, Barnett, R. L., MacClement, E. A. E., Fyfe, W. S., Morrison, G., MacRae, N. R. and Starkey, J., 1975. Zeolite facies metamorphism, geochemistry and some aspects of trace element redistribution in altered basalts of Leg. 37, DSDP. In: DSDP Initial Reports, v. 37, F. Aumento et al., eds. (U.S. Government Printing Office, Washington, D. C.).

Ault, W., 1959. Isotopic fractionation of sulfur in geochemical

processes. In: Researches in Geochemistry. P.H. Abelson, ed. (Wiley, New York) p. 241-259.

_____ and Jensen, M. L., 1973. Summary of sulfur isotopic standards. In: Biogeochemistry of Sulfur Isotopes. M. L. Jensen, ed., Natl. Sci. Found., Symposium Proc., Yale University.

_____ and Kulp, J. L., 1960. Sulfur isotopes and ore deposits. Economic Geology, v. 55, p. 73-100.

Aumento, F., Mitchell, W. S. and Fratta, M., 1976. Interaction between seawater and oceanic Layer 2 as a function of time and depth. Canadian Mineralogist, v. 14, p. 269-290.

Bachinski, D. J., 1969. Bond strength and sulfur isotopic fractionation in co-existing sulfides. Economic Geology, v. 64, p. 56-65.

Bancroft, J. A., 1912. A report on the geology and natural resources of certain parts of the drainage basins of the Harricanaw and Nottaway Rivers, to the north of the National Transcontinental Railway in north-western Québec. Québec Bureau of Mines, Report on Mining Operations, p. 131-198.

Barnes, H. L., 1979. Solubilities of ore minerals. In: Geochemistry of Hydrothermal Ore Deposits. H. L. Barnes, ed. (Wiley-Interscience, New York) p. 405-460.

_____ and Czamanske, G. K., 1967. Solubilities and transport of ore minerals. In: Geochemistry of Hydrothermal Ore Deposits. H. L. Barnes, ed. (Wiley and Sons,

New York) p. 334-381.

Barton, P. B. and Skinner, B. J., 1979. Sulfide mineral stabilities. In: Geochemistry of Hydrothermal Ore Deposits. H. L. Barnes, ed. (Wiley-Interscience, New York) p. 278-403.

Béland, R., 1953. Allard River area. Québec Department of Mines, Geological Report No. 57, 30pp.

Bell, R., 1895. Geological Survey of Canada, Annual Report, Volume III, Part A, p. 74-85.

———, 1900. Geology of the basins of the Nottoway River. Geological Survey of Canada, Volume XIII, Part K.

Bernard, P. Geology of the Norita mine A-zone, Matagami, Québec: a distal volcano-sedimentary Fe-Cu-Zn sulfide deposit. M.Sc. thesis, McGill University, Montreal, Québec (in preparation).

Berner, R. A., 1972. Sulfate reduction, pyrite formation and the oceanic sulfur budget. In: The Changing Chemistry of the Oceans. D. Dryssen & D. Jagner, eds. (John Wiley and Sons, New York) Nobel Symposium 20, p. 347-361.

Beswick, A. E. and Soucie, G., 1978. A correction procedure for metasomatism in an Archean greenstone belt. Precambrian Research, v. 6, p. 235-248.

Bischoff, J. L., 1969. The Red Sea geothermal deposits: their mineralogy, chemistry and genesis. In: Hot Brines and Recent Heavy Metal Deposits in the Red Sea.

E. T. Degens and D. Ross, eds. (Springer Verlag, New York) p. 368-401.

_____. and Dickson, F. W., 1975. Seawater-basalt interaction at 200°C and 500 bars: implications for the origin of sea-floor heavy-metal deposits and regulation of seawater chemistry. *Earth and Planetary Science Letters*, v. 25, p. 385-397.

_____. Radtke, A. S. and Rosenbauer, R. J., 1981. Hydrothermal alteration of graywacke by brine and seawater: roles of alteration and chloride complexing on metal solubilization at 200° and 350°C. *Economic Geology*, v. 76, p. 659-676.

Bonavia, F., 1982. The geology and geochemistry of Radiore 2 mine, Matagami, Québec. M.Sc. thesis, McGill University, Montreal, Québec.

Brotzen, O., 1966. The average igneous rock and the geochemical balance. *Geochimica et Cosmochimica Acta*, v. 30, p. 863-868.

Bryan, W. B. and Moore, J. G., 1977. Compositional variations of young basalts in the mid-Atlantic Ridge rift valley near latitude 36°49' N. *Geological Society of America Bulletin*, v. 88, p. 556-570.

Burnham, C. N., 1979. Magmas and hydrothermal fluids. In: *Geochemistry of Hydrothermal Ore Deposits*. H. L. Barnes, ed. (Wiley-Interscience, New York) p. 71-136.

Cameron, E. M. and Baragar, W. R. A., 1970. Distribution of ore elements in rocks for evaluating ore potential:

frequency distribution of copper in the Coppermine River Group volcanic rocks, N. W. T., Canada. In: Geochemical Exploration, Proceedings of the 3rd International Geochemical Exploration Symposium. C.I.M. Special Volume No. 11. R. W. Boyle, ed. (Montreal) p. 570-576.

_____, Siddely, G. and Durnham, C. G., 1971. Distribution of ore elements in rocks for evaluating ore potential: nickel, copper, cobalt and sulfur in ultramafic rocks of the Canadian Shield. In: Geochemical Exploration, Proceedings of the 3rd International Geochemical Exploration Symposium. C.I.M. Special Volume No. 11. R. W. Boyle, ed. (Montreal) p. 298-313.

Carmichael, I. S. E., Turner, J. F. and Verhoogen, J., 1974. Igneous Petrology. McGraw-Hill, New York. 739pp.

Connolly, J. W. D. and Haughton, D. R., 1972. The valence of sulfur in glass of basaltic composition formed under conditions of low oxidation potential. American Mineralogist, v. 57, p. 1515-1517.

Corliss, J. B., 1971. The origin of metal-bearing submarine hydrothermal solutions. Journal of Geophysical Research, v. 76, p. 8128-8138.

Craig, H., 1966. Isotopic composition and origin of Red Sea and Salton Sea geothermal brines. Science, v. 154, p. 1544-1548.

Crerar, D. A. and Barnes, H. L., 1976. Ore solution chemistry V. Solubilities of chalcopyrite and chalcocite assemblages in hydrothermal solutions at 200°C to 350°C. Economic

Geology, v. 71, p. 772-794.

Czamanske, G. K., 1974. The FeS content of sphalerite along chalcopyrite-pyrite-bornite sulfur fugacity buffer. Economic Geology, v. 69, p. 1328-1334.

_____ and Moore, J. G., 1977. Composition and phase chemistry of sulfide globules in basalt from the mid-Atlantic Ridge rift valley near 37°N latitude. Geological Society of America Bulletin, v. 88, p. 587-599.

Degens, E. T. and Ross, D. A. (eds.), 1969. Hot brines and recent heavy metal deposits in the Red Sea. Springer, New York.

Elsheimer, N. H. and Fabbi, B. P., 1974. A versatile XRF method for the analysis of sulfur in geologic materials. Advances in X-Ray Analysis, v. 17, p. 236-246.

Ewers, W. E. and Hudson, D. R., 1972. An interpretive study of a nickel-iron sulfide ore intersection, Lunon Shoot, Kambala, Western Australia. Economic Geology, v. 67, p. 1075-1092.

Fabbi, B. P. and Moore, W. J., 1970. Rapid XRF determination of sulfur in mineralized rocks from the Bingham mining district, Utah. Applied Spectroscopy, v. 24, p. 426-428.

Field, C. W., Dymond, J. R., Heath, G. R., Corliss, J. B. and Dasch, E. J., 1976. Sulfur isotope reconnaissance of epigenetic pyrite in ocean floor basalts, Leg 34 and elsewhere. In: DSDP Initial Reports, vol. 34. R.S. Yeats et al.; eds. (U.S. Government Printing Office, Washington, D.C.) p. 381-384.

Fincham, C. J. B. and Richardson, F. D., 1954. The behavior of sulfur in silicate and aluminate melts. Proceedings of the Royal Society of London, Series A, v. 223, p.40-62.

Francheteau, J., Needham, H. D., Chaukroune, P., Juteau, T., Séguret, M., Ballard, R. D., Fox, P. J., Normark, W., Corranza, A., Cordoba, D., Guerrero, J., Rangin, C., Bougoult, H., Cambon, P. and Hekinian, R., 1979. Massive deep-sea sulfide ore deposits discovered on the East Pacific Rise. Nature, v. 277, p. 523-528.

Freeman, B. C., 1936. Mattagami Lake. Geological Survey of Canada, Map 571A.

_____ and Black, J.M., 1944. The Opaóka River. Québec Department of Mines, Geology Report No. 16.

Fudali, R. F., 1965. Oxygen fugacities of basaltic and andesitic magmas. Geochimica et Cosmochimica Acta, v. 29, p. 1063-1075.

Gary, M., McAfee, R. and Wolf, C. L. (eds.), 1973. Glossary of Geology. American Geological Institute, 2nd Edition.

Gast, P. W., 1968. Trace element fractionation and the origin of tholeiitic and alkaline magma types. Geochimica et Cosmochimica Acta, v. 32, p. 1057-1086.

Gélinas, L. and Brooks, C., 1974. Archean quench texture tholeiites. Canadian Journal of Earth Science, v. 11, p. 324-340.

Goodwin, A. M. and Ridler, R. H., 1970. Abitibi orogenic belt. Geological Survey of Canada, Paper 70-40.

Grootenboer, J. and Schwarcz, H. P., 1969. Experimentally determined sulfur isotope fractionations between sulfide minerals. *Earth and Planetary Science Letters*, v. 7, p. 162-166.

Groves, D. I., Solomon, M. and Rafter, T. A., 1970. Sulfur isotope fractionation and fluid inclusion studies at the Rex Hill mine, Tasmania. *Economic Geology*, v. 65, p. 459-469.

Hagash, A., 1974. An experimental investigation of high-temperature seawater-basalt interactions. *Geological Society of America, 87th Annual Meeting, Abstracts with Programs*, v. 6, p. 771.

Hamilton, D. L., Burnham, C. W. and Osborn, E. F., 1964. The solubility of water and the effects of oxygen fugacity and water content on crystallization in mafic magmas. *Journal of Petrology*, v. 5, p. 21-29.

Harrigan, D. B. and MacLean, W. H., 1976. Petrography and geochemistry of epidote alteration patches in gabbro dykes in Matagami, Québec. *Canadian Journal of Earth Science*, v. 13, p. 500-511.

Hart, R. A., 1970, Chemical exchange between seawater and deep ocean basalts. *Earth and Planetary Science Letters*, v. 9, p. 269-279.

———, 1973. A model for chemical exchange in the basalt-seawater system of ocean Layer II. *Canadian Journal of Earth Science*, v. 10, p. 799-816.

Haughton, D. R. and Roeder, P.L., 1972. Iron and sulfur in

basaltic liquids. (Abstract) Canadian Mineralogist, v. 11, p. 574-575.

_____, Roeder, P. L. and Skinner, B. J., 1974. Solubility of sulfur in mafic magmas. Economic Geology, V. 69, p. 451-467.

_____ and Skinner, B. J., 1972. Chemistry of sulfur in melts. (Abstract) 24th International Geological Congress. p. 420.

Hawley, J. E., 1962. The Sudbury ores, their mineralogy and origin. Canadian Mineralogist, v. 7, p. 207.

Helgeson, H. C., 1964. Complexing and hydrothermal ore deposition. Macmillan, New York.

_____, 1968. Geologic and thermodynamic characteristics of the Salton Sea geothermal system. American Journal of Science, v. 266, p. 129-166.

_____, 1969. Thermodynamics of hydrothermal systems at elevated temperatures and pressures. American Journal of Science, v. 267, p. 729-804.

_____, 1970. A chemical and thermodynamic model of ore deposition in hydrothermal systems. Mineralogical Society of America, Special Paper 3, p. 155-186.

Holland, H. D., 1972. Granites, solutions and base metal deposits. Economic Geology, v. 67, p. 281-301.

Hudson, D. R., 1972. Evaluation of genetic models for Australian sulfide nickel deposits. Proceedings, Australian

Institute of Mining and Metallurgy, p. 59-69.

Irvine, T. N. and Baragar, W. R. A., 1971. A guide to the chemical classification of the common volcanic rocks. Canadian Journal of Earth Science, v. 8, p. 523-548.

Jenney, C. P., 1961. Geology and ore deposits of the Matagami area, Québec. Economic Geology, v. 56, p. 740-757.

Jensen, M. L., 1967. Sulfur isotopes and mineral genesis. In: Geochemistry of Hydrothermal Mineral Deposits. H. L. Barnes, ed. (Holt, Rinehart and Winston Inc., New York) p. 143-165.

Joklik, G. F., 1960. The discovery of a copper-zinc deposit at Garon Lake, Québec. Economic Geology, v. 55, p. 338-353.

Jolly, T. W., 1977. Relations between Archean lavas and intrusive bodies of the Abitibi greenstone belt, Ontario-Québec. Geological Association of Canada, Special Paper No. 16.

Kajiwara, Y. and Krouse, H. R., 1971. Sulfur isotope partitioning in metallic sulfide systems. Canadian Journal of Earth Science, v. 8, p. 1397-1408.

Kanehira, K., Yui, S., Sakai, H. and Sasaki, A., 1973. Sulfide globules and sulfur isotope ratios in abyssal tholeiite from the mid-Atlantic Ridge near 30°N latitude. Geochemical Journal of Japan, v. 7, p. 89-96.

Katsura, T. and Nagashima, S., 1974. Solubility of sulfur in some magmas at 1 atmosphere. Geochimica et Cosmochimica Acta, v. 38, p. 517-531.

Kerrich, R. and Fryer, B. J., 1979. Archean precious-metal hydrothermal systems, Dome mine, Abitibi greenstone belt. II. REE and oxygen isotope relations. Canadian Journal of Earth Science, v. 16, p. 440-458.

Kiline, I. A. and Burnham, C. W., 1972. Partitioning of chloride between a silicate melt and co-existing aqueous phase from 2 to 8 kilobars. Economic Geology, v. 67, p. 231-235.

Krauskopf, K. B., 1967. Introduction to Geochemistry. McGraw-Hill, New York. 488pp.

Krouse, H. R., Brown, H. M. and Farguharson, R. B., 1977, Sulfur isotope compositions of sulfides and sulfates, DSDP Leg 37. Canadian Journal of Earth Science, v. 14, p. 787-793.

Latulippe, M., 1959. The Matagami area of northwestern Québec. Geological Association of Canada, Proceedings, v. 11, p. 46-54.

_____, 1966. The relationship of mineralization to Precambrian stratigraphy in the Matagami Lake and Val d'Or districts of Québec. Geological Association of Canada, Special Paper No. 3, p. 21-42.

Longley, W. N., 1943. Kitchigama Lake area. Québec Department of Mines, Geology Report No. 12, 34pp.

MacGeehan, P. J., 1977. A model for the formation of volcanogenic massive sulfide deposits in the Matagami Mining Camp, Québec. (Abstract) GAC/MAC Program with Abstracts, v. 2, Annual Meeting, Vancouver, B. C.

_____, 1978. The geochemistry of altered volcanic rocks at Matagami, Québec: a geothermal model for massive sulfide genesis. Canadian Journal of Earth Science, v. 15, p. 551-570.

_____, 1979. The petrology and geochemistry of volcanic rocks at Matagami, Québec and their relationship to massive sulfide mineralization. Ph.D. thesis, McGill University, Montréal, Québec.

_____ and MacLean, W. H., 1980a. Tholeiitic basalt-rhyolite magmatism and massive sulfide deposits at Matagami, Québec. Nature, v. 283, No. 5743, p. 153-157.

_____ and MacLean, W. H., 1980b. An Archean sub-seafloor geothermal system, "calc-alkaline" trends and massive sulfide genesis. Nature, v. 286, p. 767-771.

MacLean, W. H., 1969. Liquidus phase relations in the FeS-FeO-Fe₃O₄-SiO₂ system and their application in geology. Economic Geology, v. 64, p. 865-884.

_____, 1977. Sulfides in Leg 37 drill core from the mid-Atlantic Ridge. Canadian Journal of Earth Science, v. 14, No. 4, p. 674-683.

_____, 1981. Position of massive sulfide deposits in the volcanic sequence at Matagami, Québec. GAC/MAC Abstract 6, 36.

_____ and MacGeehan, P. J., 1976. Garon Lake mine, Matagami, Québec. Case History 76-1, Mineral Exploration Research Institute, McGill University - Ecole Polytechnique de Montréal.

Mathez, E. A., 1976. Sulfur solubility and magmatic sulfides in submarine basaltic glass. *Journal of Geophysical Research*, v. 81, p. 4269-4275.

_____ and Yeats, R. S., 1976. Magmatic sulfides in basalt glass from DSDP hole 319A and site 320, Nazca Plate. In: *DSDP Initial Reports*, vol. 34. R.S. Yeats and S.R. Hart, eds. (U.S. Government Printing Office, Washington, D.C.) p. 363-373.

✓ Meyers, R. E., 1979. The geology and origin of the New Inco copper deposit, Noranda district, Québec. M.Sc. thesis, McGill University, Montréal, Québec.

Moore, J. G. and Calk, L., 1971. Sulfide spherules in vesicles of dredged pillow basalt. *American Mineralogist*, v. 56, p. 476-488.

_____ and Fabbi, B. P., 1971. An estimate of juvenile sulfur content of basalt. *Contributions to Mineralogy and Petrology*, v. 33, p. 118-127.

_____ and Fabbi, B. P., 1971. Sulfur content of submarine versus subaerial basalt. *American Geophysical Union, Transactions*, v. 52, No. 11, p. 925-926.

_____ and Schilling, J. G., 1973. Vesicles, water and sulfur in Reykjanes Ridge basalts. *Contributions to Mineralogy and Petrology*, v. 41, p. 105-118.

Mottl, M. J., Corr, R. F. and Holland, H. D., 1974. Chemical exchange between seawater and mid-ocean ridge basalt during hydrothermal alteration: an experimental study. *Geological Society of America*, 87th Annual Meeting,

Abstracts with Programs, 6, p. 879-880.

_____ and Holland, H. D., 1978. Chemical exchange during hydrothermal alteration of basalt by seawater - I. Experimental results for major and minor components of seawater. *Geochimica et Cosmochimica Acta*, v. 42, p. 1103-1115.

Muehlenbacks, K. and Clayton, R. N., 1976. Oxygen isotope composition of the oceanic crust and its bearing on seawater. *Journal of Geophysical Research*, v. 81, p. 4365-4369.

Nagamori, M. and Kameda, M., 1965. Equilibria between Fe-S-O system melts and CO-CO₂-SO₂ gas mixtures at 1200°C. *Japanese Institute of Metallurgy, Transactions*, v. 6, p. 21-30.

Nagashima, S. and Katsura, T., 1973. The solubility of sulfur in Na₂O-SiO₂ melts under various oxygen partial pressures. *Chemical Society of Japan, Bulletin*, v. 46, p. 3099-3103.

Naldrett, A. J., 1969. A portion of the system Fe-S-O between 900° and 1080°C and its application to sulfide ore magmas. *Journal of Petrology*, v. 10, p. 171-201.

_____, 1973. Nickel sulfide deposits - their classification and genesis, with special emphasis on deposits of volcanic association. *Transactions of the Canadian Institute of Mining and Metallurgy*, v. 76, p. 183-201.

_____ and Gasparrini, E. L., 1971. Archean nickel sulfide deposits in Canada: their classification, geo-

logical setting and genesis with some suggestions as to exploration. Geological Society of Australia, Special Publication, No. 3, p. 201-226.

_____ and Goodwin, A. M., 1977. Volcanic rocks of the Blake River Group, Abitibi greenstone belt, Ontario and their sulfur content. Canadian Journal of Earth Science, v. 14, p. 539-550.

_____, Goodwin, A. M. and Fisher, T. L., 1977. Sulfur in Leg 37 basalts. In: DSDP Initial Reports, vol. 37. F. Aumento et al., eds. (U.S. Government Printing Office, Washington, D.C.) p. 561-562.

_____, Goodwin, A. M. and Fisher, T. L., 1978. The sulfur content of Archean volcanic rocks and a comparison with ocean floor basalts. Canadian Journal of Earth Science, v. 15, p. 715-728.

_____ and Kullerud, G., 1967. A study of the Strathcona mine and its bearing on the origin of Ni-Cu ores of the Sudbury district, Ontario. Journal of Petrology, v. 8, p. 453-531.

Nicholls, G. D. and Islam, M. R., 1971. Geochemical investigations of basalts and associated rocks from the ocean floor and their implications. Royal Society of London Philosophical Transactions, Series A, v. 268, p. 469.

Nockolds, S. R., 1966. The behavior of some elements during fractional crystallization of magmas. Geochimica et Cosmochimica Acta, v. 30, p. 267-278.

Norrish, K. and Chappell, B. W., 1967. X-ray fluorescence

spectrography. In: Physical Methods in Determinative Mineralogy. J. Zussman, ed. (Academic Press, London) p. 161-214.

Ohmoto, H., 1972. Systematics of sulfur and carbon isotopes in hydrothermal ore deposits. Economic Geology, v. 67, p. 551-578.

_____, Kajiwara, Y. and Date, J., 1970. The Kuroko ores in Japan - products of seawater? (Abstract) Geological Society of America, Abstracts with Programs, v. 2, p. 640-641.

_____ and Rye, R. O., 1974. Hydrogen and oxygen isotopic compositions of fluid inclusions in the Kuroko deposits, Japan. Economic Geology, v. 69, p. 947-953.

_____ and Rye, R. O., 1979. Isotopes of sulfur and carbon. In: Geochemistry of Hydrothermal Ore Deposits. H. L. Barnes, ed. (Wiley-Interscience, New York) p. 509-567.

Ol'shanskii, Y. I., 1951. The system Fe-FeS-FeO-SiO₂. (in Russian) Izvest. Akad. Nauk. S.S.S.R., Geological Series 6, p. 128-152.

Page, N. J., 1971. Comments on the role of oxygen fugacity in the formation of immiscible sulfide liquids in the H chromite zone of the Stillwater Complex. Economic Geology, v. 66, p. 607-610.

Parmentier, E. M. and Spooner, E. T. C., 1978. A theoretical study of hydrothermal convection and the origin of the ophiolitic sulfide ore deposits of Cyprus. Earth and Planetary Science Letters, v. 40, p. 33-44.

Pugh, D. T., 1967. Origin of hot brines in the Red Sea. *Nature*, v. 214, p. 1003-1004.

Ringwood, A. E., 1966. The chemical composition and origin of the earth. In: *Advances in Earth Science*. P.M. Hurley, ed. (M.I.T. Press, Cambridge, Mass.).

Ripley, E. M. and Ohmoto, H., 1977. Mineralogic, sulfur isotope and fluid inclusion studies of the stratabound copper deposits at the Raul mine, Peru. *Economic Geology*, v. 72, p. 1017-1041.

Roberts, R. G., 1966. Geology of the Matagami Lake mine, Galinée Township, Québec. Ph.D. thesis, McGill University, Montréal, Québec.

_____, 1975. The geological setting of the Matagami Lake mine, Québec: a volcanogenic massive sulfide deposit. *Economic Geology*, v. 70, p. 115-129.

Romberger, S. B. and Barnes, H. L., 1970. Ore solution chemistry III. Solubility of CuS in sulfide solutions. *Economic Geology*, v. 65, p. 901-919.

Rye, R. O. and Ohmoto, H., 1974. Sulfur and carbon isotopes and ore genesis: a review. *Economic Geology*, v. 69, p. 826-842.

Sakai, H., 1957. Fractionation of sulfur isotopes in nature. *Geochimica et Cosmochimica Acta*, v. 12, p. 150.

_____, 1968. Isotopic properties of sulfur compounds in hydrothermal processes. *Geochemical Journal*, v. 2, p. 29-49.

_____ and Nagasawa, H., 1958. Fractionation of sulfur isotopes in volcanic gases. *Geochimica et Cosmochimica Acta*, v. 15, p. 32-39.

Sangster, D. F., 1968. Relative sulfur isotope abundance of ancient seas and stratabound sulfide deposits. *Geological Association of Canada, Proceedings*, v. 19, p. 79-86.

_____, 1972. Precambrian volcanogenic massive sulfide deposits in Canada: a review. *Canadian Geological Survey, Paper 72-22*, 44pp.

Sasaki, A., 1970. Re-examination of sulfur isotopic composition of the earth's upper mantle. (Abstract) In: *International Symposium of Hydrogeochemistry and Biogeochemistry*. Clarke, ed. (Washington, D.C.) p. 129.

Sato, M. and Wright, T. L., 1966. Oxygen fugacities directly measured in magmatic gases. *Science*, v. 153, p. 1103-1105.

Schneider, A., 1970. The sulfur isotope composition of basaltic rocks. *Contributions to Mineralogy and Petrology*, v. 25, p. 95-124.

Scott, S. D. and Barnes, H. L., 1971. Sphalerite geothermometry. *Economic Geology*, v. 66, p. 653-669.

Seccombe, P. K. and Clark, G. S., 1981. Sulfur isotope and element variations in the South Bay mine, northwestern Ontario. *Economic Geology*, v. 76, p. 621-636.

Seyfried, W. and Bischoff, J. L., 1977. Hydrothermal transport of heavy metals by seawater: the role of seawater-basalt

ratio. Earth and Planetary Science Letters, v. 34,
p. 71-77.

Sharpe, J. I., 1964. Precambrian geology and sulfide deposits of the Matagami area, Québec. Ph.D. thesis, McGill University, Montréal, Québec.

_____, 1968. Geology and sulfide deposits of the Matagami area, Abitibi-east county. Québec Department of Natural Resources, Geology Report 137, 122pp.

Shaw, D. M. and Muysson, J. R., 1976. Granitophile trace elements and alteration in Leg 37 drill core. In: DSDP Initial Reports, vol. 37. F. Aumento, et al., eds. (U.S. Government Printing Office, Washington, D.C.)

Shima, H. and Naldrett, A. J., 1975. Solubility of sulfur in an ultramafic melt and the relevance of the system Fe-S-O. Economic Geology, v. 70, p. 960-967.

Shimazaki, H. and Clark, L. A., 1973. Liquidus relations in the FeS-FeO-SiO₂-Na₂O system and geological implications. Economic Geology, v. 68, p. 79-96.

Skinner, B. J., 1979. The many origins of hydrothermal mineral deposits. In: Geochemistry of Hydrothermal Ore Deposits. H.L. Barnes, ed. (Wiley-Interscience, New York) p. 1-20.

_____ and Peck, D. L., 1966. The solubility of sulfur in basic magmas. (Abstract) Economic Geology, v. 61, p. 802.

_____ and Peck, D. L., 1969. An immiscible sulfide

melt from Hawaii. Symposium: Magmatic Ore Deposits.

H.D.B. Wilson, ed. (Economic Geology Publ. Co.) p. 310-322.

_____, White, D. E., Rose, H. J. and Mays, R. E., 1967.
Sulfides associated with the Salton Sea geothermal
brine. Economic Geology, v. 62, p. 316-330.

Smitheringale, W. G. and Jensen, M. L., 1963. Sulfur isotopic
composition of the Triassic igneous rocks of eastern
U.S. Geochimica et Cosmochimica Acta, v. 27, p. 1183-1207.

Spooner, E. T. C. and Fyfe, W. S., 1973. Sub-sea floor me-
tamorphism and mass transfer. Contributions to Mineralogy
and Petrology, v. 42, p. 287-304.

Stanton, R. L., 1972. Ore Petrology. McGraw Hill, New York.
713 pp.

Sullivan, C. J., 1959. The origin of massive sulfide ores.
C.I.M. Bulletin, v. 52, p. 613-619.

Swallow, J. C. and Crease, J., 1965. Hot salty water at the
bottom of the Red Sea. Nature, v. 205, p. 165-166.

Taylor, H. P. Jr., 1974. The application of oxygen and hy-
drogen isotope studies to problems of hydrothermal
alteration and ore deposition. Economic Geology, v. 69,
p. 843-883.

Thode, H. G., Dunford, H. B. and Shima, M., 1962. Sulfur
isotope abundances in rocks of the Sudbury district and
their geological significance. Economic Geology, v. 57,
p. 565-578.

- _____, Monster, J. and Dunford, H. B., 1961. Sulfur isotope geochemistry. *Geochimica et Cosmochimica Acta*, v. 25, p. 159-174.
- Thompson, G., 1973. A geochemical study of the low-temperature interaction of seawater and oceanic igneous rocks. American Geophysical Union, Transactions, v. 54, p. 1015-1019.
- Thompson, M. and Howarth, R. J., 1976. Duplicate analysis in geochemical practice. Part 1: Theoretical approach and estimation of analytical reproducibility. *Analyst*, v. 101, p. 690-698.
- Vakhrushev, V. A. and Prokoptsev, N. G., 1972. Primary magmatic formations in basalts from the oceanic crust and inclusions of ultrabasic rocks in basalts. *International Geological Review*, v. 14, p. 125-135.
- Verhoogen, J., 1954. Petrologic evidence on temperature distributions in the mantle of the earth. American Geophysical Union, Transactions, v. 35, p. 85-92.
- Wager, L. R., Vincent, E. A. and Smales, A. A., 1957. Sulfides in the Skaergaard Intrusion, East Greenland. *Economic Geology*, v. 52, p. 855-895.
- Webber, G. R. and Newbury, M. L., 1971. X-ray fluorescence determination of minor and trace elements in silicate rocks. *Canadian Spectroscopy*, v. 16, p. 3-7.
- Wedepohl, K. (ed.), 1978. *Handbook of Geochemistry*. Springer Verlag, New York.

(.) Weissberg, B. G., Browne, P. R. L. and Seward, T. M., 1979. Ore metals in active geothermal systems. In: Geochemistry of Hydrothermal Ore Deposits. H.L. Barnes, ed. (Wiley-Interscience, New York) p. 738-780.

White, D. E., 1968. Environments of generation of some base metal ore deposits. Economic Geology, v. 63, p. 3-335.

_____, Muffler, L. J. P. and Truesdell, A. H., 1971. Vapor-dominated hydrothermal systems compared to hot-water systems. Economic Geology, v. 66, p. 75-97.

Wolery, T. J. and Sleep, N. H., 1976. Hydrothermal circulation and geochemical flux at mid-ocean ridges. Journal of Geology, v. 84, p. 249-275.

Woodall, R. and Travis, G. S., 1969. The Kambala nickel deposits, Western Australia. Publ. 9th. Commonwealth Mining and Metallurgical Congress, Paper 26, p. 17.

Yoder, H. S. Jr. and Tilley, C. E., 1962. Origin of basalt magmas: an experimental study of natural and synthetic systems. Journal of Petrology, v. 3, p. 342-532.

APPENDIX I - SAMPLE PREPARATION

General

2.3 kilograms of fresh sample was collected at each sample location. Special care was taken to ensure the freshness of the samples, thereby guarding against possible loss of sulfur from these rocks. Each of the samples was numbered and its sample location tagged. The sample was then subdivided into two parts. One portion of every sample was retained as a handspecimen while the remaining portion was put aside for subsequent crushing. All of the samples which were put aside for this purpose were first crushed to -1/4 inch in a gyratory jaw crusher. Following this, each sample was put into a Bico rotary grinder where it was ground to -50 mesh (Endecott) between two ceramic plates. Each sample was then mixed and quartered. At this stage, one quarter of each sample was set aside for subsequent finer grinding while the rest was retained as is. The selected quarter of each sample was then placed in a Tema puck grinder for four minutes where it was ground to -200 mesh. As a final precaution, the samples which were ground in the puck grinder were sieved to ensure that all particles were no larger than -200 mesh.

Preparation of Standards

Six standards were prepared for the purpose of sulfur determination of unknowns. Each standard was prepared by

the addition of a carefully weighed amount of finely ground pyrite grains (-200 mesh) to a weighed sample of pulverized rock powder (-200 mesh) of basaltic composition. The exact proportions of pyrite to basalt used in the preparation of each of these standards are indicated below.

BASALT(g)	PYRITE(g)	%S
3.000	0.000	0.000
2.997	0.003	0.050
2.994	0.006	0.100
2.985	0.015	0.250
2.970	0.030	0.500
2.940	0.060	1.000

Each standard sample was then placed in an agate mortar. Sufficient acetone was added to each basalt-pyrite mixture in order to facilitate mixing. Following the addition of acetone, each standard sample was mixed for three minutes with an agate pestle until the mixture appeared homogeneous. After the samples were dry, each was pelletized following the procedure outlined below.

Powder Pellets for XRF Analysis

Three grams of -200 mesh sized particles were placed over the base of a steel cylinder and mixed with four drops of 2% mowiol solution. Following mixing, approximately two grams of boric acid were spread evenly over the sample as a backing to the pellet. Pelletization was achieved by subjecting the sample to a pressure of 23 tonnes/cm² for one minute.

The pressure was then released gradually over a period of 25 seconds.

Preparation of Samples for LECO Analysis

Since the LECO analytical method is currently thought to be the best technique for the determination of sulfur content, several samples were sent out for such analyses. Some of these samples were analyzed by Dr. C. Riddle of the Ontario Geological Survey using the Canmet certified standard SL-1, while others were analysed by Dr. C. E. Rees of McMaster University.

The analytical procedure of this method involves initial combustion of samples in a stream of oxygen in a LECO induction furnace. The sulfur dioxide produced is then swept by the oxygen into a flask containing bromine water, and oxidized to sulfate. The latter is precipitated as barium sulfate and the sulfur content is determined gravimetrically at this stage.

I-2 Determination of Sulfur Concentration in Basalts

(A) X-Ray Fluorescence Analysis

A total of 200 sample pellets were analysed for sulfur using a Philips PW 1200 X-Ray Fluorescence Spectrometer and a chromium tube. The sulfur peak was measured at $2\theta = 106.50^\circ$ while the background measurement was obtained at $2\theta = 105.00^\circ$. The net counts per second (ie. peak - background) of unknowns was compared with the net counts per second of sulfur standards.

The sulfur content of unknowns was determined by using the equation of the least squares regression line obtained by plotting the sulfur content of each standard against the ratio of net counts per second of each standard to the net counts per second of a reference standard (ie. 0.5 %S). The least squares regression line has been illustrated in the text in Figure 3.1. The equation derived from this figure can be represented by the following relation:

$$\text{ppm } S_{\text{unk}} = X[5300 + 100]_{\text{ppm}}$$

where ppm S_{unk} is the amount of sulfur present in the unknown and X is the ratio of net counts per second of the unknown to the net counts per second of the reference standard. The value 5300 is the X co-ordinate of the reference standard against which all of the unknowns were run and the value 100 is the x intercept. Thus, given the x co-ordinate and the x intercept and knowing the value of X , one can readily calculate the amount of sulfur present in any unknown.

(1) Standards

(a) Precision of XRF Analyses

The precision of XRF analyses of sulfur standards was checked by periodically re-analysing several samples. A summary of these analyses is presented in Table I-a. The precision at the 95% confidence level was found to be within 6.1% of the sulfur concentration for the 0 %S standard, $\pm 3.5\%$ for 0.05 %S, $\pm 1.8\%$ for 0.1 %S, $\pm 1.6\%$ for 0.25 %S and

TABLE I-a: Precision of XRF Analyses of Sulfur Standards

<u>0 %S</u>	<u>0.05 %S</u>	<u>0.1 %S</u>	<u>0.25 %S</u>	<u>1.0 %S</u>	
0.032	0.056	0.110	0.244	0.995	
0.032	0.056	0.110	0.249	0.994	
0.032	0.058	0.112	0.242	0.994	
0.037	0.055	0.108	0.243	0.995	
0.033	0.057	0.109	0.243	0.995	
0.033	0.056	0.110	0.245	0.994	
0.032	0.058	0.111	0.244	0.995	
					n = 7
0.033	0.057	0.110	0.244	0.995	\bar{X}
0.001	0.001	0.001	0.002	0.001	S_X
0.0004	0.0004	0.0004	0.0008	0.0004	$S_{\bar{X}}$
					f = 6
					$t_{95} = 2.447$
0.002	0.002	0.002	0.0039	0.002	$t(S_{\bar{X}})$
6.1%	3.5%	1.8%	1.6%	0.2%	P(%)

±0.2% for the 1.0 %S standard. In general, better precision was obtained with increasing sulfur concentration of the standards. This is as expected because addition of larger amounts of pyrite to a given amount of basalt powder is less difficult as compared to the addition of very small and exact amounts of pyrite to the same quantity of rock powder. In addition, it is often more difficult to obtain a truly homogeneous mixture when the quantities of components are drastically different.

(2) Unknowns

(a) Precision of XRF Analyses in Unknowns

The precision of XRF analyses was checked by analysing a given powder pellet twice during each day's run and by re-analysing other powder pellets as well. A summary of these analyses is presented in Table I-b. The precision, on average, is 4.4% at a level of confidence of 95%.

(b) Accuracy of XRF Analyses in Unknowns

The accuracy of XRF analyses has been determined by comparing values of sulfur concentration obtained by XRF with the values obtained by LECO analysis. This was done on the assumption that the LECO analytical method provides "true" sulfur values. On the basis of the data presented in Table I-c, there is 90% confidence that the difference between the two sets of values is real and that the XRF values will generally be greater than the LECO values.

TABLE I-b: Precision of XRF Analyses in Unknowns

Sample No.	X_1 (ppmS)	X_2 (ppmS)	$ X_1 - X_2 $	\bar{X}	S_x	P(%)
AP5	1267	1193	74	1230	52.3	4.3
AP13	2019	1919	100	1969	70.7	3.6
AP14	1325	1309	16	1317	11.3	0.9
AP15	848	816	32	832	22.6	2.7
AP20	853	832	21	843	14.8	1.8
AP27	1092	1018	74	1055	52.3	5.0
AP38	1707	1696	11	1702	7.8	0.5
AP42	906	864	42	885	29.7	3.4
M2	1076	1065	11	1071	7.8	0.7
M70	769	731	38	750	26.9	3.6
M246	2459	2427	32	2443	22.6	0.9
M252-2	5258	5109	149	5184	105	2.0
M330	3291	3323	82	3307	58.0	1.8
M371	610	599	11	605	7.8	1.3
M372	1685	1670	15	1678	10.6	0.6
M397	747	720	27	734	19.1	2.6

$\bar{P}(\%) = 2.2$ at 68% C.L.

$\bar{P}(\%) = 4.4$ at 95% C.L.

()
TABLE I-c: Accuracy of XRF Analyses of Unknowns

Sample No.	%S _{XRF}	%S _{LA}	(X _{XRF} - Y _{LA})
AP1	0.032	0.028	0.004
AP5	0.119	0.112	0.007
AP7	0.021	0.018	0.003
AP9	0.053	0.052	0.001
AP13	0.192	0.162	0.030
AP18	0.008	0.007	0.001
AP26	0.017	0.018	-0.001
AP29	0.234	0.193	0.041
AP30	1.612	1.663	-0.051
AP31	0.466	0.452	0.014
AP38	0.169	0.142	0.027
AP39	0.013	0.014	-0.001
AP41	0.007	0.009	-0.002
AP42	0.086	0.063	0.023
AP43	0.058	0.049	0.009
AP44	0.040	0.038	0.002
AP49	0.016	0.015	0.001
AP50	0.008	0.009	-0.001
AP55	0.016	0.014	0.002
AP64	0.005	0.007	-0.002
M330	0.332	0.290	0.042
M316	0.007	0.008	-0.001
M317	0.077	0.077	0.000
M655	0.017	0.012	0.005
M38	0.019	0.015	0.004

n = 25

$\bar{X} = 0.145$ $\bar{Y} = 0.139$ $\bar{d} = 0.00628$

$S_d = 0.0178$

$S_{\bar{d}} = 0.00357$

f = 24

$t = \frac{\bar{d}}{S_{\bar{d}}} = 1.76$ (90% C.L.)

At C.L. = 68%

$$A = \frac{\bar{d}}{\bar{y}} = \frac{0.00628}{0.139} = 4.5\%$$

At C.L. = 95%,

$$t_f = 24 = 2.064$$

$$t(S_{\bar{d}}) = 0.0074$$

$$A = \frac{t(S_{\bar{d}}) + \bar{d}}{\bar{y}} = \frac{0.0136}{0.139} = 9.8\%$$

The accuracy of the XRF analytical method is 9.8% at a level of confidence of 95%.

(B) LECO Analysis

(a) Precision of LECO Sulfur Analyses of Unknowns

The precision of these analyses was estimated on the basis of duplicate results supplied by the Ontario Geological Survey. A summary of these analyses is presented in Table 1-d. The precision, at a level of confidence of 95%, is 4.2%, on average.

(b) Reliability of LECO Sulfur Analyses of Unknowns

The reliability of LECO analyses was checked by analysing two powder pellets by two commercial labs. One set of results was provided by Dr. C. Riddle of the Ontario Geological Survey while the other set was provided by Dr. C. E. Rees of McMaster University. A summary of these analyses is presented in Table 1-e. On the basis of the data shown in this table, there is 50% confidence that the analytical bias between the two commercial labs is real and the interlab bias, expressed as an average deviation, is 0.083 %S.

I-3 Determination of FeO Concentration in Basalts

Atomic Absorption

The total iron content (expressed as FeO) of 44 samples was determined by A. M. Collins, geochemist. The analytical procedure involved initial pre-ignition of graphite crucibles

TABLE I-d: Precision of LECO Sulfur Analyses

Sample No.	X_1 (%S)	X_2 (%S)	\bar{X}	S_x	P(%)
AP1	0.028	0.027	0.028	0.0007	2.5
AP5	0.112	0.112	0.112	0.000	0.0
AP7	0.018	0.018	0.018	0.000	0.0
AP9	0.052	0.052	0.052	0.000	0.0
AP13	0.162	0.156	0.159	0.004	2.5
AP18	0.007	0.006	0.007	0.007	10
AP26	0.017	0.019	0.018	0.001	5.6
AP29	0.194	0.192	0.193	0.001	0.5
AP30	1.71	1.72	1.72	0.007	0.4
AP31	0.454	0.450	0.452	0.003	0.7
AP38	0.143	0.140	0.142	0.002	1.4
AP39	0.014	0.013	0.014	0.0007	5.0
AP41	0.009	0.009	0.009	0.000	0.0
AP44	0.039	0.040	0.040	0.0007	1.8
AP50	0.009	0.009	0.009	0.000	0.0
AP55	0.013	0.014	0.014	0.0007	5.0
AP64	0.007	0.007	0.007	0.000	0.0

$\bar{P}(\%) = 2.1$ at 68% C.L.

$\bar{P}(\%) = 4.2$ at 95% C.L.

TABLE I-e: Reliability of the LECO Analytical Method

Sample No.	$X_1(\%S)$	$X_2(\%S)$	$X_1 - X_2$
AP30	1.72	1.56	0.16
AP44	0.04	0.035	0.005
$n = 2$	$\bar{X}_1 = 0.88$	$\bar{X}_2 = 0.80$	$\bar{d} = 0.083$
			$s_d = 0.11$
			$s_{\bar{d}} = 0.077$
			$f = 1$
			$t = \frac{\bar{d}}{s_{\bar{d}}} = 1.1(50\% \text{ C.L.})$

()

in a muffle furnace at 1000°C for 15 minutes. Following this, the crucibles were set aside to cool for about 35 minutes. Once they had cooled, 1.0 g of lithium metaborate was added to each crucible. Between 200-205 mg of sample was weighed out and added to the lithium metaborate already in the crucibles. The contents of each crucible were mixed with a thin glass rod and set aside while 40 ml of 6% HNO₃ solution was pipetted into 150-200 ml beakers. A Teflon stirring bar was added to each of the beakers which were then placed over magnetic stirrers. Meanwhile, the covered crucibles were placed in a pre-heated furnace at 1000°C for 15 minutes and then removed. As the crucibles were removed from the furnace, the contents of each were swirled and poured into an appropriately labeled beaker containing 40 ml of HNO₃ solution. While the samples were dissolving in their respective beakers, 80 ml of 15,000 ppm Sr solution was pipetted into each 200 ml volumetric flask. As the samples in the beakers dissolved, the sample solutions were added to the volumetric flasks. Each beaker was rinsed with distilled water five times so that each flask eventually contained 200 ml of solution. The contents of each volumetric flask was then filtered into a 200 ml LPE bottle using a Whatman No. 1 filter paper. After all the samples had been filtered, a blank solution was prepared following the exact same procedure, except omitting the sample. Once this was done, the samples were analysed for iron using a Perkin-Elmer

403 Atomic Absorption Spectrophotometer. The results were reported in terms of ppm Fe present in each sample. However, these values were later converted to %Fe and then to %FeO using the following formula:

$$\%FeO = \frac{\text{mol. wt. FeO}}{\text{at. wt. Fe}} \times \text{wt. \% Fe}$$

The results of these iron analyses are included in Table II-a which summarizes the geochemical composition of each sample.

APPENDIX II - GEOCHEMICAL COMPOSITION OF BASALT UNITS B1 - B7

The geochemical composition of these basalts is presented in Table II-a.

The major element analyses of the M-series rocks have been determined by MacGeehan (1979).

The FeO values shown in this table represent total iron contents of the samples, calculated as FeO. The FeO content of the M-series rocks is the result of determinations by X-Ray Fluorescence spectrometry while that of the AP-series rocks is the result of atomic absorption analysis.

The sulfur analyses which supplement the above were determined by X-Ray Fluorescence. A total of 200 samples have been analysed.

Unit	No. of Samples
NR	5
B1	12
B2	14
B3	43 + 46
B4	44
GLR	6
B5	15
B6	9
B7	<u>6</u>
	200

Individual units are presented in order of increasing stratigraphic height. Samples belonging to any one of these units are always presented in order of increasing SiO₂ content.

Finally, all of the samples appearing in Table II-a are identified on sample location Maps 1 and 2.

TABLE II-a: Geochemical Composition of Units NR - B7

Unit	Sample No.	SiO ₂	FeO	S
NR	M567	71.90	5.39	39
NR	M557	73.82	4.67	138
NR	M591	73.99	4.49	79
NR	M563	75.08	4.22	99
NR	M590	77.53	5.29	53
B1	M274	52.23	16.48	111
B1	M598	54.50	12.58	121
B1	M492	54.97	16.43	19,277
B1	M597	55.29	12.59	116
B1	M561	56.71	11.88	371
B1	M596-1	56.99	12.63	11,236
B1	M560-1	58.87	13.25	3821
B1	M596-2	59.71	10.98	1606
B1	M558	61.87	12.29	7696
B1	M560-2	64.67	9.45	2480
B1	M513	66.30	7.67	3041
B1	M516	66.38	9.39	7328
B2	M319	49.52	13.59	201

Unit	Sample No.	SiO ₂	FeO	S
B2	M584	50.63	13.07	3291
B2	M322	51.10	13.18	392
B2	M585	51.36	12.37	747
B2	M317	51.38	12.26	770
B2	M569	51.50	13.28	509
B2	M321	51.86	13.22	710
B2	M578	54.91	15.78	1712
B2	M568	56.61	11.40	509
B2	M579	57.37	11.50	2687
B2	M316	58.97	9.64	75
B2	AP33	—	13.62	413
B2	AP34	—	13.67	477
B2	AP35	—	13.79	297
B3	M310	46.37	16.20	278
B3	M305	48.59	15.03	133
B3	M19	49.01	15.23	465
B3	M307	49.61	16.66	716
B3	M343	50.05	16.56	906
B3	M9	50.13	16.66	2152
B3	M309	50.21	15.85	160
B3	M308	50.37	15.70	3858

Unit	Sample No.	SiO ₂	FeO	S
B3	M313	50.52	16.75	368
B3	M306-2	50.61	14.87	93
B3	M329	50.96	14.97	385
B3	M312	51.00	16.75	848
B3	M18	51.29	14.83	293
B3	M306-1	51.66	12.92	48
B3	M3	51.85	14.68	238
B3	M300	52.19	15.03	185
B3	M338	53.96	15.76	308
B3	M14	54.58	14.06	101
B3	M332	56.55	15.16	779
B3	M334	56.67	13.97	201
B3	M333	57.23	13.97	227
B3	M334-2	57.34	13.46	196
B3	M326	57.73	13.55	191
B3	M335	58.54	11.56	111
B3	M337	58.81	13.88	91
B3	M331	59.03	13.29	159
B3	M314	59.30	10.05	551
B3	M337-2	59.70	14.12	139
B3	M262	60.36	12.45	2390
B3	M330	60.46	14.31	3323

Unit	Sample No.	SiO ₂	FeO ^a	S
B3	M335-2	60.56	10.11	106
B3	M1009	61.88	9.78	6302
B3	M265	62.32	8.22	42
B3	M1010	62.74	9.35	1097
B3	M264	63.44	6.43	901
B3	M261	63.87	10.26	159
B3	M267	64.71	7.87	200
B3	M303	65.54	8.67	170
B3	AP3	—	12.12	175
B3	AP7	—	15.05	207
B3	AP36	—	13.89	408
B3	AP37	—	12.97	101
B3	AP39	—	16.38	133
B4	M92	46.63	20.07	2205
B4	M372	47.12	16.81	1670
B4	M89	48.07	17.36	210
B4	M256	49.13	15.57	1198
B4	M1	49.75	16.04	450
B4	M253	49.87	16.16	472
B4	M252	50.61	16.10	5109
B4	M350	51.19	15.13	253

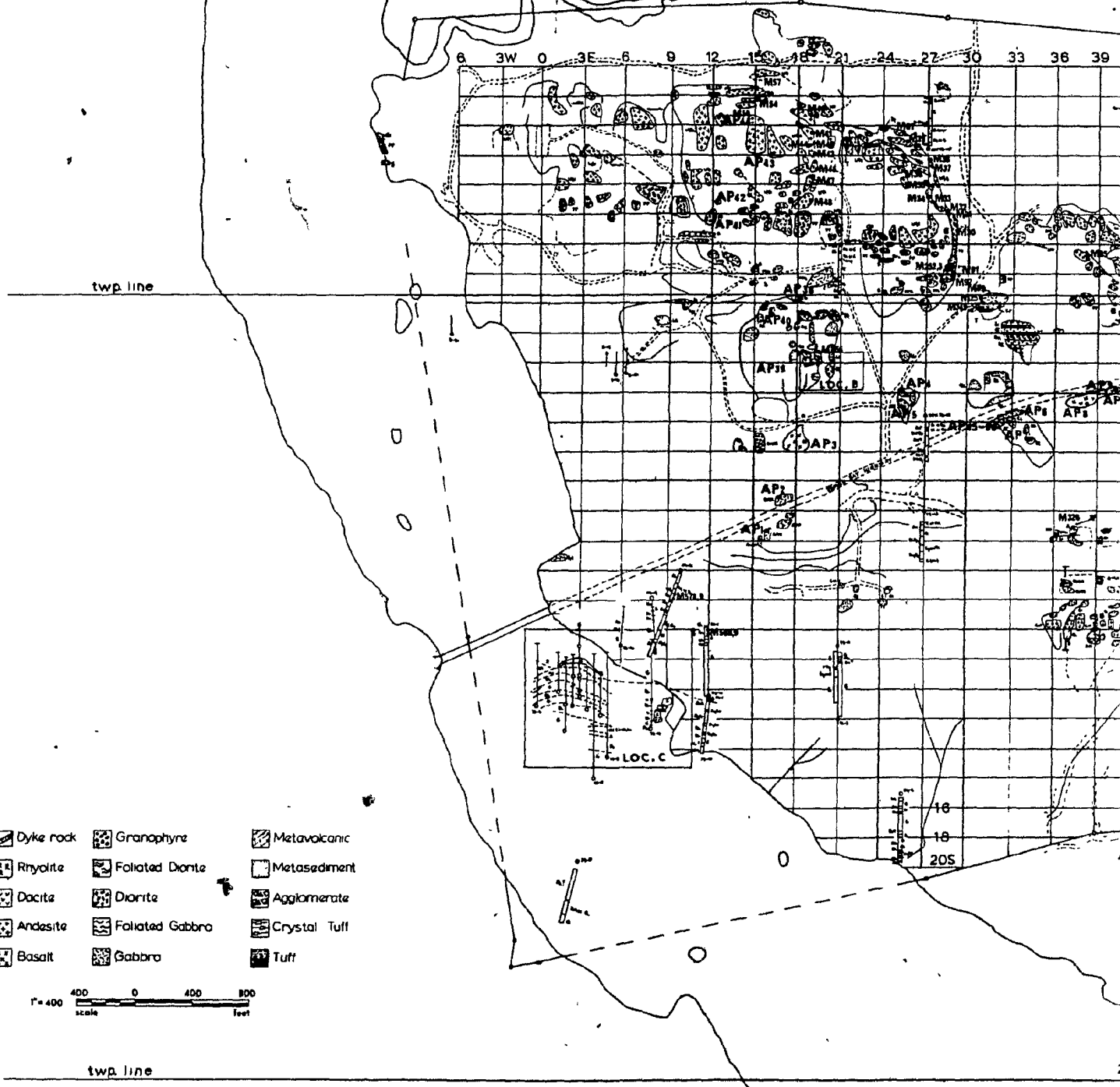
Unit	Sample No.	SiO ₂	FeO	S
B4	M655	52.32	15.56	170
B4	M369	52.60	13.99	9545
B4	M91	52.70	14.67	5067
B4	M368	54.28	15.12	3758
B4	M654	56.97	12.03	80
B4	M371	57.28	13.19	599
B4	M474	58.75	14.39	451
B4	M349	59.65	10.84	80
B4	M473	59.76	13.05	631
B4	M397	61.44	11.35	720
B4	M1008	62.09	10.04	816
B4	M256-2	63.28	10.10	1049
B4	M24	64.23	8.38	7369
B4	M23	67.00	7.28	110
B4	M1003	74.39	5.26	484
B4	M27	74.91	5.79	1542
B4	M252-2	—	16.92	5109
B4	M395	—	15.66	213
B4	M398	—	14.61	490
B4	AP9	—	13.06	530
B4	AP10	—	8.05	117
B4	AP12	—	12.89	292

Unit	Sample No.	SiO ₂	FeO	S
B4	AP13	_____	13.31	1919
B4	AP14	_____	12.65	1309
B4	AP15	_____	8.55	816
B4	AP17	_____	12.52	80
B4	AP18	_____	7.56	82
B4	AP20	_____	15.76	832
B4	AP21	_____	14.46	498
B4	AP23	_____	15.94	1113
B4	AP24	_____	15.36	2327
B4	AP25	_____	14.72	138
B4	AP26	_____	16.23	170
B4	AP27	_____	14.19	1018
B4	AP38	_____	9.02	1696
B4	AP40	_____	21.90	58
GLR	M672-2	62.63	6.19	143
GLR	M671	69.16	6.04	254
GLR	M657	70.47	6.00	175
GLR	M667	70.89	6.53	191
GLR	M693	71.85	9.01	228
GLR	M64	78.45	2.19	191

Unit	Sample No.	SiO ₂	FeO	S
B5	M48	49.92	17.76	1076
B5	M85	51.21	17.59	742
B5	M47	51.73	17.35	1383
B5	M33	53.24	14.48	2162
B5	M32	53.89	14.31	1887
B5	M46	54.22	15.87	806
B5	M30	54.41	16.28	2030
B5	M34	54.62	15.46	5597
B5	M31	55.20	15.46	779
B5	M383	—	27.40	3811
B5	M384	—	15.53	1012
B5	M386	—	13.58	2528
B5	M388	—	6.14	101
B5	M389	—	11.94	3949
B5	AP42	—	17.36	864
B6	M42	54.48	14.68	583
B6	M40	54.53	15.00	758
B6	M43	54.81	14.79	478
B6	M41	55.29	14.69	758
B6	M36	55.37	13.70	392

Unit	Sample No.	SiO ₂	FeO	S
B6	M37	55.84	13.94	270
B6	M50	56.02	14.24	705
B6	M35	56.54	15.03	6281
B6	AP43	—	15.99	583
B7	M54	54.10	14.76	398
B7	M61	55.55	13.61	207
B7	M57	56.18	12.66	143
B7	M39	57.94	12.35	647
B7	M38	64.07	7.05	188
B7	AP44	—	15.35	398

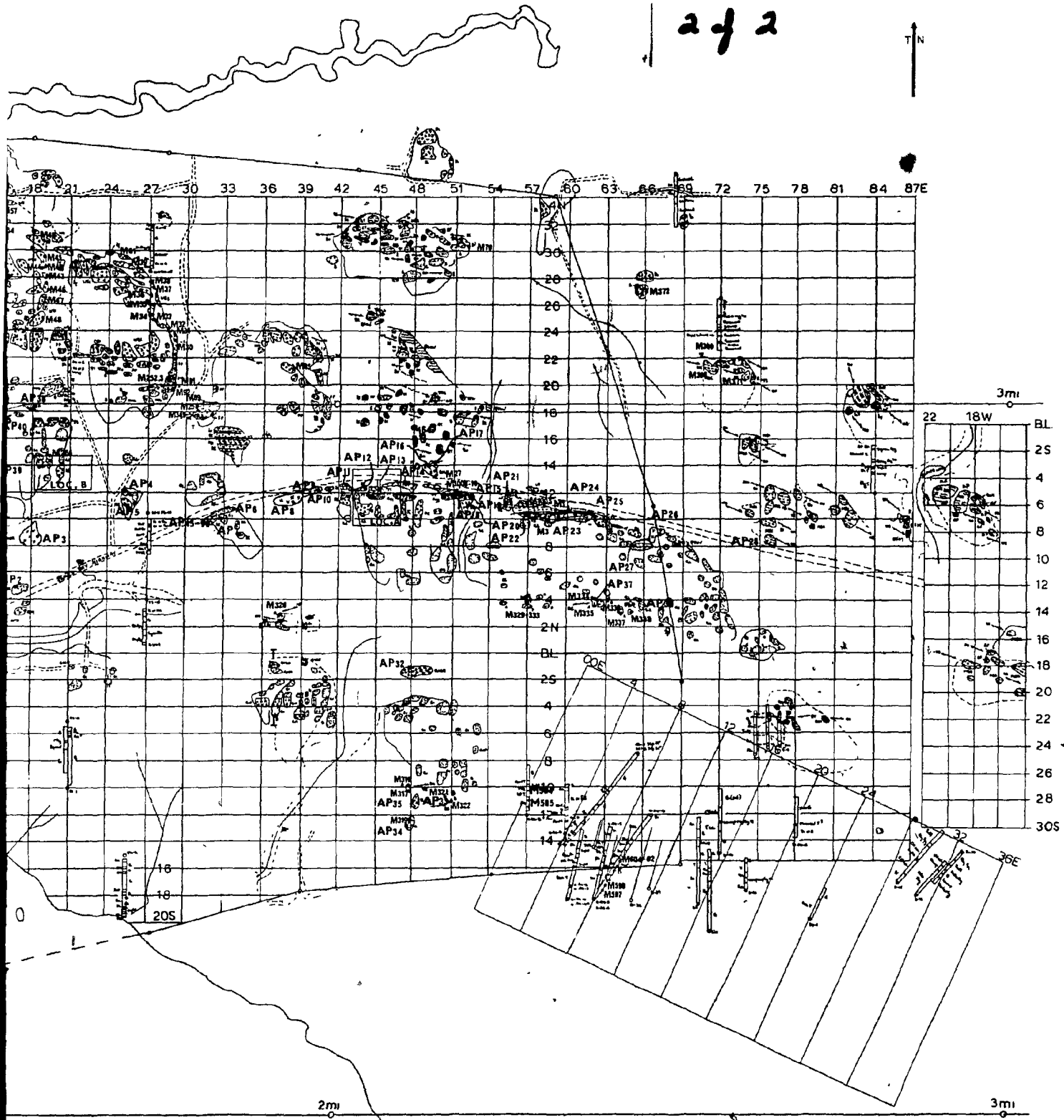
18



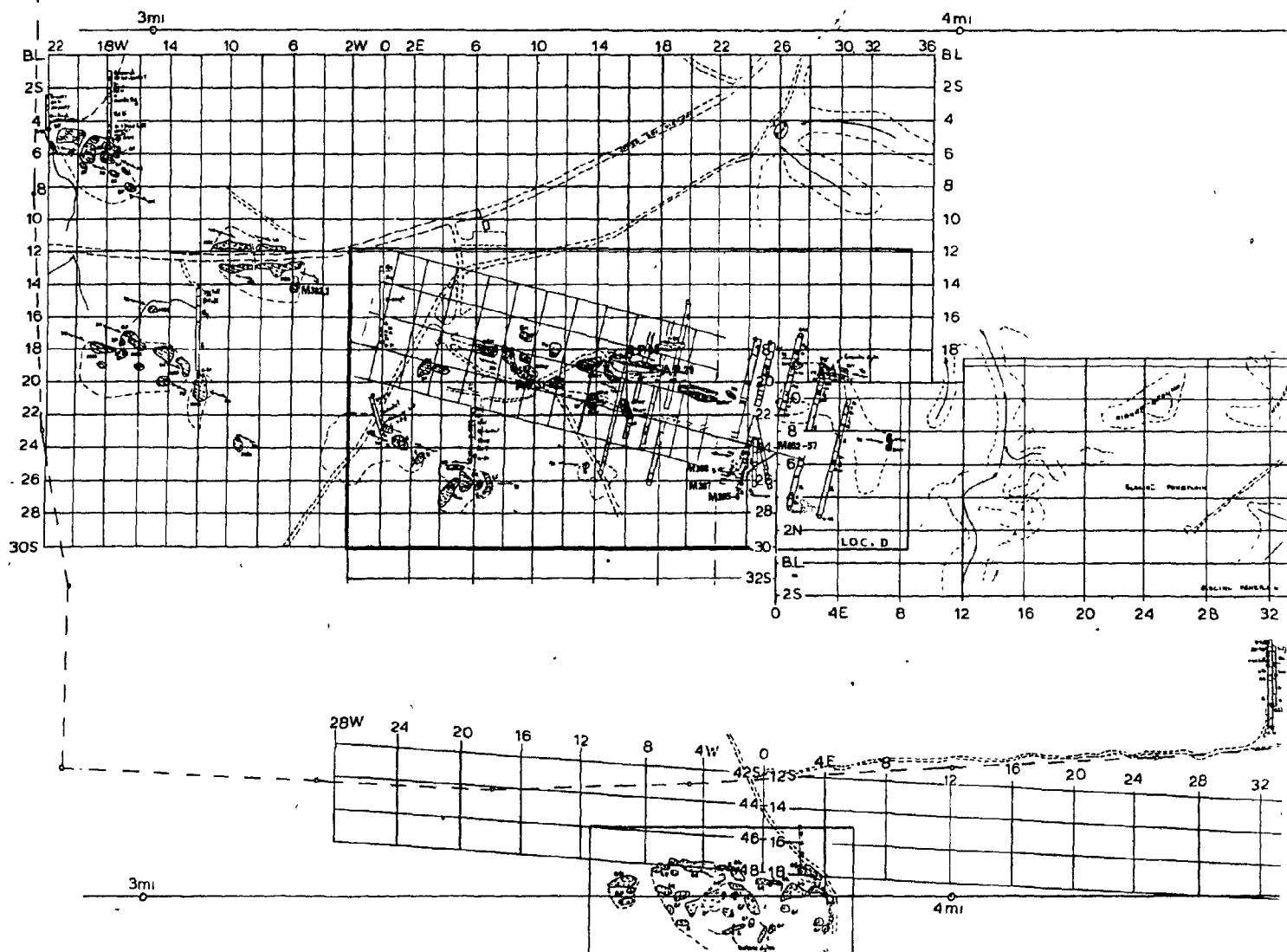
- | | | |
|-----------|------------------|--------------|
| Dyke rock | Granophyre | Metavolcanic |
| Rhyolite | Foliated Diorite | Metasediment |
| Dacite | Diorite | Agglomerate |
| Andesite | Foliated Gabbro | Crystal Tuff |
| Basalt | Gabbro | Tuff |



272



18

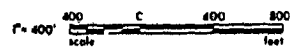


272



twp. bdy

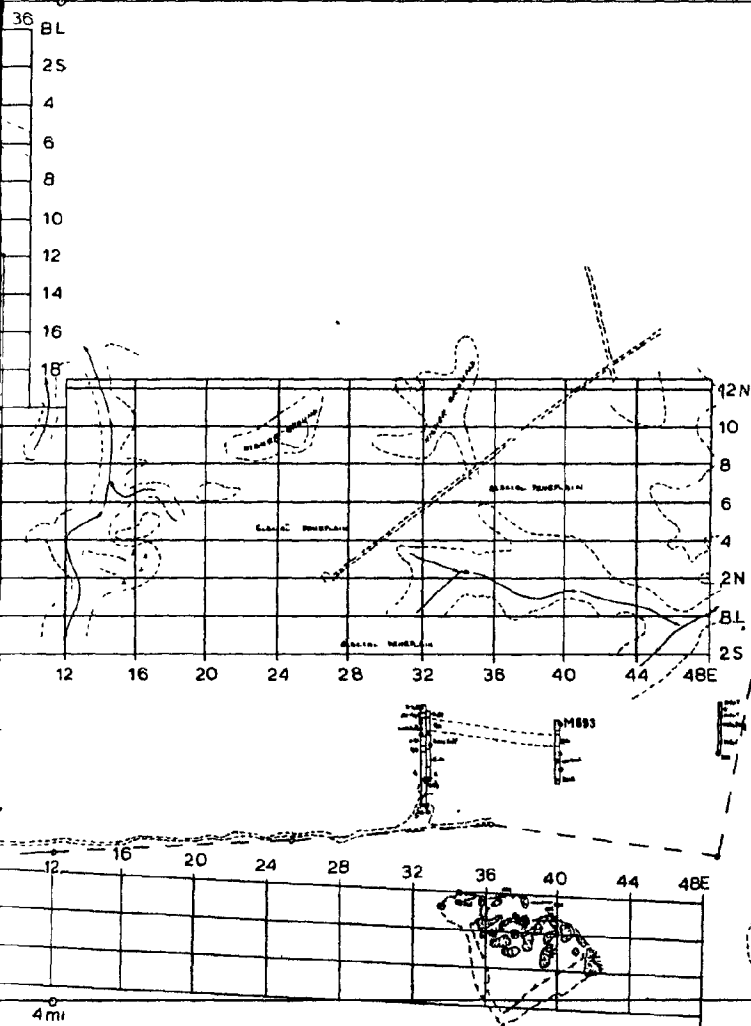
- | | | |
|-----------|------------------|--------------|
| Dyke rock | Granophyre | Metavolcanic |
| Rhyolite | Foliated Diorite | Metasediment |
| Dacite | Diorite | Agglomerate |
| Andesite | Foliated Gabbro | Crystal Tuff |
| Basalt | Gabbro | Tuff |



5mi

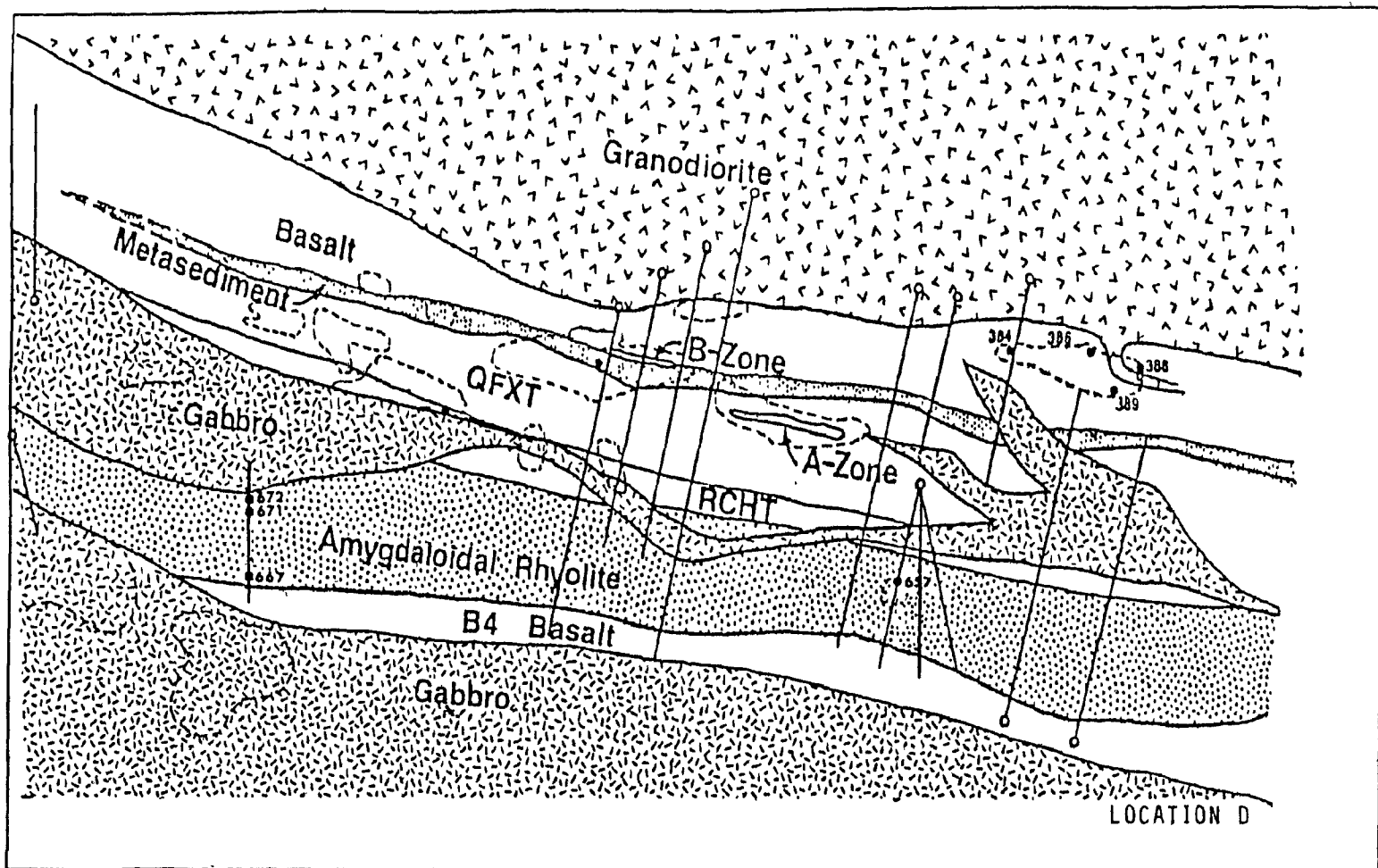
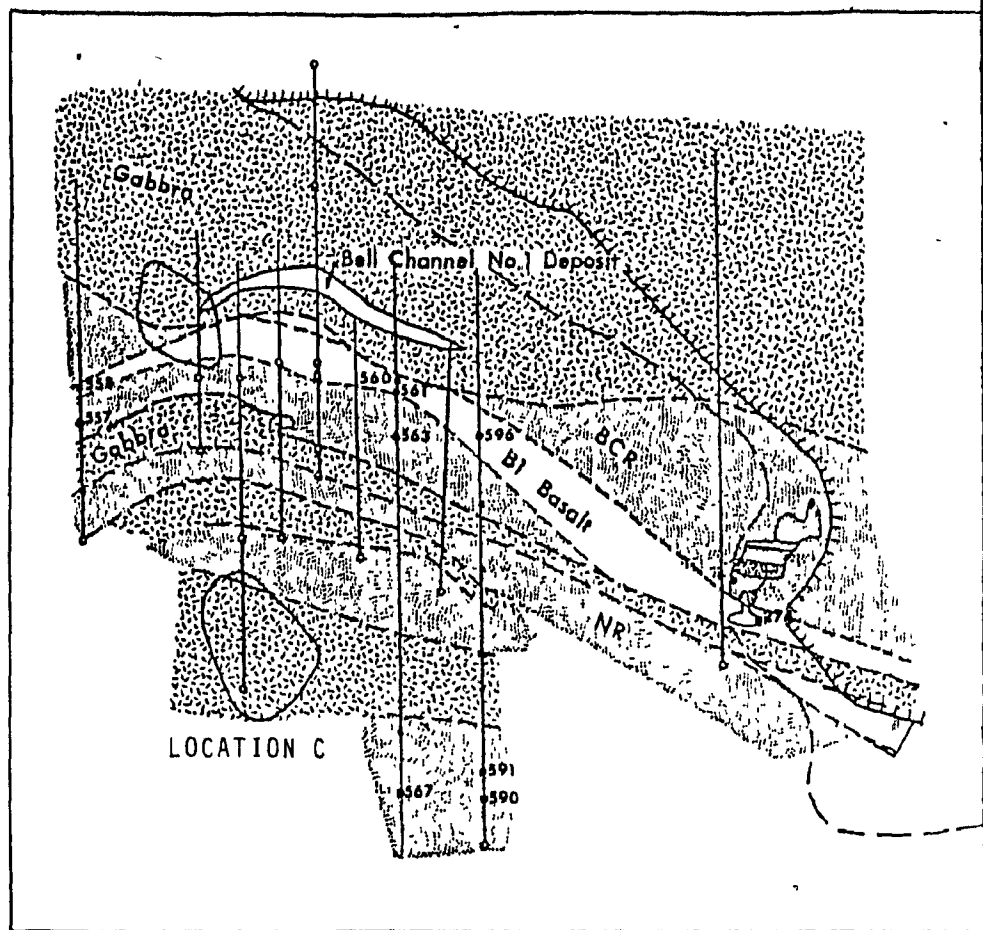
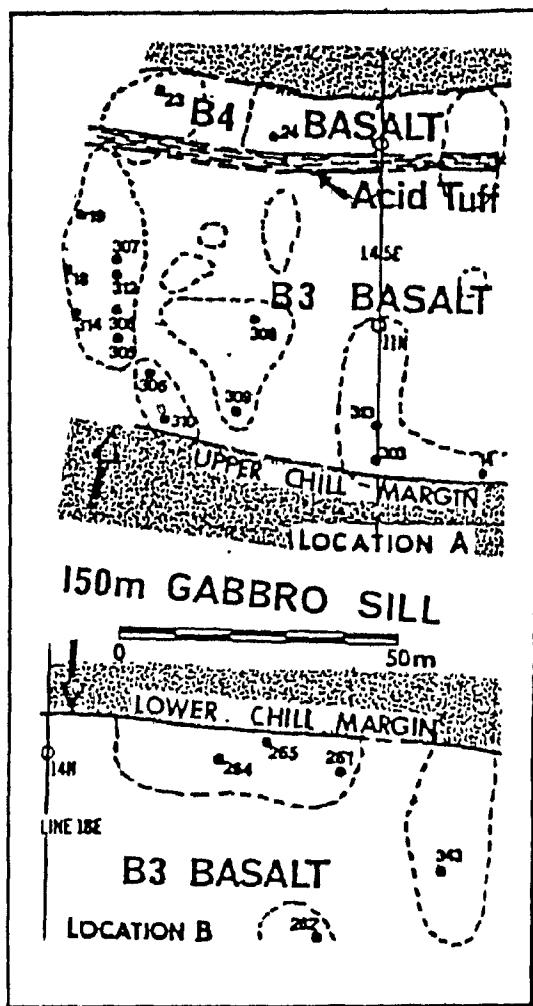
twp. line

4mi

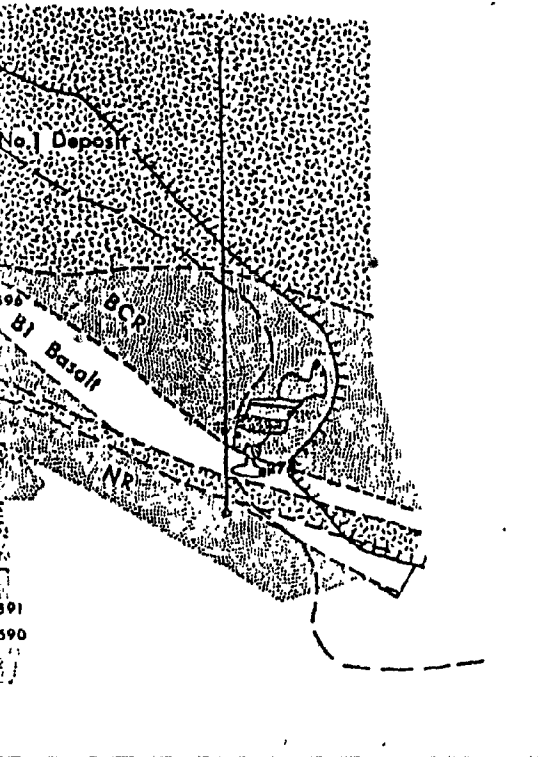


MAPPED BY MacGehee, P.J., 1979

GARON LAKE MAP 2



272



- | | | |
|-----------|------------------|--------------|
| Dike rock | Granophyre | Metavolcanic |
| Rhyolite | Foliated Diorite | Metasediment |
| Dacite | Diorite | Agglomerate |
| Andesite | Foliated Gabbro | Crystal Tuff |
| Basalt | Gabbro | Tuff |